ISOTOPES AND RADIATION TECHNOLOGY

THE UNIVERSITY OF MICHIGAN
JAN 28 1965
PHORMIX

A Quarterly Technical Progress Review

Prepared for DIVISION OF TECHNICAL INFORMATION / DIVISION OF ISOTOPES DEVELOPMENT, UNITED STATES ATOMIC ENERGY COMMISSION, by P. S. BAKER, A. F. RUPP, and ASSOCIATES, OAK RIDGE NATIONAL LABORATORY

Fall 1964

● VOLUME 2

● NUMBER 1

TECHNICAL PROGRESS REVIEWS

To meet the needs of industry for concise summaries of current atomic developments, the Atomic Energy Commission is publishing this series, Technical Progress Reviews. Issued quarterly, each of the reviews digests and evaluates the latest findings in a specific area of nuclear technology and science.

The five journals published in this series are:

Isotopes and Radiation Technology, P. S. Baker, A. F. Rupp, and associates, Oak Ridge National Laboratory

Nuclear Safety, Wm. B. Cottrell, W. H. Jordan, and associates, Oak Ridge National Laboratory

Power Reactor Technology, W. H. Zinn and J. R. Dietrich, General Nuclear Engineering Corporation

Reactor Fuel Processing, Stephen Lawroski and associates, Chemical Engineering Division, Argonne National Laboratory

Reactor Materials, R. W. Dayton, E. M. Simons, and associates, Battelle Memorial Institute

Each journal may be purchased from the Superintendent of Documents, U. S. Government Printing Office, Washington, D. C., 20402. *Isotopes and Radiation Technology* at $2.00 per year for subscription or $0.55 for individual issues; the other four journals at $2.50 per year and $0.70 per issue. See back cover for remittance instructions and foreign postage requirements.

The views expressed in this publication do not necessarily represent those of the United States Atomic Energy Commission, its divisions or offices, or of any Commission advisory committee or contractor.

Availability of Reports Cited in This Review

Unclassified AEC reports are available for inspection at AEC depository libraries and are sold by the Office of Technical Services, Department of Commerce, Washington, D. C., 20230. Some of the reports cited are not available owing to their preliminary nature; however, the information contained in them will eventually be made available in formal progress or topical reports.

Unclassified reports issued by other Government agencies or private organizations should be requested from the originator.

Unclassified British and Canadian reports may be inspected at AEC depository libraries. British reports are sold by the British Information Service, 45 Rockefeller Plaza, New York, N. Y.; Canadian reports (AECL series) are sold by the Scientific Document Distribution Office, Atomic Energy of Canada, Ltd., Chalk River, Ontario, Canada.

Classified U. S. and foreign reports identified in this journal as Classified may be purchased by properly cleared Access Permit Holders from the Division of Technical Information Extension, U. S. Atomic Energy Commission, P. O. Box 1001, Oak Ridge, Tenn., 37831. Such reports may be inspected at classified AEC depository libraries.

ISOTOPES AND RADIATION TECHNOLOGY

A REVIEW OF RECENT DEVELOPMENTS

Prepared for DIVISION OF TECHNICAL INFORMATION / DIVISION OF ISOTOPES DEVELOPMENT, UNITED STATES ATOMIC ENERGY COMMISSION, by P. S. BAKER, A. F. RUPP, and ASSOCIATES, OAK RIDGE NATIONAL LABORATORY

FALL 1964

VOLUME 2

NUMBER 1

Foreword

Isotopes and Radiation Technology is a Technical Progress Review prepared by the Isotopes Development Center, Oak Ridge National Laboratory, at the request of the Divisions of Technical Information and Isotopes Development, U. S. Atomic Energy Commission. This Review is intended to assist those interested in keeping abreast of significant developments in the fields of isotopes and radiation technology. It is not a comprehensive review of all literature published in this field during a given quarter; rather, it is a mechanism for presenting concise, selected reviews of information on subjects of prevailing Commission interest as it becomes available.

This Review attempts to relate the published results of research and development sponsored by the Division of Isotopes Development to significant developments in radioisotopes and radiation technology, as reported in the world literature. Coverage includes isotope production and development, isotope technology development, isotope applications technology, process radiation development, and radiation processing of food and medical supplies.

In addition to reviews of current literature and special review articles dealing with specific isotopes, facilities, and applications, this publication occasionally contains feature articles prepared by recognized experts on specific topics of current interest. Critical evaluations and interpretations presented are those of the editors and invited reviewers; therefore readers are encouraged to consult the original references in order to obtain all the background of the work reported and the interpretation of the results given by the original authors.

The subject headings listed below have been adopted to help maintain continuity and order, from one issue to the next, in the material reviewed. All reviews, except Feature Articles, will be arranged under these headings; but any one issue will not necessarily contain all the headings.

Isotope Production and Development
Isotope Technology Development
Food Irradiation
Process Radiation Development
Source Development
Isotopic Power Development
Applications in Medicine
Safety
Miscellaneous Items of Interest

P. S. BAKER, ROBERT H. LAFFERTY, Jr.,
MARTHA GERRARD, D. A. FUCCILLO, and
R. E. GREENE, Editors
A. F. RUPP, Advisory Editor
Oak Ridge National Laboratory

Issued quarterly by the U. S. Atomic Energy Commission. Use of funds for printing this publication approved by the Director of the Bureau of the Budget on December 31, 1962.

DEPOSITED BY THE
UNITED STATES OF AMERICA

Contents

I Isotope Production 1
Isotope Separations Chemistry 1
Ion-Exchange Purification of Radioisotopes at the ORNL Isotopes Development Center.
ORNL Target Fabrication Center 5
Isotopic Magnesium Targets • Technetium-99 Targets.
Production of ^{28}Mg: State of the Art 8
Production Procedures Manuals for Isotopes 10
Mound and Savannah • Brookhaven and Oak Ridge.
References 16

II Isotope Technology Development 18
Radioactive Tracer Uses in the Mining Industry 18
Radioisotope Tracers in Research with Coal • Radioactive Tracers for Concentration of Ores.
Recent Developments in Counting Methods 34
Geiger Counters in Flexible Materials • Anion- and Cation-Exchange Resins with Scintillating Properties.
Radio-Snow Gages: A Review of the Literature 41
Fixed-Location Snow Gages • Portable Neutron and Gamma Probes.
References 47

III Food Irradiation 50
Effect of Gamma Irradiation on Shasta Strawberries Under Marketing Conditions . . . 50
Experimental Work • Selection of Optimum Radiation Dose • Materials and Methods. Summary.
References 53

IV Source Development 55
Beta-Ray-Excited Sources for Radiography 57
^{147}Pm as a Source of Secondary Radiation 58
Source Requirements and Design • Spectrum and Output • Results of Experimental Applications • Limitations and Applications • Economics of ^{147}Pm Source.
^{85}Kr for Beta-Excited Radiation 62
Mixture Configuration • Transmission Configuration • Reflection Configuration. Sandwich Configuration • Specific Applications.
Other Isotopes for Radiography 67
References 70

V Safety 72
Shielding Requirements for Isotopic Power Sources 72
Isotopes Studied • Reliability of the Data • Allowable Radiation Levels and Biological Hazards • Method for Calculating Radiation Levels • Radiation Production in Decay Processes • Radiation Characteristics and Shielding Requirements.
References 80

VI Medicine 82
Iodine-132 82
Physical Properties of ^{132}I • Production of ^{132}I.
Reference 85

VII Miscellaneous Items of Interest 86

Section

I

Isotopes and Radiation Technology

Isotope Production

Isotope Separations Chemistry

The separation and purification of isotopes involve many of the traditional chemical procedures but also take advantage of numerous specialized techniques developed by the processing chemists. In the next several issues of *Isotopes and Radiation Technology*, we plan to cover some of the procedures used—both for general separations and for isolation of specific products.

Processes for purification of enriched stable isotopes lean, perhaps, toward the conventional quantitative procedures ordinarily encountered in gravimetric analysis, since macroquantities of products are involved. Of course, many modifications have been introduced through the years. The isolation and purification of radioisotopes, on the other hand, often concern trace quantities of products, and the techniques must reflect this. Again, the many modifications that have crept in through the years have provided procedures which, in many cases, are almost unique.

The methods for separating radioisotopes include such techniques as solvent extraction, ion exchange, precipitation, and distillation. The principal difference between isolating radionuclides and ordinary compounds lies in the minute quantities of the former. Table I-1 shows the weights associated with usable amounts of several isotopes. Hence the procedures must frequently be adapted to trace-quantity recovery.

Chemical separation of any two or more species is based on differences in their physicochemical properties and usually takes advantage of preferential distribution between two phases. The phases may be solid-liquid, liquid-liquid, solid-gas, or liquid-gas. The phases may comprise the substances to be separated or may be the matrixes carrying the desired materials. The efficiency of separation is represented by the distribution coefficient, or distribution factor, D_A, which is simply the ratio of the concentrations of the chemical species, A, in the two phases at equilibrium. The ratio of distribution coefficients for two species, D_A/D_B, is called the "separation factor" and is a measure of the separation efficiency. Obviously, high separation factors are desirable, and the ideal case is one in which separation can be accomplished by a single equilibration of the two phases. In other cases, several or numerous stages may be necessary. (The basic concept of a "stage" applies equally to all separation processes, whether precipitation, distillation, chromatography, or liquid-liquid extraction.)

The review in this issue is devoted to the separation of radioisotopes by ion exchange.

Table I-1 MASS-ACTIVITY RELATIONS FOR SELECTED NUCLIDES

Isotope	Half-life	Mass per millicurie, g
^{137}Cs	29.7 years	1×10^{-5}
^{60}Co	5.2 years	9×10^{-7}
^{35}S	89 days	2×10^{-8}
^{59}Fe	44 days	2×10^{-8}
^{51}Cr	28 days	1×10^{-8}
^{131}I	8 days	8×10^{-9}
^{32}P	14 days	3×10^{-9}
^{82}Br	36 hr	9×10^{-10}
^{24}Na	15 hr	1×10^{-10}

Ion-Exchange Purification of Radioisotopes at the ORNL Isotopes Development Center

By P. B. Orr

Much of the pioneer work on ion-exchange separation of adjacent elements of the same

chemical family was done at what is now Oak Ridge National Laboratory (ORNL)[1–7] and at Iowa State College,[8,9] In some cases, ion-exchange processing was found to be a superior method of chemical separation, particularly in the purification of the rare earths. Because it was the only way to separate subgram amounts of rare earths at that time and such techniques were urgently needed in many phases of chemical work on the Manhattan Project, the new technique was readily accepted and rapidly developed. One of the most notable pieces of work at that time was the ion-exchange purification and identification of element 61 by Marinsky and coworkers[10] at ORNL, and thus the filling of the last gap in the main body of the periodic table.

In the recovery and purification of radioisotopes, ion exchange is often used in conjunction with solvent-extraction or precipitation techniques. For example, an element or group of elements in a solution of an irradiated target or a solution of fission products may first be extracted with an organic solvent. The product of this group separation may then be passed through an ion-exchange column for removal of impurities, concentration of a subgroup of elements, or separation of the desired element. The final step may be precipitation. Organic ion-exchanger materials, or resins, are primarily used in this work. Some separation work has been done with inorganic exchange materials, chiefly synthetic zeolites, but they are generally used to sorb fission products from liquids for concentration and to provide a solid medium for safe shipment of the sorbed radioisotopes.

CHOICE OF ION-EXCHANGE MATERIAL

Most of the radioisotopes prepared in the Isotopes Development Center by ion exchange are separated as cations, and sulfonated styrene-divinylbenzene copolymers, e.g., the commercial products Dowex 50 and Amberlite IR-120 are used extensively. Anion-exchange resins are much more susceptible to damage by radiation, but they have been used successfully, for example, in the purification of the alpha emitters plutonium and neptunium, as well as for many gamma emitters.

The degree of cross-linkage in the ion-exchange material is important in ion-exchange separation efficiency, since the diffusion rate of ions into and out of the resin appears to be the rate-controlling factor in the process.[11] For example, with a 4% cross-linked resin, separation of the rare earths was found[12] to be significantly better than with a 12% cross-linked one. On the other hand, with 4% cross-linked resin, separation and purification of ^{140}Ba and ^{89}Sr have been found to be unsuccessful, whereas separations are routinely good with 12%.

Resin Decomposition. When organic resins are used to purify large quantities of a highly radioactive element, such as ^{144}Ce, ^{90}Sr, or even ^{147}Pm, the resin capacity is gradually decreased due to radiation damage. If glass columns are used, this loss in capacity may be observed and estimated visually, since the bands from a given amount of activity become progressively wider as the damage increases. The amount of organic matter in the product also increases greatly.

In experiments to determine the extent of resin damage by radiation, Yee[13] passed demineralized water through a column of Dowex 50 resin, which was set up in a ^{60}Co irradiator to simulate process conditions. After an exposure of 2 watt-hr per gram of dry resin, 40 to 50% of the strong acid sorption capacity was lost, roughly equivalent to 20 to 25% per watt-hour. From standard moisture content analysis (resin swelling), he found, with the same radiation exposure, a 120% increase in the number of molecules of water per sulfonate group which remained on the irradiated resin. He interprets these data as indicating a decrease in cross-linkage as a result of the irradiation.

COLUMN PREPARATION AND LOADING

Resin used in the separation and purification of radioisotopes is sized on classifying screens prior to use to ensure uniform flow throughout the bed. The smallest mesh size consistent with an adequate flow rate is used to produce as sharp a band front as possible. The sized resin is washed with 6*M* HCl until extraneous cations are completely removed and then with distilled water to remove excess acid. The resin, now in the hydrogen form, is ready for use.

When being filled with resin, the column must be exactly vertical, and the top of the bed must be kept as flat as possible. If either of these conditions is compromised, there is a tendency for the ions to form an uneven band. This uneven configuration will generally be maintained as the band passes down the column

during elution, and product purity will be decreased. A flat loading band also usually retains its shape.

The acidity of the feed for the ion-exchange column is carefully adjusted to about 0.1*M* to ensure a well-defined small band of the cations at the top of the resin. If large quantities of highly ionizing radioisotopes emitting energetic alpha and beta radiation are being processed, the solution concentration should be high to permit a short loading time. The longer a radioisotope is permitted to remain in contact with the resin with relatively no movement, the greater the danger of damage to the resin.

In commercial rare-earth separation, only a third of the column length is loaded with feed. This practice is also followed in the separation of radioisotopes, particularly in the final purification step. However, it has been found[14] that, when the first pass is made through a column, particularly when large quantities of material are to be processed, as in the purification of ^{147}Pm, the loading length may be increased to as much as half the total resin-column length to speed up the processing time. In this case the first pass through the column is not so much a purification step as it is one of concentration of the wanted radioisotope.

ELUANT CHOICE

Eluting agents used in radioisotope recovery and purification are aqueous solutions of chelating or other complexing agents. Of many such agents reported in the literature, only three—ethylenediaminetetraacetic acid (EDTA), diethylenetriaminepentaacetic acid (DTPA), and citric acid—are, or have been, used extensively by the Isotopes Development Center (Table I-2). The choice of eluant is determined by the quantity and the nature of the isotopes.

EDTA is one of the best complexing agents in ion-exchange separation; it is usually used as the sodium salt. In industry it is used to purify stable rare earths but, since its acid form is insoluble, retaining* ions that are eluted ahead of the rare-earth fraction are added to prevent precipitation of the acid, which occurs in the presence of a hydrogen-form resin. Wheelwright et al.[15] successfully used yttrium as a retaining ion in the purification of kilocurie quantities of ^{147}Pm. Copper is used in commercial rare-earth separations, but these workers found that the high radiation fields reduced the copper ions to metal on the resin, stopping the flow.

*A "retaining" ion is one that is sorbed on the resin to replace the hydrogen and is, in turn, replaced by the rare earth in the rare-earth sorption step.

Table I-2 SOME ELUANT SYSTEMS USED FOR ISOTOPE SEPARATION IN THE ORNL ISOTOPES DEVELOPMENT CENTER

Eluant	Elements
0.078*M* Na-form EDTA, *p*H 6.3	^{140}Ba, ^{140}La, and ^{89,90}Sr
0.5% DTPA, *p*H 5.5–6.5	^{147}Pm and ^{144}Ce
	Stable fission-product Nd, Pr, and Sm
0.2*M* citric acid, *p*H 2.8–2.9	^{161}Tb
	Short-lived rare earths
0.2*M* citric acid, *p*H 6.0–6.5	^{140}Ba and ^{89,90}Sr

DTPA, a higher homolog of EDTA, is the complexing agent chosen in the Isotopes Development Center for separating the long-lived and stable fission-product rare earths. Although it is only slightly soluble (0.4% at 25°C), the acid forms supersaturated solutions of good stability, and hydrogen-form resin is used in the column. The *p*H of a 0.5% solution of DTPA buffered with NH_4OH can vary from 5.5 to 7.5 with little or no effect on the separation.

When DTPA is used in separating ^{147}Pm from the other fission rare earths and actinides by ion exchange, the order of elution of ^{241}Am (which ordinarily is eluted with ^{147}Pm) is changed so that it is eluted with the europium fraction. At the same time, however, the order of elution of yttrium is also changed. With many ion-exchange systems, yttrium behaves as a heavy rare earth, being eluted between terbium and dysprosium and thus having an apparent atomic number of 65.5. With DTPA it is eluted with the promethium. This does not pose a great problem since yttrium can be largely removed in the preceding solvent-extraction step. Any yttrium remaining after ion-exchange purification may be completely removed by solvent extraction or ion exchange with a system in which the order of elution corresponds to the apparent atomic number of 65.5. Table I-3 gives the orders of elution of the rare earths and ^{241}Am with citric acid and DTPA as eluants.

Citric acid, one of the first chelating agents to be used in separation by ion exchange, has been almost completely replaced by the organic amines, which have proved superior in large-scale separations. However, 0.2*M* citric acid is still used for separation of microgram

Table I-3 ORDERS OF ELUTION OF THE RARE EARTHS AND ^{241}Am

Citric acid as eluant	DTPA as eluant
1. Lu	1. Dy
2. Yb	2. Ho
3. Tm	3. Er
4. Er	4. Tm
5. Ho	5. Yb
6. Dy	6. Lu
7. Y	7. Tb
8. Tb	8. Eu-Am
9. Gd	9. Gd
10. Eu	10. Sm
11. Sm	11. Y-Pm
12. Pm-Am	12. Nd
13. Nd	13. Pr
14. Pr	14. Ce
15. Ce	15. La
16. La	

quantities of short-lived fission rare earths and alkaline earths.

Eluant Decomposition. The eluants are used as aqueous solutions, and radiation decomposition of the water may present major problems. The nature of this decomposition has been reported by Hochanadel[16] as two reactions, which yield primary products and free radicals:

$$2H_2O \rightsquigarrow H_2 + H_2O_2$$

$$H_2O \rightsquigarrow H + OH$$

Later work indicates that what was originally thought to be a free radical, H, was probably really an electron.[17]

If curie amounts of energetic radioisotopes are permitted to remain on a column without flow for half an hour or more, the released gas may cause the column to become locked with gas bubbles. To minimize this gassing problem, the resin particle size is controlled to one that permits a flow rate of two to three column volumes per hour. The column is loaded at maximum flow and is promptly washed with one column volume of distilled water to remove the excess acid. Elution is started immediately so that any gas formed in the loaded portion will be kept in solution and removed from the column. When heated columns are used, heat is applied to the column jacket after one column volume of eluant, which has been boiled to remove dissolved air, has been put through. The increased temperature decreases the viscosity of the eluant and increases the rates of diffusion and reaction, permitting faster flow and better removal of the dissolved gases.

Decomposition of the organic eluant may also occur. In work[17] done to determine the relative radiation stability of DTPA and EDTA in a ^{60}Co irradiator, 0.5% solutions were exposed to 5×10^6 r, and the solutions were examined for *p*H change and discoloration. The *p*H of the EDTA solution rose from 7.34 to 8.36, changing from a water-white to a pale-green color, while that of DTPA changed from 5.47 to 7.55. The color of the DTPA after irradiation was darker green than that of the EDTA. Both had an unpleasant odor after exposure, indicating amine degradation.

Blanco, Higgins, and Kibbey[18] reported experiments in which the EDTA was destroyed at an initial rate of 0.6 millimole per watt-hour of energy absorbed per gram of solution, the rate decreasing with time. They used 0.065*M* solutions of EDTA containing 0.33*M* to 0.48*M* sodium, 0.16*M* to 0.31*M* nitrate, 0.018*M* diethanolglycine, 0.03*M* lead, and traces of barium, strontium, and cerium and irradiated with 5400- and 14,000-r/min ^{60}Co sources. Damage, which became objectionable above 0.04 watt-hr/g, was characterized by an increase in the solution *p*H, the presence of nitrate ions, a color change from water-white to yellow, and precipitation of barium, strontium, cerium, and lead. In applying these findings to the purification of kilocurie amounts of ^{140}Ba, it was necessary to adjust the *p*H of the EDTA solution to compensate for the change that took place while the solution was in contact with the high-energy ^{140}Ba-^{140}La gamma radiation on the column and to maintain the highest flow rate consistent with good separation.

With 0.2*M* citric acid buffered to a *p*H of 3.0 as the eluant in the separation of 20,000 curies of ^{147}Pm, Pressly et al. found that eluant decomposition was not a problem.[19] However, three passes through the column were necessary to produce a product of about 65% purity, and close *p*H control was essential. It was necessary to make the citric acid eluant 1% in phenol in the makeup vessel prior to elution to protect it from a mold growth, which, upon long standing, can be sufficient to reduce or even stop the flow through a column. Even with phenol, mold growth was inhibited only 2 or 3 days. This citric acid system for ^{147}Pm separation was largely replaced in 1961 by the

DTPA system, which gives better separation factors.

ELUANT FLOW RATE

The eluant flow rate depends on the resin size, column size, temperature, loading length, and, to some extent, the eluant used. A rule of thumb for an unheated column is one column volume per hour; for a column heated to 80°C, it is about two volumes per hour. At the higher temperature the exchange rate and, to some extent, the diffusion rate are speeded up.

When trace quantities of radioisotopes are being eluted, the fractions may be as small as 25 to 100 ml, for example, in columns 15 mm in inside diameter by 18 in. in height. It is convenient to pass the column discharge line through an ion-chamber–electrometer arrangement so that each activity peak may be observed as it is eluted.

PROCESSING EQUIPMENT

Practically all equipment used at ORNL for ion-exchange work is custom glassware. Column sizes vary from 10 mm in diameter by 4 in. in height, used in concentration of trace quantities of many radioisotopes, to 3 in. in diameter by 8 ft in length, used, for example, to separate ^{147}Pm from the other fission-product rare earths. It is usually considered good practice to use a column small enough in diameter for good banding and long enough that no more than a third of the length is required for starting the band. Many of the columns are jacketed for uniform hot-water heating of the column. They have a porous sintered-glass filter disk at the bottom to support the resin and to permit as uniform a flow of process liquid as possible. The sintered disk causes loss of flow along the wall of the column at the point of fusion of the disk to the column, resulting in some channeling of the ions to the center of the disk as they reach the bottom of the bed. In an effort to overcome this difficulty, experimental columns have been successfully made with fine platinum mesh as the resin retainer.

Columns with a constant taper from the top to the bottom have been successfully used to lengthen the bands as they come off the resin. The same result has been obtained by eluting through more than one column in series, the last one having a smaller diameter than the first.

In a heated column, gassing will occur even with nonradioactive elements if the dissolved air in the eluant is not removed prior to elution. To prevent this difficulty, provision is made to heat and degas the eluant in a section of the tube between the feed tank and the column.

Sampling equipment is very simple. Eluate fractions are collected in bottles from which samples may be taken with medicine droppers by means of remote-control manipulators. Sample bottles are removed in small lead shields, through shielded removal locks, to the outside of the cell. Finished products are removed similarly and transferred to other sections of the Isotopes Development Center for analysis, packaging, and shipping.

ORNL Target Fabrication Center

The Target Fabrication Center at ORNL was established in 1961 and described in a report[20] prepared for EANDC* in 1963. The activities carried out include:

1. Preparation of isotopes of high chemical and isotopic purity to meet requirements
2. Preparation of chemical forms suitable for target fabrication
3. Fabrication of targets to meet exacting physical specifications
4. Measurement of the chemical and physical characteristics of the finished target
5. Packaging to ensure shipment without damage
6. Recovery of enriched material not actually shipped as target
7. Development of procedures to minimize target cost
8. Publishing of new developments in the fabrication of targets

Among the target facilities, some of which are shown in Fig. I-1, are a 5-in. Fenn rolling mill, several resistance-heat vacuum evaporators, an electron-bombardment vacuum-evaporation furnace, an induction heater, an electroplating apparatus, a 20 × to 2000 × metallographic microscope, a 30-ton press, and a refrigerated vacuum glove box. Data relevant to the types of targets which can be fabricated are shown in Table I-4.

*European-American Nuclear Data Committee, Organization for Economic Cooperation and Development.

Table I-4 TARGET FABRICATION DATA

Element	Thickness	Method of preparation*	Backing†
Hydrogen	Zr, Y, or Ti: 100 to 5000 $\mu g/cm^2$	f (Zr, Y, and Ti on 10-mil Pt followed by ^2H sorption)	2
Deuterated polyethylene	>0.2 mil	f	1
Lithium	1 mg/cm^2 to any cast size	b, d	1
LiH	200 to 500 $\mu g/cm^2$	a	3
Beryllium	25 to 500 $\mu g/cm^2$	a	3
Boron	20 to 500 $\mu g/cm^2$	a	1, 2
	500 to 1000 $\mu g/cm^2$	a	2
Carbon	10 to 100 $\mu g/cm^2$	a normal	1 normal
		f isotopic	2 isotopic
Fluorine (as fluoride)	25 to 500 $\mu g/cm^2$	a	2
Sodium	7.5 mg/cm^2 to any cast size	b, d	1
Magnesium	5 to 8000 $\mu g/cm^2$	a	3
Aluminum	5 to 12,000 $\mu g/cm^2$	a	2
	250 $\mu g/cm^2$ up	b	1
Silicon	30 to 100 $\mu g/cm^2$	a	1
	10 to 100 $\mu g/cm^2$	a	2
Sulfur	5 mg/cm^2 up	d	1
Chlorine (as chloride)	5 mg/cm^2 up	a	2
		d	1
Potassium	7.5 mg/cm^2 to any cast size	b, d	1
Calcium	1 mg/cm^2 up	b	1
Scandium	1 mg/cm^2 up	b	1
Titanium	1 mg/cm^2 up	b	1
Vanadium	1 mg/cm^2 up	b	1
Chromium	10 to 5000 $\mu g/cm^2$	c	2
Iron, cobalt, and nickel	1 mg/cm^2 up	b	1
	800 mg/cm^2 up	d	1
	10 to 1000 $\mu g/cm^2$	c	2
Copper	1 mg/cm^2 up	b	1
	10 to 1000 $\mu g/cm^2$	c	2
Zinc	1 mg/cm^2 up	b	1
	10 to 1000 $\mu g/cm^2$	c	2
Germanium	10 to 200 $\mu g/cm^2$	a	2
Arsenic	10 to 200 $\mu g/cm^2$	a	2
Selenium	300 to 5000 $\mu g/cm^2$	a	1
	10 to 5000 $\mu g/cm^2$	a	2
Bromine (as bromide)	5 mg/cm^2 up	a	2
		d	1
Rubidium (salt)	10 to 1000 $\mu g/cm^2$	a	2
	40 mils up	d	1
Yttrium	10 to 5000 $\mu g/cm^2$	a	2
Zirconium	1 mg/cm^2 up	b	1
	10 to 5000 $\mu g/cm^2$	a	2
Niobium	2 mg/cm^2 up	b	1
Molybdenum	10 to 1000 $\mu g/cm^2$	a	2
Technetium	10 to 1000 $\mu g/cm^2$	a	2
Palladium	1 mg/cm^2 up	b	1
Silver	1 mg/cm^2 up	b	1
	100 to 5000 $\mu g/cm^2$	a	1
	10 to 1000 $\mu g/cm^2$	a	2
	40 mils up	d	1
Cadmium	1 mg/cm^2 up	b	1
Indium	5 mg/cm^2 up	b	1
Tin	3 mg/cm^2 up	b	1
	10 to 1000 $\mu g/cm^2$	a	2
	0.5 to 3 mg/cm^2	a	1
Antimony	10 to 1000 $\mu g/cm^2$	a	2
Tellurium	10 to 1000 $\mu g/cm^2$	a	2, 3
Cesium (salt)	10 to 1000 $\mu g/cm^2$	a	2
Barium (salt)	10 to 1000 $\mu g/cm^2$	a	2
Lanthanum (metal) and rare-earth oxides	10 to 1000 $\mu g/cm^2$	a	2
Hafnium	Undetermined	b	1
Tantalum	2 mg/cm^2 up	b	1
	10 to 1000 $\mu g/cm^2$	a	2
Tungsten	In Cu matrix: >2 mg/cm^2	b, d	2
Rhenium	Undetermined	a	2
Iridium	Undetermined	a	2
Platinum	3 mg/cm^2 up	b	1
Mercury	1 to 4 mg/cm^2	c	2 on Au
Thallium	8 mg/cm^2 up	b	1
Lead	8 mg/cm^2 up	b	1
	1 to 8 mg/cm^2	a	1
	10 to 1000 $\mu g/cm^2$	a	2
Bismuth	Undetermined	a	2

*Processes used to fabricate the targets are noted according to the following letter codes:

a. Evaporation
b. Rolling
c. Electrolytic deposition
d. Pressing or casting
e. Vapor plating
f. Miscellaneous

†The various substrates or backing materials used for target fabrication are noted according to the following number codes:

1. Self-supporting
2. Metal backing (specified by customer)
3. Thin carbon: 20 to 100 $\mu g/cm^2$

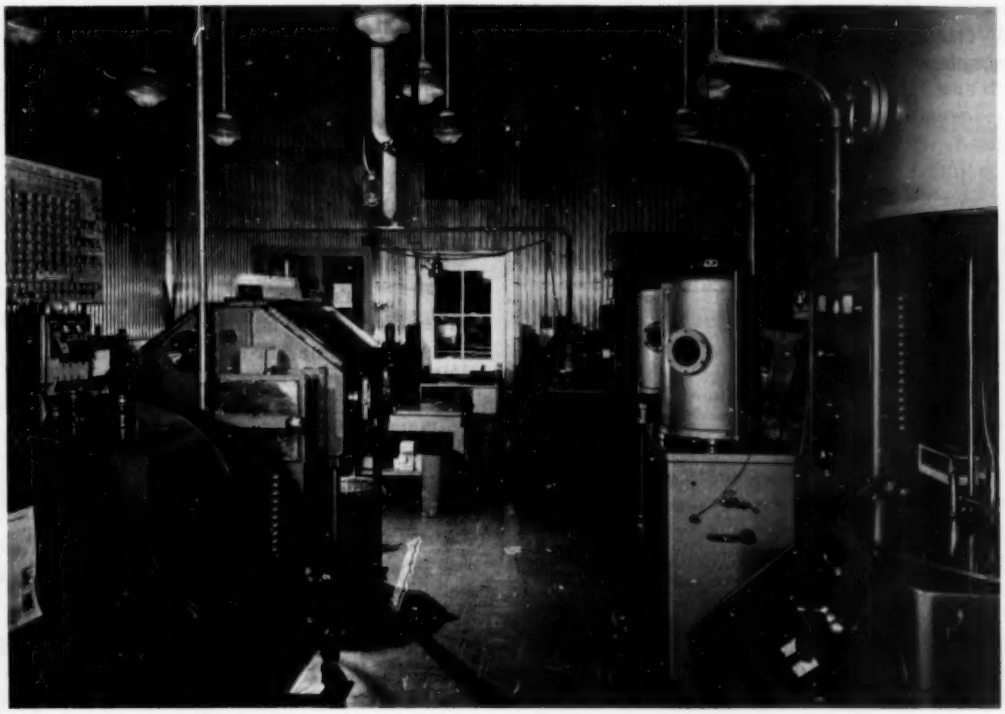

Fig. I-1 Some target fabrication facilities at ORNL.

Major emphasis of the Center is on development and improvement of target fabrication techniques. This often involves chemical and metallurgical procedures to prepare suitable materials for the fabrication work.

Isotopic Magnesium Targets

Elemental enriched magnesium isotopes have been available from ORNL for a number of years;[21] however, in some instances there has been difficulty in obtaining sufficient purity for certain uses (e.g., in preparation of ^{28}Mg from enriched ^{26}Mg at BNL).[22,23] A distillation procedure has been developed by Box[24] which produces >99% pure magnesium by thermochemical reduction of MgO with aluminum powder at 1250°C and 10^{-6} torr and simultaneous distillation of the resulting magnesium. When 2-g batches are used, yields of ~95% can be expected in about 3 hr. Table I-5 lists typical amounts of impurities as shown by spectrophotometric analysis. The apparatus as shown in Fig. I-2 is suitable for quantities up to 5 g. The resulting magnesium can be fabricated into foils by hot rolling procedures or evaporated again onto suitable backings.

Relatively thick adherent magnesium or scandium targets (up to 0.005 in.) can be deposited[25] by successively evaporating thin (5 mg/cm^2) layers of magnesium on a water-cooled copper backing and wiping the thin layers between evaporations to remove any powdery layers of material. Adherence is assured by pretreatment of the copper, including thorough de-

Table I-5 SPECTROPHOTOMETRIC ANALYSIS OF VACUUM-DISTILLED MAGNESIUM

Element	Amount present, wt.%	
	1250°C	1350°C
Al	0.30	2.69
Be	<0.001	Not found
Ca	<0.0001	<0.001
Cr	Not found	Not found
Cu	<0.01	<0.001
Fe	<0.01	<0.001
Mn	<0.01	<0.1
Nb	Not found	Not found
Si	<0.01	<0.01

greasing, cleaning with dilute hydrochloric acid, and etching by glow discharge in an argon atmosphere.

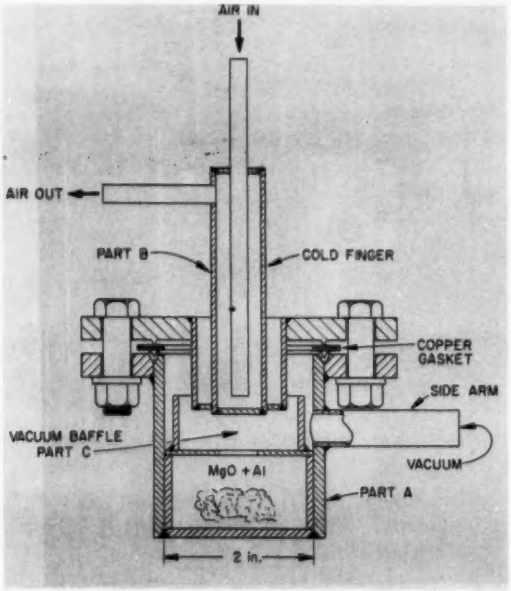

Fig. I-2 Apparatus for reducing and evaporating magnesium.

Technetium-99 Targets

A recent report by Box[26] describes a method for the efficient electroplating of ^{99}Tc from dilute pertechnetate solutions. Film thicknesses up to 18 mg/cm^2 on copper, gold, silver, and platinum can be obtained by electroplating from acid oxalate solutions of ammonium pertechnetate solutions at a current density of approximately 1.3 amp/cm^2.

Oxides of technetium have been plated previously in a number of instances,[27–31] and there are several reports of the deposition of technetium metal.[32] However, yields of metal from the sulfuric acid–fluoride solutions ordinarily used have varied from 25 to 75%, and other difficulties have been encountered.

A possible use of electroplated ^{99}Tc foils is in the preparation of beta sources for medical use,[33] for example, to effect coagulation of blood incident to eye surgery, thereby minimizing formation of scar tissue. Other possible uses are as beta calibration sources, static eliminators, and low-energy bremsstrahlung radiography sources.

Production of ^{28}Mg: State of the Art*

By Allen J. Weiss and Manny Hillman†

Magnesium-28 has been produced by several methods over the past 10 years by the following reactions:

1. By spallation of sodium chloride,[34–36] silicon,[37–39] potassium sulfate,[37,38] and copper[40–42] targets with protons.
2. By gamma irradiation of silicon: $^{30}Si(\gamma,2p)^{28}Mg$ (Ref. 43).
3. By alpha irradiation of magnesium and aluminum: $^{26}Mg(\alpha,2p)^{28}Mg$ (Refs. 39 and 43 to 45) and $^{27}Al(\alpha,3p)^{28}Mg$ (Ref. 46).
4. By triton irradiation of magnesium: $^{26}Mg(t,p)^{28}Mg$ (Refs. 36 and 47 to 49).
5. By fast-neutron irradiation of silicon: $^{29}Si(n,2p)^{28}Mg$ and $^{30}Si(n,^3He)^{28}Mg$ (Refs. 50 and 51).

Sheline and Johnson[43,44] made ^{28}Mg by the $^{30}Si(\gamma,2p)^{28}Mg$ and $^{26}Mg(\alpha,2p)^{28}Mg$ reactions to characterize and determine a decay scheme for the new nuclide. Lindner[34] separated a magnesium fraction from the spallation products of the irradiation of chlorine, as sodium chloride, with 340-Mev protons. The 21-hr activity present was deduced to be ^{28}Mg from the 2.3-min half-life of the ^{28}Al milked from it. Marquez,[37] Wapstra and Veenindaal,[45] and Olsen and O'Kelley[35] prepared ^{28}Mg to study its beta spectrum. None of the above-listed references indicate the ^{28}Mg yields.

Lindner[52] prepared carrier-free ^{28}Mg by spallation of sodium chloride with 340-Mev protons to determine the beta and gamma spectrums. Results were similar to those reported by Sheline and Johnson[44] and by Marquez.[37] The half-life of ^{28}Mg was found to be 21.2 ± 0.2 hr, which agrees with Sheline and Johnson's value[39,43] of 21.3 ± 0.2 hr and Wapstra and Veenindaal's value[45] of 21.4 ± 0.6 hr but differs measurably from the value 22.1 ± 0.3 hr reported by Jones and Kohman.[38] The cross-section for the reaction $^{37}Cl(p,2\alpha 2p)^{28}Mg$ with 340-Mev protons on sodium chloride was calculated to be ~0.003 barn. Olsen and O'Kelley[35] used Lindner's carrier-free ^{28}Mg to measure the beta-ray de-

*USAEC Report BNL-6607, Brookhaven National Laboratory, no date; received Jan. 21, 1963.

†Brookhaven National Laboratory.

cay. Weiss and Hillman[53] recently remeasured the ^{28}Mg half-life, using a specially prepared "ultrapure" sample. The average of 20 determinations was 20.88 ± 0.06 hr.

Jones and Kohman[38] report having made ^{28}Mg in the synchrocyclotron with 350-Mev protons and the reaction ^{30}Si(p,3p)^{28}Mg prior to learning of the work of Sheline and Johnson. In each of two 1-hr irradiations of 2 g of silicic acid, the ^{28}Mg yield was 8×10^5 dis/min. The circulating current was estimated to be 0.2 μa. From comparative yields they estimated the cross-section to be 10^{-4} barn.

Friedlander et al.[40] separated ^{28}Mg as a spallation product from copper targets that were irradiated with 2.2-Gev protons. The formation cross-section at this energy is 0.41 mb ± 20%. Rudstam et al.[41] report spallation cross-sections of 0.25 mb with 24-Gev protons and 0.65 mb with 5.7-Gev protons. The cross-sections for spallation produced above 1 Gev hardly vary with energy. Crespo[42] reports a cross-section of 0.049 mb for spallations of copper with 700-Mev protons. He also gives cross-sections for targets of silver, gold, and uranium bombarded with alpha particles of 320, 500, 700, and 880 Mev energy.

Hudis[46] made microcurie amounts of carrier-free ^{28}Mg by irradiating ^{27}Al with 41-Mev alpha particles by the reaction ^{27}Al(α,3p)^{28}Mg. Stacked-foil experiments showed that the practical threshold that gave sufficient activity to definitely identify ^{28}Mg is 35 ± 1 Mev, and the cross-section for the reaction with 41-Mev alpha particles is ~0.0002 barn. The ^{28}Mg yield in an alpha bombardment of 100 μa-hr of a 1-mil aluminum target is 1.5×10^7 dis/min.

The specific activity of the ^{28}Mg prepared from aluminum targets depends on the amount of magnesium impurity in the target. A simple chemical procedure,[54] based on the formation of a radiocolloid of carrier-free magnesium in alkaline solution and its retention on a fine-glass frit, yields ^{28}Mg free from Al^{3+} and ^{24}Na. In this procedure the aluminum target is dissolved in concentrated sodium hydroxide, the solution is filtered through a fine-glass frit, the frit is washed with sodium hydroxide solution and then with water, and the magnesium hydroxide on the frit is dissolved in dilute acid.

Iwerson, Koski, and Rasetti[47] used the ^{26}Mg(t,p)^{28}Mg reaction to prepare ^{28}Mg. A significant difference between this method and previous ones is the use of reactor rather than accelerator irradiation. Reactor irradiation of lithium-magnesium alloy first produced tritons, ^{6}Li(n,α)T, and ^{28}Mg was formed by the reaction ^{26}Mg(t,p)^{28}Mg. The irradiation product was dissolved in acid, to which carriers of suspected impurities were added. Several sulfide precipitations, followed by precipitation of magnesium hydroxide, purified the ^{28}Mg. The half-life was reported to be 21.8 ± 0.3 hr.

In 1956, ^{28}Mg was made routinely available by the Hot Laboratory Division of Brookhaven National Laboratory (BNL).[48] A lithium-magnesium alloy, 70 wt.% lithium, irradiated in the research reactor at a thermal-neutron flux of 3.5×10^{12} neutrons/(cm^2)(sec) for 4 days produces ^{28}Mg with a specific activity of 100 μc per gram of magnesium. Substitution of ^{6}Li for natural lithium made possible specific activities of >1000 μc/g, and substitution of ^{26}Mg for natural magnesium further increased the specific activity.

Currently at BNL, irradiation of a 10-mil foil of ^{6}Li-^{26}Mg alloy (75 wt.% ^{6}Li) for 3 days in a thermal-neutron flux of 2×10^{13} neutrons/(cm^2)(sec) produces ^{28}Mg with a specific activity of 40,000 μc per gram of magnesium.[55]

Mellish and Crockford[36] described two methods of producing ^{28}Mg at Harwell: the (t,p) reaction on magnesium in a lithium-magnesium alloy and cyclotron spallation of chlorine by proton bombardment. The yield in the first method was determined to be a function of the percentage of lithium in the alloy in the range 2 to 25% lithium. The specific activity increased with increasing percentage of lithium up to 45 μc per gram of magnesium saturation equilibrium activity in a flux of 1.5×10^{12} neutrons/(cm^2)(sec). The second method uses the reactions ^{35}Cl(p,6p2n)^{28}Mg and ^{37}Cl(p,6n4p)^{28}Mg. The cross-section for producing ^{28}Mg was studied as a function of proton energy up to 160 Mev and found to be still sharply increasing with energy. The yield of ^{28}Mg-^{28}Al equilibrium mixture for 160-Mev protons was studied as a function of target thickness. The yield in a typical irradiation of 15 to 20 g of potassium chloride at 1 μa was ~40 μc/hr.

Rodriguez Pasques[50] made ^{28}Mg by irradiating silicon as silicic acid with neutrons of energies >20 Mev, obtained by bombarding beryllium with 28-Mev deuterons. The nuclear reactions are ^{29}Si(n,2p)^{28}Mg, $Q = -13.3$ Mev, and ^{30}Si(n,^{3}He)^{28}Mg, $Q = -16.3$ Mev. The amount of ^{28}Mg produced at the end of the irradiation calculated on the basis of 90% chemical yield,

saturation irradiation, and 100% isotopic abundance for 2 to 3 g of silicic acid is 2.93×10^5 counts/min by the $(n,2p)$ reaction and 4.45×10^5 counts/min by the $(n,^3He)$ reaction.

Since neither the beam current nor the neutron flux was indicated, the meaningfulness of the ^{28}Mg yield is indeterminate. The work was repeated by Weiss.[51] Five grams of quartz was irradiated with fast neutrons from the $^7Li(d,2n)^7Be$ and $^6Li(d,n)^7Be$ reactions for ~1 hr with a total beam of 55 μa-hr of 20-Mev deuterons. The yield at the end of the bombardment was 0.3 μc of ^{28}Mg.

Hinds, Marchant, and Middleton[49] prepared ^{28}Mg targets with tritons up to 6.8 Mev energy by the $^{26}Mg(t,p)^{28}Mg$ reaction in order to measure the ^{28}Mg energy levels. The Q value for the reaction was calculated to be 6.466 Mev, which agrees well with the mass Q value of 6.460 Mev.

Although ^{28}Mg now available from BNL is used by many institutions for medical research, it is desirable to use carrier-free ^{28}Mg for many applications. For example, magnesium is found in very low concentrations in some living tissue. For some physiological studies, then, a very high specific activity is required in order not to upset the magnesium balance in the system by administering large amounts of stable magnesium. Carrier-free ^{28}Mg has been produced with an accelerator. However, the amount that can be produced in an accelerator is limited because of the target size and the prohibitive cost for long irradiations. On the other hand, it may be possible to increase the specific activity of ^{28}Mg produced in a reactor by the (t,p) reaction by utilizing the recoil phenomenon of the reaction.

There are many possible systems for utilizing this phenomenon. One, the Szilard-Chalmers reaction, involves incorporating the target nuclide in a compound. The recoil of the product nuclide breaks the bonds of the compound. Chemical separation may be possible. In another system the target nuclide is placed in one matrix, and recoil causes the product nuclide to move to a second matrix. The matrixes may be separated chemically or physically. Investigation of these systems as applied to ^{28}Mg production is under way at BNL. No success has been obtained with the first system because of rapid exchange of the products in some cases and excessive radiation damage of the magnesium compound (principally the thenoyltrifluoroacetonate) in others. The second system has been unsuccessful with a dispersion of lithium-magnesium alloy in an organic medium because of radiation damage. However, preliminary results indicate the possibility of success when the recoils from a very thin magnesium target are caught in a matrix separated from the magnesium.

Production Procedures Manuals for Isotopes

Four reports[56–59] that summarize current procedures in radioisotope production and chemical separation were released simultaneously June 11–12, 1964, at an information meeting at AEC's Germantown, Md., headquarters. The purpose of the meeting was to provide industry with the technology of AEC production methods for radioisotopes for general distribution. More than 100 persons attended, among whom were U. S. industrial producers and processors of radioisotopes, Atomic Industrial Forum members, foreign representatives of firms having radioisotopes programs, and reporters.

AEC laboratories issued reports in two forms—a "cookbook" variety from Oak Ridge and Brookhaven National Laboratories and descriptive ones from Mound Laboratory and the Savannah River Plant. The manuals are summarized in the following paragraphs, and further details on papers given at the meeting are reported in Sec. VII of this review.

Mound and Savannah

Allen[58] of Savannah and Lonadier and Huddleston[59] of Mound described the isotopes, ^{60}Co and ^{210}Po, respectively, with which their laboratories are concerned. Mound has had the responsibility for polonium chemistry, separation technology, and separation since 1943; weighable quantities were produced as early as 1946. The isotope is now made by the reaction

$$^{209}Bi + {}^1_0n \longrightarrow {}^{210}Bi \xrightarrow[5.4\ days]{\beta} {}^{210}Po$$

The laboratory determines that the bismuth target is at least 99.5% pure, and 1.3433- by 6.000-in. slugs are shipped directly from a manufacturer to Hanford Laboratories for jacketing and irradiation. Ten to 20 curies of polonium per pound of bismuth is produced. Mound dissolves

the target jacket in HCl and the bismuth in HCl and HNO_3. A series of concentration steps increases the polonium in the bismuth from about 5 to 14,800 ppm. Polonium is reduced with stannous chloride and hydrazine hydrochloride solutions, further processed, and assayed. In a final step, ^{210}Po is electrodeposited onto platinum gauzes, up to 50 curies of ^{210}Po per gauze. Figure I-3 shows the three main steps in ^{210}Po processing. A decay scheme, physical properties of the isotope, typical bismuth-target and polonium-product analyses, and sales from 1955–1963 are given in the report.

Since 1955 the Savannah River Plant has produced close to 4 million curies of ^{60}Co by irradiating ^{59}Co in production reactors. Past, present, and expected cobalt irradiations are summarized in Table I-6. The largest single irradiation was 1.3 million curies for the Food Process Development Irradiator at Natick, Mass. Slugs are specially designed for each cobalt irradiation, and several designs are illustrated in the manual. Figure I-4 shows production yields for cobalt at several values of neutron flux. Cobalt production at Savannah River is usually incidental to the production of other materials; hence the standard tolerance on an irradiation is ±20% of the activity requested, in addition to a ±5% variation from piece to piece. Plant capacity and costs also are discussed in the manual, and it is pointed out that Savannah River reactors are capable of producing large quantities of inexpensive, high-activity ^{60}Co. Less-than-100,000-curie amounts normally have to be obtained elsewhere.

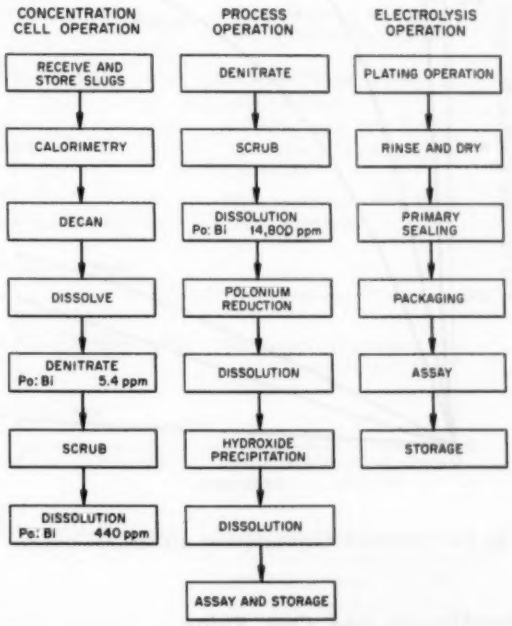

Fig. I-3 Polonium-210 procedures at Mound Laboratory.

Table I-6 COBALT IRRADIATIONS AT SAVANNAH RIVER PLANT

Date	Activity: Total, curies	Activity: Specific, curies/g	Shape	Purpose
1955–1963	975,700	27–83	Wafers	ORNL, therapeutic; Japanese, experimental
1958–1964	1,256,900	15–100	Slabs	BNL; MPDI; SRL; Curtiss-Wright
1959–1960	150,000	99–120	Pellets	ORNL, radiography
1961–1962	1,448,000	6–17	Rods	FPDI; USBM
	3,830,600			
In process	240,000	400–500	Pellets	DID—develop uses for high-specific-activity cobalt
	75,000	400–500	Wafers	
	150,000	300	Slabs	
	465,000			
	52,000	150–300	Pellets	Flux control for transuranium irradiation
	125,000	275–400	Wafers	
	113,000	175–275	Slabs	
	290,000			
Expected (within fiscal year)	20,000	15–20	Rods	USBM
	700,000	150	Slabs	BNL
	175,000	30	Wafers	ORNL; Japanese
	895,000			

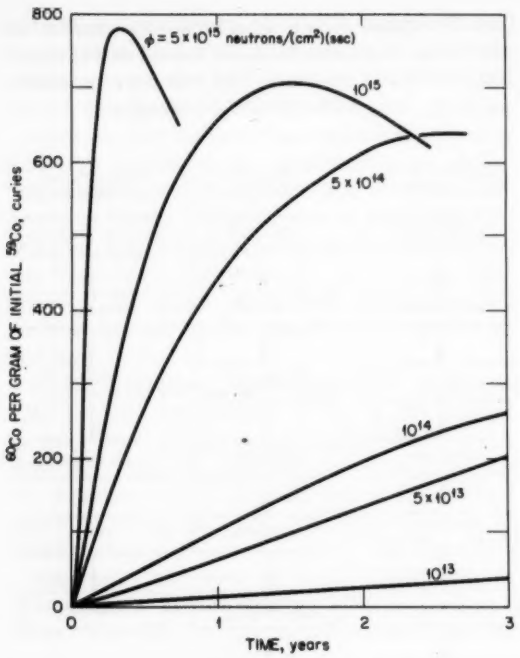

Fig. I-4 Cobalt-60 production at six neutron fluxes.

Brookhaven and Oak Ridge

The manuals from BNL and ORNL have a common purpose: the collection and presentation of the detailed procedures for routinely producing the more than 100 isotopes that require chemical processing after irradiation. Bibliographies totaling about 100 references to work by ORNL and BNL people are given. Two-thirds of these are open-literature citations. Economic data are not included in either report; but separate notebooks and talks by AEC, BNL, and ORNL representatives covered this subject (see Sec. VII).

The method of presenting information on activities at the two laboratories differs mostly in details. The preliminary BNL report gives a historical-procedural introduction, discusses instruments and handling of isotopes, and then describes production, processing, and preparation of each isotope product. The ORNL report contains (1) a chapter on target selection, preparation, reactor irradiation, and chemical processing principles; (2) the detailed processing procedures for each radioisotope; (3) information on storage, shipping, and handling; and (4) appendixes covering descriptions of the Oak Ridge Research Reactor (ORR) and the chemical processing facilities, tabulated reactor production data for each radioisotope product, and analytical techniques. More than 80 reactor-produced radioisotopes are discussed in the ORNL report, and 17 reactor-, cyclotron-, and Cockcroft-Walton-produced isotopes are described in the BNL manual. Most of the ORNL isotopes are produced by (n,γ) reactions in a target composed of the same element as the product in a neutron flux of $\sim 2 \times 10^{14}$ neutrons/$(cm^2)(sec)$. Some of the BNL data are given in Table I-7 as an illustration of the diversity of existing methods of production. Figure I-5 shows the flow of radioisotopes operations at ORNL and some of the end uses of the products. A summary of fission-product flow was given in an earlier issue of this review.[60]

The separation and purification of radioisotopes require many standard unit processes, among them solvent extraction, ion exchange, gas chromatography, and precipitation. The detailed steps of both the BNL and ORNL reports stem from the application of these processes to radiochemical separation. Figure I-6 is a page taken from ORNL-3633 showing the detailed procedures for processing ^{90}Y by solvent extraction. In addition to such postirradiation processing steps, procedures are given in the BNL report on target preparation and postirradiation handling. Preceding the processing procedures in each manual are descriptions of targets used, yields, and isotope characteristics (e.g., Fig. I-7). Preparation, loading, and milking of generators also are described in the BNL report.

As mentioned earlier, both manuals briefly describe the respective laboratories, including hot cells, equipment, and general procedures. The ORNL manual, in addition, briefly discusses radiation areas, monitoring, and waste disposal.

Radioisotope product solutions are analyzed to determine whether they conform to certain specifications. The processing procedure for each radioisotope in ORNL-3633 is referenced to the appropriate analytical procedures in another ORNL manual,[61] and assay methods also are described.

Calculations of the specific activities of radioisotopes produced by neutron capture are given in another appendix of ORNL-3633. Burnup of target atoms and of the product radioisotope are taken into consideration in these calculations, which were made with the help of CDC 1604-A and IBM 7090 computers. Specific ac-

Table I-7 SELECTED DATA ON ISOTOPES PRODUCED AT BNL

Isotope	Method of production	Half-life	Shipping form	Comments
^{28}Al	^{28}Mg parent	^{28}Al, 2.24 min ^{28}Mg, 20.9 hr	Generator ("cow") $Na^{28}AlO_2$ in 1*M* NaOH	~30% yield; see ^{28}Mg below
^{38}Ar	$^{37}Cl(n,\gamma)^{38}Cl$ $^{38}Cl \xrightarrow[37.3\ min]{\beta^-} {}^{38}Ar$	(Stable)	Gas in ampule	NaCl crystals for 56 days at 10^{13} neutrons/(cm^2)(sec)
^{67}Cu	$^{64}Ni(\alpha,p)^{67}Cu$	61.6 hr	$^{67}Cu(NO_3)_2$ in 6*M* HNO_3	Enriched ^{64}Ni in ~40-Mev cyclotron beam
^{18}F	$^{6}Li(n,t)^{4}He$ $^{16}O(t,n)^{18}F$	110 min	$Na^{18}F$ plus trace of $NaAlO_2$ in 0.1*M* NaOH	Mev radiations: 0.65 (100%) positron; 0.51 annihilation gammas
^{68}Ga	$^{69}Ga(p,2n)^{68}Ge$ ^{68}Ge parent	^{68}Ga, 68 min ^{68}Ge, 275 days	^{68}Ga-EDTA, $^{68}GaCl_3$ in ether, or $^{68}Ga_2(SO_4)_3$ "weightless" solid	ORNL cyclotron; ~70% yield from generator
^{124}I	$^{121}Sb(\alpha,n)^{124}I$	4.2 days	$H^{124}I$ in $NaHSO_3$ or Na_2SO_3	
^{132}I	^{132}Te parent	^{132}I, 2.3 hr ^{132}Te, 77 hr	Generator $Na^{132}I$ in 0.01*M* NH_4OH	~70% yield; see ^{132}Te below
^{133}I	Fission of ^{235}U	^{133}I, 21 hr ^{133}Xe, 5.3 days	$Na^{133}I + Na^{133}IO_3$ in dilute NaOH	Unenriched U_3O_8 target; ^{131}I and ^{135}I also present in product
^{28}Mg	$^{6}Li(n,t)^{4}He$ $^{26}Mg(t,p)^{28}Mg$	^{28}Mg, 20.9 hr ^{28}Al, 2.3 min	$^{28}MgCl_2$ in dilute HCl	
^{99}Mo	Fission of ^{235}U	^{99}Mo, 67 hr ^{99m}Tc, 6 hr	$(NH_4)_2\ ^{99}MoO_4$ in 1*M* NH_4OH	Target is alloy of Al with enriched, 93.15%, ^{235}U
^{43}K	$^{40}Ar(\alpha,p)^{43}K$	22 hr	As required	
^{48}Sc	$^{51}V(n,\alpha)^{48}Sc$	44 hr	$^{48}ScCl_3$ as "weightless" solid	Cockcroft-Walton generator; ~5×10^8 neutrons/(cm^2)(sec); neutron source, $^{3}H(d,n)^{4}He$
^{87m}Sr	$^{85}Rb(\alpha,2n)^{87}Y$ ^{87}Y parent	^{87m}Sr, 2.8 hr ^{87}Y, 80 hr	Generator $^{87m}Sr_3(C_6H_5O_7)_2$ in 0.005% citric acid	Radiochemical purity >99.9% at time of milking
^{99m}Tc	^{99}Mo parent	^{99m}Tc, 6 hr ^{99}Mo, 67 hr	Generator $^{99m}TcO_4^-$ in 0.1*M* HCl	See ^{99}Mo above
^{132}Te	Fission of ^{235}U	^{132}Te, 77 hr ^{132}I, 2.3 hr	$H_2{}^{132}TeO_2$ in 1*M* HNO_3	See ^{99}Mo comment
^{128}Xe	$^{127}I(n,\gamma)^{128}I$ $^{128}I \xrightarrow[25\ min]{\beta^-} {}^{128}Xe$	(Stable)	Gas in ampule	
^{90}Y	Fission of ^{235}U	^{90}Y, 64.2 hr ^{90}Sr, 28 years	Generator ~0.98 mc ^{90}Y per milliliter of citric acid solution at radioactive equilibrium	

tivities for 50 radioisotopes are listed in three extensive tables. [Three neutron fluxes are assumed: 2×10^{13}, 2×10^{14}, and 2×10^{15} neutrons/(cm^2)(sec).] It is noted that it may be difficult to attain these calculated yields in some cases. For example, materials with high neutron-capture cross-sections will cause a decrease in neutron flux near the target, and yields will be lower. Irradiations in the reactor are presented in the tables in half-life units ($t/T_{1/2}$, where t is time of irradiation and $T_{1/2}$ is the half-life of the product isotope) from 0.01 to 5.0. Generally speaking, for radioisotopes with short half-lives, a sample may be irradiated for five or more half-lives; for those with half-lives from a week to a few months, the irradiation time varies from one to three half-life units; for those with extremely long half-lives, a small half-life unit is chosen. The tables show the buildup in curies per gram of irradiated material for each half-life unit, and a value of T_{max} shows the irradiation time in days at which the specific activity of the product radioisotope passes through a maximum.

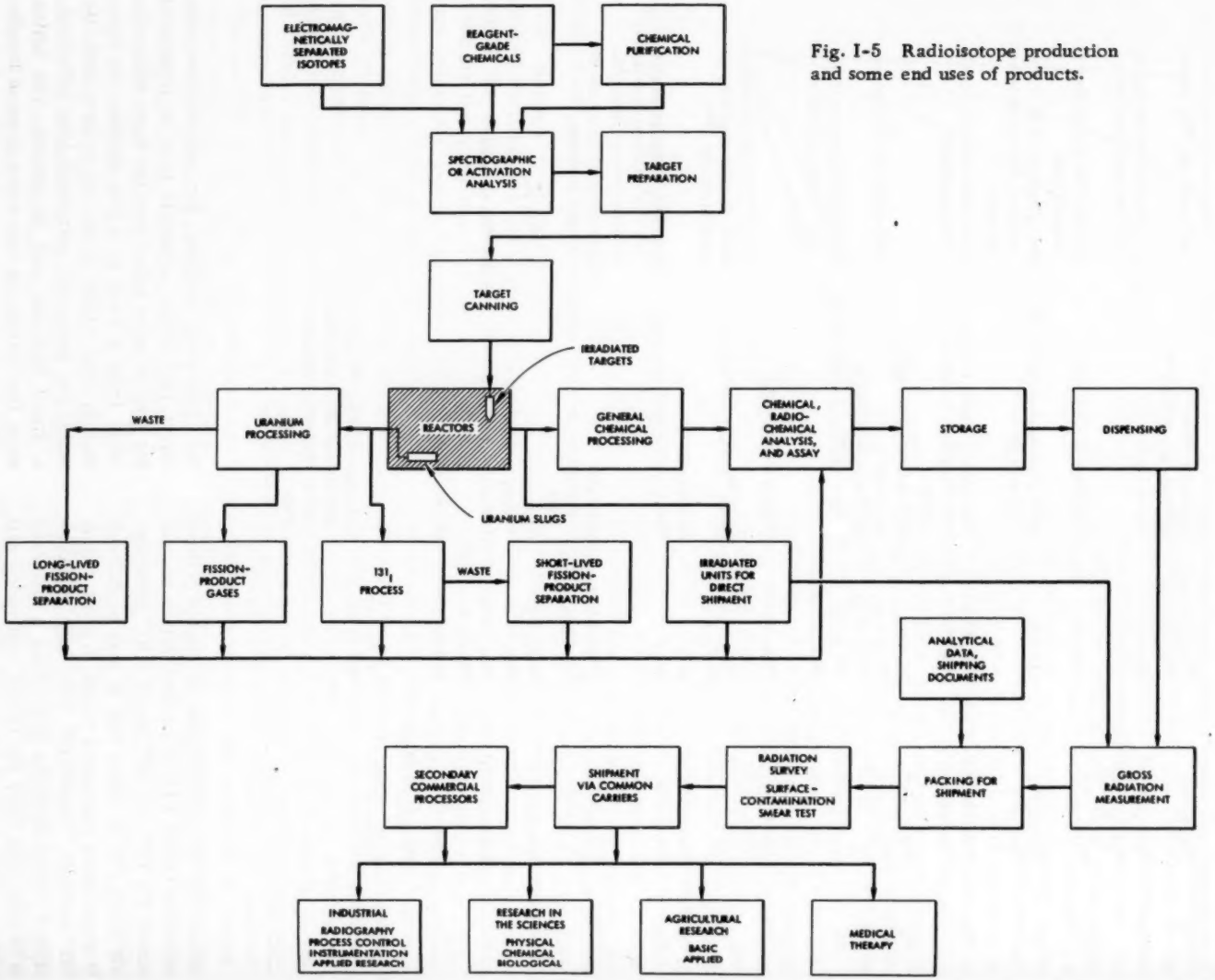

Fig. I-5 Radioisotope production and some end uses of products.

1. Prepare equipment.	100-ml separatory funnel Two 250-ml Pyrex beakers Two 150-ml Pyrex beakers Hot plate Ten 100-ml product bottles
2. Equilibrate 25 ml of di-2(ethylhexyl) phosphoric acid (HDEHP) (10 ml HDEHP and 15 ml Amsco 120) with 25 ml of 0.1 *M* HCl by manually shaking together in separatory funnel. Save organic phase. Discard aqueous phase.	This step adjusts acidity of HDEHP to ~0.1 *M* HCl.
3. Add 25 ml of 0.1 *M* HCl solution of ^{90}Sr-^{90}Y to the 25 ml of organic phase in separatory funnel. Manually shake mixture for ~5 min. Let phases settle out.	Yttrium-90 extracts into organic phase and ^{90}Sr into aqueous phase. See ^{90}Sr procedure for preparation of ^{90}Sr feed solution.
4. Drain off bottom phase (aqueous) to clean bottle. Save.	Organic phase contains ^{90}Y and some ^{90}Sr contamination.
5. Wash organic phase four times with 25 ml of 0.1 *M* HCl each time. Shake funnel. Allow to settle and drain off aqueous phase into same bottle from step 4 each time.	Washing removes most of ^{90}Sr contaminant. Save bottle with original separation plus washes. This can be used after two to three weeks for another ^{90}Y separation after ^{90}Y appears again.
6. Add 25 ml of 6 *M* HCl to funnel. Shake for ~5 min. Settle. Draw off aqueous phase.	Aqueous solution contains most of ^{90}Y.
7. Repeat step 6. Discard organic phase.	This removes remainder of ^{90}Y.
8. Boil down aqueous solution to dryness. Adjust volume to 25 ml with 0.1 *M* HCl.	This removes acid.
9. Use new glassware, and repeat steps 2 through 8.	The ^{90}Sr contaminant is further reduced.
10. Fume twice with 25 ml of concentrated HNO_3.	Organic matter is destroyed.
11. Fume twice with concentrated HCl.	Yttrium-90 is converted to $^{90}YCl_3$ and HNO_3 removed.
12. Adjust volume to 25 ml with 1.0 *M* HCl and transfer to 100-ml product bottle.	
13. Sample and analyze for: ^{90}Y concentration Total solids Molarity of HCl ^{90}Sr concentration Heavy metals	Refer to *ORNL Master Analytical Manual* (TID-7015), procedure No. 9 0733960.

Fig. I-6 Yttrium-90 processing procedure from ORNL-3633.

CHROMIUM-51

Production method:	$^{50}Cr(n,\gamma)^{51}Cr$
Cross section:	17 barns
Target:	Chromium metal enriched to 98% ^{50}Cr
Target weight:	15 mg
Neutron flux:	2×10^{14} neutrons cm^{-2} sec^{-1}
Irradiation-time:	26 weeks
Reactor yield:	11 curies
Processing yield:	>95%
Radiochemical purity:	>99%

Half-life: 27.8 days

Radiations:

Beta	Gamma	Others
None	0.32 (~8%)	EC

Processing facility and shielding required: manipulator cell, ~2 in. lead equivalent

Fig. I-7 Example of production data given in ORNL and BNL reports.

References

Isotope Separations Chemistry

1. E. R. Tompkins, J. X. Khym, and W. E. Cohn, Ion Exchange as a Separations Method. I. Separation of Fission-produced Radioisotopes, Including Individual Rare Earths, by Complexing Elution from Amberlite Resin, *J. Am. Chem. Soc.*, 69: 2769-77 (1947).
2. D. H. Harris and E. R. Tompkins, *ibid.* II. Separations of Several Rare Earths of the Ce Group (La, Ce, Pr, and Nd), *J. Am. Chem. Soc.*, 69: 2792-800 (1947).
3. E. R. Tompkins and S. W. Mayer, *ibid.* III. Equilibrium Studies of the Reactions of Rare Earth Complexes with Synthetic Ion Exchange Resins, *J. Am. Chem. Soc.*, 69: 2859-65 (1947).
4. S. W. Mayer and E. R. Tompkins, *ibid.* IV. Theoretical Analyses of the Column Separations Process, *J. Am. Chem. Soc.*, 69: 2866-74 (1947).
5. G. E. Boyd, J. Schubert, and A. W. Adamson, Exchange Adsorption of Ions from Aqueous Solutions by Organic Zeolites. I. Ion Exchange Equilibria, *J. Am. Chem. Soc.*, 69: 2818-29 (1947).
6. B. H. Ketelle and G. E. Boyd, *ibid.* IV. Separation of the Y Group Rare Earths, *J. Am. Chem. Soc.*, 69: 2800-12 (1947).
7. E. R. Tompkins, D. H. Harris, and J. X. Khym, Study of the Effect of a Number of Column Variables, *J. Am. Chem. Soc.*, 71: 2504-10 (1949).
8. F. H. Spedding, A. F. Voigt, E. M. Gladrow, and N. R. Sleight, Separation of Rare Earths by Ion Exchange. I. Ce and Y, *J. Am. Chem. Soc.*, 69: 2777-81 (1947).
9. F. H. Spedding, A. F. Voigt, E. M. Gladrow, N. R. Sleight, J. E. Powell, J. M. Wright, T. A. Butler, and P. Figard, *ibid.* II. Nd and Pr, *J. Am. Chem. Soc.*, 69: 2786-92 (1947).
10. J. A. Marinsky, L. E. Glendenin, and C. D. Coryell, Chemical Identification of Radioisotopes of Nd and of Element 61, *J. Am. Chem. Soc.*, 69: 2781-5 (1947).
11. R. D. Hansen and K. S. Chaberek, Dow Chemical Co., Ion Exchange Separation of Y from Rare Earths with Diethylenetriaminepentaacetic Acid, informal note.
12. P. B. Orr, Ion Exchange Purification of ^{147}Pm and Its Separation from ^{241}Am with Diethylenetriaminepentaacetic Acid as the Eluant, USAEC Report ORNL-3271, Oak Ridge National Laboratory, 1962.
13. W. C. Yee, Oak Ridge National Laboratory, personal communication, April 1964, reported in Chemical Technology Division Annual Progress Report, May 31, 1964, USAEC Report ORNL-3627, page 233, October 1964.
14. P. B. Orr, R. S. Pressly, and E. J. Spitzer, Evidence of the Nonexistence of Long-lived Isotopes of Promethium from Fission of Uranium and the Purification of Pm for Establishment of a Primary Spectrographic Standard, USAEC Report ORNL-3631 (in preparation).
15. E. J. Wheelwright and F. P. Roberts, Development and Demonstration of an Ion Exchange Process for Kilogram-Scale Production of High Purity Promethium, USAEC Report HW-78651(Rev.), Hanford Atomic Products Operation, 1963.
16. C. J. Hochanadel, Effects of Co γ Radiation on Water and Aqueous Solutions, *J. Phys. Chem.*, 56: 587-94 (1952).
17. A. O. Allen, *Radiation Chemistry of Water and Aqueous Solutions*, Van Nostrand, New York, 1961.
18. R. E. Blanco, I. R. Higgins, and A. H. Kibbey, Separation of Fission Products from Aluminum Waste Solutions by Ion Exchange, USAEC Report ORNL-301(Rev.), Oak Ridge National Laboratory, 1956 (first published in 1953).
19. R. S. Pressly, C. L. Ottinger, P. B. Orr, and E. E. Beauchamp, Purification of Kilocurie Quantities of ^{147}Pm by Ion Exchange, USAEC Report ORNL-2928, Oak Ridge National Laboratory, 1960.

ORNL Target Fabrication Center

20. E. H. Kobisk, Oak Ridge National Laboratory Target Preparation Program, EANDC(US)-32, USAEC Report ORNL-3400 (Special), Oak Ridge National Laboratory, 1963.
21. *Oak Ridge National Laboratory Catalog (of) Radio and Stable Isotopes*, USAEC Report TID-18870(4th Rev.), April 1963.
22. Catalog of *Processed Isotopes Available from Brookhaven National Laboratory*, 1960.
23. A. J. Weiss and Manny Hillman, Production of ^{28}Mg — State of the Art, USAEC Report BNL-6607, Brookhaven National Laboratory, 1962.
24. W. D. Box, Vacuum Distillation of Isotopic Magnesium Metal, USAEC Report ORNL-TM-749, Oak Ridge National Laboratory, August 1964.
25. E. H. Kobisk, H. L. Adair, H. G. Hunter, and E. B. Olszewski, Target Development, USAEC Report ORNL-TM-718, Oak Ridge National Laboratory, 1964.
26. W. D. Box, Electrodeposition of Technetium-99, USAEC Report ORNL-TM-748, Oak Ridge National Laboratory, September 1964.
27. C. Perrier and E. Segrè, Some Chemical Properties of Element 43, *J. Chem. Phys.*, 7: 155-6 (1939).
28. J. F. Flagg and W. E. Bleidner, The Electrodeposition of Element 43 and the Standard Potential of the Reaction Tc—TcO_4^-, *J. Chem. Phys.*, 13: 269-76 (1945).
29. E. E. Motta, Q. V. Larson, and G. E. Boyd, Studies of the Tracer Chemistry of Element 43, Clinton Laboratories (ORNL), USAEC Report MonC-99, 1947.
30. L. B. Rogers, Electroseparation of Tc from Re and Mo, *J. Am. Chem. Soc.*, 71: 1507-8 (1949).
31. N. Matsura and H. Yumoto, Deposition Potential of ^{99}Tc from Alkaline Solution and Its Application

to Standard Pure β Source on Thin Metallic Foils, *Radioisotopes (Tokyo)*, 8: 32-3 (1959).
32. J. D. Eakins and D. G. Humphries, Preparation of Tc Metal, *J. Inorg. Nucl. Chem.*, 25: 737 (1963).
33. K. W. Christenberry, M. D., Christenberry Optical Dispensary, Knoxville, Tenn., private communications, May 1963.

Production of ^{28}Mg: State of the Art

34. M. Lindner, Heavy Isotopes of Mg and Si, *Phys. Rev.*, 89: 1150 (1953).
35. J. L. Olsen and G. D. O'Kelley, Beta-Ray Spectrum of ^{28}Mg, *Phys. Rev.*, 93: 1125-6 (1954).
36. C. E. Mellish and G. W. Crockford, Production of ^{28}Mg in the Pile and Cyclotron at Harwell, *Intern. J. Appl. Radiation Isotopes*, 1: 299-304 (1957).
37. L. Marquez, The Beta Spectrum of ^{28}Mg, *Phys. Rev.*, 90: 330-1 (1953).
38. J. W. Jones and T. P. Kohman, Synchrocyclotron Production and Properties of ^{28}Mg, *Phys. Rev.*, 90: 495-6 (1953).
39. R. K. Sheline, N. R. Johnson, P. R. Bell, R. C. Davis, and F. K. McGowan, Study of the Isobaric Triplet ^{28}Mg-^{28}Al-^{28}Si, *Phys. Rev.*, 94: 1642-51 (1954).
40. G. Friedlander, J. Miller, R. Wolfgang, J. Hudis, and E. Baker, Nuclear Reactions of Cu with 2.2-Bev Protons, *Phys. Rev.*, 94: 727-8 (1954).
41. G. Rudstam, E. Bruninx, and A. C. Pappas, Spallation of Copper with 24-Gev Protons, *Phys. Rev.*, 126: 1852-7 (1962).
42. V. P. Crespo, Ejection of Large Fragments in High-energy Nuclear Reactions, USAEC Report UCRL-9683, University of California Radiation Laboratory, Sept. 6, 1961.
43. R. K. Sheline and N. R. Johnson, New Long-lived ^{28}Mg Isotope, *Phys. Rev.*, 89: 520-1 (1953).
44. R. K. Sheline and N. R. Johnson, Decay Scheme of ^{28}Mg, *Phys. Rev.*, 90: 325 (1953).
45. A. Wapstra and A. Veenindaal, Decay of ^{28}Mg, *Phys. Rev.*, 91: 426 (1953).
46. J. Hudis, Production of Carrier-Free ^{28}Mg from Al, *J. Inorg. Nucl. Chem.*, 4: 237-8 (1957).
47. E. Iwerson, W. S. Koski, and F. Rasetti, Triton-induced Activities in Mg and Al, *Phys. Rev.*, 91: 1229-31 (1953).
48. L. G. Stang, Jr., W. D. Tucker, R. F. Doering, A. J. Weiss, M. W. Greene, and H. O. Banks, Development of Methods for the Production of Certain Short-lived Radioisotopes, *Radioisotopes Sci. Res., Proc. Intern. Conf., Paris, Sept. 9–20, 1957*, 1: 50-70 (1958).
49. S. Hinds, H. Marchant, and R. Middleton, The Energy Levels of the Mg Isotopes of Mass 25 to 28, *Proc. Phys. Soc. (London)*, 78: 473-90 (1961).
50. R. H. Rodriguez Pasques, Reacciones Poco Frecuentes Observadas por Irradiacion de Silico con Neutrones, *Publs. Com. Nacl. Energia Atomica (Buenos Aires) Ser. Quim.*, 1(8): 81-9 (1957).
51. A. J. Weiss and M. Hillman, Nuclear Engineering Department Progress Report, May 1–August 31, 1962, Brookhaven National Laboratory.
52. M. Lindner, New Nuclides Produced in Chlorine Spallation, *Phys. Rev.*, 91: 642-4 (1953).
53. A. J. Weiss and M. Hillman, The ^{28}Mg-^{28}Al System: An ^{28}Al Generator, *Intern. J. Appl. Radiation Isotopes*, 14: 628-9 (1963).
54. W. M. Garrison and J. G. Hamilton, Production and Isolation of Carrier-free Radioisotopes, *Chem. Rev.*, 49: 237-72 (1951).
55. Brookhaven National Laboratory Annual Report, p. 56, USAEC Report BNL-682, Brookhaven National Laboratory, July 1, 1961.

Production Procedures Manuals for Isotopes

56. ORNL Radioisotopes Procedures Manual, USAEC Report ORNL-3633, Oak Ridge National Laboratory, June 1964.
57. Manual of Isotope Production Processes, Preliminary draft of USAEC Report BNL-864, Brookhaven National Laboratory (final report was scheduled to be issued August 1964).
58. H. F. Allen, Cobalt-60 Production at Savannah River, USAEC Report DPSPU-64-30-16A, Savannah River Plant (presented at Process Radiation Meeting sponsored by Washington Section, American Nuclear Society, Washington, D. C., May 13, 1964).
59. F. D. Lonadier and F. M. Huddleston, Polonium-210 Processing, Monsanto Research Corporation Report, May 26, 1964.
60. *Isotopes Radiation Technol.*, 1: 35-43 (1963).
61. ORNL Master Analytical Manual, USAEC Report TID-7015, 1957 and annual supplements, available from Office of Technical Services, Department of Commerce, Washington, D. C.

Section

II

Isotopes and Radiation Technology

Isotope Technology Development

In both the Spring and Summer 1964 issues of *Isotopes and Radiation Technology*, new uses of both radioactive and stable tracers in industrial and other large-scale engineering applications were described. In the present issue the discussion of tracers is continued with a discussion of some selected applications of radioactive tracers in the mining industry and of some new developments in counting equipment and techniques. A review of work on the use of isotopic gages to measure snow densities and profiles is also included.

Radioactive Tracer Uses in the Mining Industry

Some specific tracer applications of radioisotopes and the use of radioisotopes in the foreign coal industry were reviewed in the Spring 1964 issue of *Isotopes and Radiation Technology*.[1] In the current issue these subjects are further developed in a discussion of specific studies on uses of radioisotopes as tracers in the mining industry in the United States. Yavorsky and Gorin in two studies at Consolidation Coal Co. have used radiotracers to study the effect of particle size on the movement of coal in a fluidized bed[2] and to follow the separation of iron pyrites from coal, also in a fluidized bed.[3] Gaudin and Ramdohr at MIT[4] in another investigation induced radioactivity in minerals and used it to sort metal-bearing particles from gangue.

Radioisotope Tracers in Research with Coal

Isotopes have been used relatively rarely in the coal industry in the United States. In 1959, Bituminous Coal Research, Inc., under a contract with the USAEC Division of Isotopes Development (DID) made a survey of applications of radioisotopes in the coal industry.[5] More than 100 applications in 11 potentially profitable areas were suggested:

Area	No. of suggestions
Borehole logging	8
Mine surveying	1
Coal mining	30
Coal preparation	14
Equipment maintenance	6
Coal transportation, weighing, and storage	8
Use of coal for power generation and heat	12
Carbonization, gasification, and other process uses	9
Control of water and air pollution	3
Coal sampling, analysis, and testing	3
Coal research	16

About 80 of these were in regular or experimental use in the coal mining or analogous industries somewhere in the world at the time the report was written.

Commercial isotope gages are used routinely to measure the density and moisture content of coal; and Semmler, Brugger, and Rieke[6–8] at the University of Chicago made an extensive study of the use of a commercial gamma-scattering density gage with coal. The Texas Nuclear Corp. under a contract[9] with DID is developing a method based on activation analysis or related technique for continuous determination of the heat value of coal. The basic feasibility[10] of this system has been demonstrated in the laboratory, and a field test is currently being set up at loading facilities of Consolidation Coal Co.'s mine near Morgantown, W. Va.[11]

Consolidation recently completed two closely related DID-sponsored studies to demonstrate the use of radioisotope techniques in industrial process research with solids.

The first study[2] was aimed at measuring the rate of mixing or diffusion of solids, the rate and degree of size segregation, settling rates of oversize particles, and fluidized-bed expansion—all as functions of particle size and of flow velocity and viscosity of the fluidizing vehicle. The second investigation,[3] in which separation of pyritic sulfur and other mineral impurities in coal was studied, broadened the previous work by introducing the factor of density differences into separation studies.

Radioisotopes that emit gamma rays are uniquely suited for tracing the mechanics, motions, or disposition of granular solids, which are often involved in industrial processes.[12–15] The gamma rays penetrate heavy industrial equipment so that the tracer is conveniently detected and located without disruption of a process. These studies[2,3] have been directed primarily at coal particle mechanics in a fluidized system with a liquid vehicle, and the data are also generally applicable to fluidized-solid-catalyst systems.

EFFECT OF PARTICLE SIZE ON SEPARATION OF COAL FRACTIONS

The first study demonstrated the use of a radioactive tracer to study the physical process of separation in a fluidized bed. Liquid-vehicle fluidized systems have attained commercial application, particularly in large coal-preparation plants and in the mineral-dressing industry, for effecting the gravity separation of minerals of different density. The basic fluidized bed used in these cases is usually sand fluidized by upwardly flowing water.

The tracers used in this work were samples of coal that had been irradiated in a reactor. This tracer was so successful that it obviated trying any other methods, such as reaction or adsorption of radiochemicals on the particles. The coal-activation method produces an ideal industrial tracer. With proper precautions the induced gamma activity can be securely bound in the coal particles, faithfully tagging the tracer. The half-life of the major radioactive material in the coal is long enough to allow unhurried tracer experiments, and yet it decays sufficiently in 1 to 2 years to alleviate disposal problems.

Radiotracers. The coal used for tracer and fluidizer inventory was Pittsburgh Seam bituminous coal from near Georgetown, Ohio. Its ash content is nominally 10%. Since the major gamma-emitting activated isotopes are metallic elements, the amount and constitution of the inorganic ash determine the gamma activity, which will vary somewhat for coals from different sources.

The neutron irradiations were carried out in the Brookhaven graphite reactor. Two pounds of coal of select particle sizes was contained in an aluminum irradiation cylinder. Irradiation was usually for 280 hr at a neutron flux of 1.2×10^{12} neutrons/(cm^2)(sec). After a week or two, during which short-lived radioisotopes decay, the specific activity in the coal is about 11 μc/g.

The gamma-ray spectrum of the activated coal, obtained with an NaI(Tl) crystal scintillation counter and a Nuclear-Chicago radiation analyzer a month after irradiation, is shown in Fig. II-1*a*. Three reports[16*a–c*] were used to interpret the spectrum. In resolving the spectrum, only radioisotopes of half-lives longer than 1 day were considered.

Gamma rays were expected from iron, a major coal ash constituent of large neutron-capture cross-section. The rays from 45-day ^{59}Fe have energies of 1.30, 1.10, and 0.19 Mev, which coincide well with three peaks on the spectrum. However, the relative heights of the two highest energy gamma peaks are out of proportion, even when the dependence of counting efficiency on gamma energy is taken into consideration. The 1.12-Mev peak is too large to be attributed to ^{59}Fe alone, and it can be tentatively surmised that another radioisotope contributes to it. Review of single isotope spectrums reveals that 85-day ^{46}Sc has gamma energies of 0.89 and 1.12 Mev. The latter would overlap the 1.10-Mev peak of ^{59}Fe, and the 0.89-Mev peak is obvious on the spectrum, thus confirming this choice. The minor peaks from 20 to 37 volts have not been identified because of the confusing contribution in this range by the Compton scattering from the iron and scandium radiation. An attempt to better resolve the low-energy spectrum by adjusting both sample size and counting geometry resulted in the identification of a peak at 14 volts which can be ascribed to the single 0.32-Mev gamma ray of 27-day ^{51}Cr.

The gamma-ray spectrum was determined again a year after activation (Fig. II-1*b*), and,

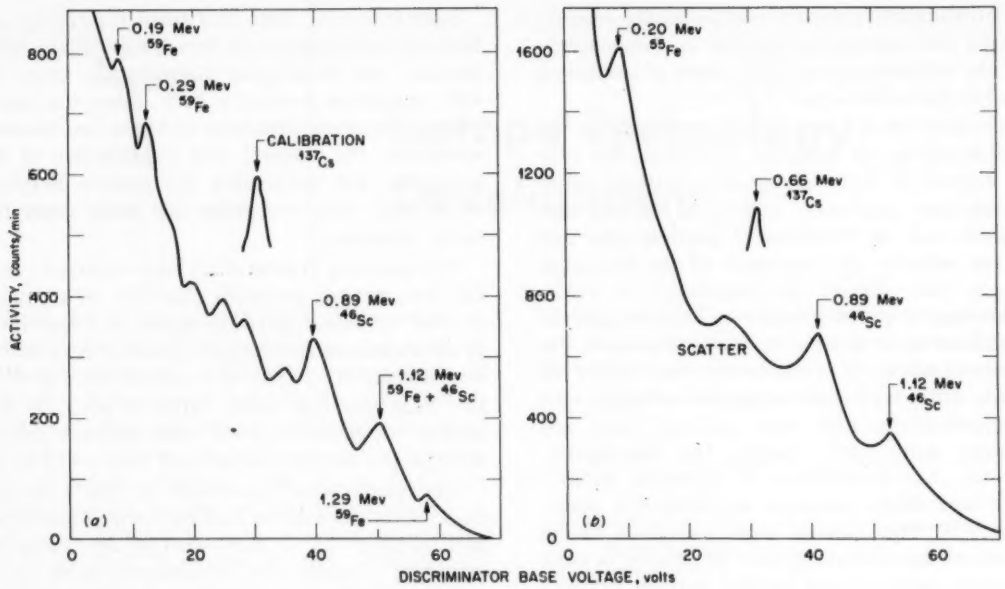

Fig. II-1 Gamma spectrum of activated coal for tracer use. *(a)* One month, and *(b)* one year after irradiation.

as expected, the ^{59}Fe peaks at 1.30 and 1.10 Mev had disappeared along with the unidentified peak at 0.27 Mev, but a strong 0.19-Mev peak remained, indicating a very long-lived radioisotope. The K X ray that is emitted following K electron capture of ^{55}Fe has this energy. In addition, ^{55}Fe has a half-life of 3.0 years, and the neutron-capture cross-section of ^{54}Fe is several times larger than even that of ^{58}Fe. The isotopic abundance is also about 20 times that of ^{58}Fe. However, because of the long half-life of ^{55}Fe, its contribution to the radioactivity of the coal is only about 10% in the year-old sample, and less than 1% in the freshly activated coal (only 0.1 mc in the 2-lb sample). The only other radiation persisting after a year is still identified with ^{46}Sc.

Data on the decay rate of the radioactive coal, plotted in the usual semilog fashion, showed a half-life of 85 days for the main portion of the curve, confirming ^{46}Sc as the main source of radioactivity in this activated coal.

If coal is not washed well before irradiation, up to 10% of the induced activity can be leached from it when it is mixed with water. The gamma spectrum of the soluble material in the wash water showed that both scandium and iron partially dissolve. The unidentified gamma peak at 0.27 Mev was especially strong in the water solution. As a precaution against leaching, which could confuse tracer studies, all coals for tracer studies were prewashed by stirring with water for 3 hr prior to irradiation. When the coal was thus treated, no activity could be leached from it after irradiation or activation.

Fluidization Unit and Associated Apparatus. A large experimental unit was constructed for radiotracer studies of the mechanics of fluidized particles. The large size facilitated accurate measurement of times for particles to move between select points in the motion studies and allowed more accurate extrapolation of data for design of commercial fluidized reactors.

A schematic drawing of the fluidizer and accessory radiation-detection equipment is shown in Fig. II-2. The basic fluidization vessel was made of 6-in.-ID by 20-ft-high pipe. The system was heated and insulated to provide temperature control for easy variation of viscosity in studies on the effect of this variable on particle mechanics.

The operation of the equipment is apparent from the drawing. The range of upflow velocities is from that just sufficient to initiate fluidization (~0.001 ft/sec) to that which is high

enough (~0.05 ft/sec) to carry over the suspended solids. The recycle system provides for separation and return of entrained solids to the bed when necessary. Prevention of passage of solids through the pump is desirable to avoid excessive solids attrition and wear.

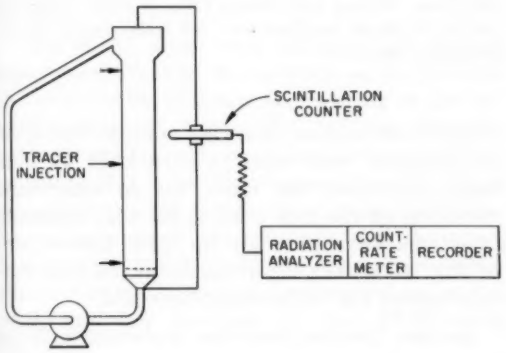

Fig. II-2 Schematic diagram of fluidization unit.

The radiotracer injector is illustrated in Fig. II-3. It can be charged, mounted, operated, and removed for recharging without significant loss of column inventory, even under pressure. The piston and plug are pulled back into the closed position, and the cylinder is moved back through the plug valve by turning the threading handle. The plug valve is then closed to prevent emptying of the fluidized column as the whole injector assembly is removed by unscrewing the injector housing from the plug-valve housing. The cylinder can be recharged with a water slurry of the labeled coal by opening the plug slightly and pouring the slurry into the cylinder above the piston. The piston plunger is pulled tight to prevent leakage of the coal slurry before injection as well as its premature diffusion into the fluidized bed. The injector housing is threaded back into position, the plug valve is opened, and the cylinder is finally inserted by threading through the plug valve until the end of the cylinder is flush with the inner wall of the fluidizing column.

The coal is injected rapidly into the bed at the proper moment by pushing in the piston plunger. The plug is pushed out into the fluidizing column while the piston pushes the coal out into the bed. It was found necessary to inject the labeled coal as a slurry, since dry coal rises extremely rapidly through the bed with little mixing, indicating that it is carried entrapped in bubbles of air before it becomes wetted by the vehicle.

A scintillation counter is used to locate the tracer or observe its passage past a selected point. A guide-rail support and cable winch are used for positioning of the counter, as shown in Fig. II-2. The lead collimator on the front of the counter restricts the viewing field to a few inches along the axis of the fluidized column, thus locating the tracer with sufficient accuracy in a total column length of 20 ft. The counter is connected to a radiation analyzer by 30-ft coaxial cables. A preamplifier in the counter housing minimizes pulse loss. The analyzer can be set to select the 0.89-Mev ^{46}Sc gamma ray, thus screening out much of the background radiation. Its output is fed to an integrating count-rate meter and then to a fast-speed strip-chart recorder to accurately measure travel time of the tracer. The travel-time measurements are important in determining the mixing rates and solids residence times in fluidized reactor systems.

Two methods of measuring fluidized-bed expansion were evaluated. In the first method, applicable to beds of narrow particle-size distribution, about 0.3 mc of tracer coal was mixed or blended with the coal, uniformly tagging it. While the bed was fluidized, the scintillation counter scanned it over the length of the column. A sudden transition in the counting rate occurred at the top of the fluidized bed, above which there were no radioactive coal particles. The expanded bed height could thus be easily located. This method was very fast, and the bed expansion could be measured in a short

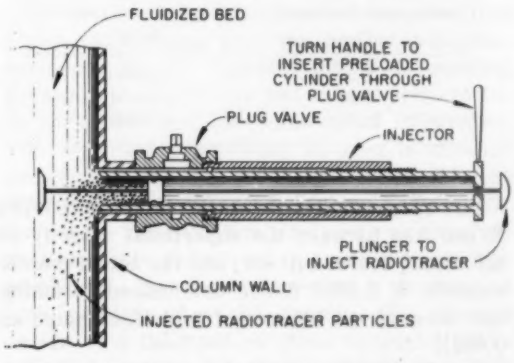

Fig. II-3 Radiotracer injector.

time for many variations in operating conditions.

A gamma-ray absorption method using a ^{137}Cs source opposite the counter was also tried for determination of the bed height. However, the disadvantage of moving the counter and source over large distances without altering their relative positions even slightly showed that the tracer method of measuring bed heights was preferable.

Typical Results. Some selected results from this study[2] are given here to illustrate the potential of the method. In the first tracer application, it was desired to learn whether or not fine coal would mix homogeneously in a fluidized bed of coarse coal or be swept out with the fluidizing vehicle and, if so, at what rate. To study the behavior of fine coal (<100 mesh), radioactive coal of this size was injected into a bed containing 50 lb of coarse coal (28/35 mesh) fluidized by water at 0.00625 ft/sec. Radiation monitoring was carried out at select positions after the injection of the tracer fine coal, and these measurements supplied information on mixing and transporting of the fine coal (Fig. II-4). Considerable mixing was indicated by the initial appearance of the fine coal at the detecting point at a velocity much greater than the superficial velocity of the fluidizing vehicle. Also, extensive tailing-out was observed after the passage of the concentration peak. The concentration peak, as reflected by the counting rate peak, appeared to have moved at nearly the same velocity to the three different stations along the fluidized column as shown below:

Height of detector above injection point, ft	Velocity of movement of radiation peak, ft/sec
2.3	0.00734
9.3	0.00737
17.3	0.00730

Not surprisingly, its mean value of 0.00734 ft/sec lies between the superficial velocity of the water, 0.00625 ft/sec, and the actual vehicle velocity of 0.0096 ft/sec determined by taking into account the fraction of voids (estimated as 0.652).

The radiation profile became very diffuse due to extensive mixing by the time the tracer

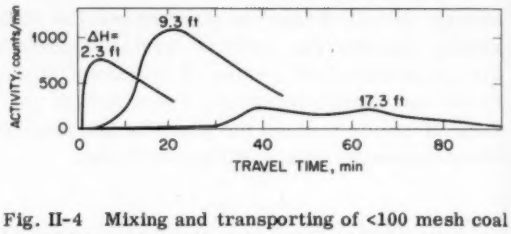

Fig. II-4 Mixing and transporting of <100 mesh coal in a 28/35 mesh fluidized bed. ΔH = distance from injection to detector.

reached the highest detection station. The level of radiation went down to zero after 90 min, which indicated that there was no substantial retention of the fine coal in the bed. Different injections were used for the three tracer runs of Fig. II-4; thus the areas under the distribution curves are not necessarily equal.

Another investigation was concerned with the mixing rate and equilibrium segregation observed when particles of various sizes were injected into the fluidized coal bed for one fluidization velocity. The bed solids were again predominantly 28/35 mesh coal, 10% of which was <35 mesh. The peak diffusion velocity and the average velocity as well as the approximate time to reach equilibrium are shown in Table II-1. These velocities illustrate the dependence of the mixing rate on particle size. The peak velocities were measured from the time of passage of the radiation peak past a position either 2 ft above the distribution plate or 10 ft above the plate, depending upon whether the

Table II-1 MIXING RATE AS A FUNCTION OF PARTICLE SIZE FOR COAL INJECTED INTO A HOMOGENEOUS FLUIDIZED BED

Coal Fluidized by Water; Bed Particle Size: 90% 28/35 Mesh, 10% <35 Mesh; Superficial Vehicle Velocity, 0.024 Ft/Sec; Velocity Through Bed, 0.031 Ft/Sec

Particle size injected, mesh	Peak velocity,* ft/sec	Average velocity,* ft/sec	Time for equilibrium, min
6/8	−0.152	−0.182	1
14/20	−0.0534	−0.0341	2
28/35	−0.0595,† +0.0521†		60
48/65	+0.0204	+0.0185	8
<100	+0.027	+0.024	Swept out

*Negative values mean the peak moved down the column, and positive values, up.

†Maximum velocities.

injected coal fell or rose through the bed. The tracer coal was injected at the $5\frac{1}{2}$-ft position.

When the injected coal was larger than the bed solids, it fell rapidly through the bed to reach its equilibrium position. Finer coal rose rapidly through the bed and, in the vicinity of <100 mesh, approached the velocity of the fluidizing water, confirming the above observations.

The 28/35 mesh coal diffused both upward and downward from the injection point. This fact is noted by the plus and minus signs on the two values given in Table II-1 for the diffusion velocity of this size coal. Maximum velocities in Table II-1 were determined from the initial appearance of the tracer at the detection station. Here the counter was far away from the injection point so that too much diffusion or broadening occurred to permit determination of the peak with any accuracy for the 28/35 mesh tracer.

The mixing of injected particles that have the same size as the uniform fluidized bed is a relatively slow process at low fluidization velocities, while movement of injected particles of sizes different from those of the bed into distinct segregated positions is a very rapid process, as expected. Injected tracer particles that are the same size as most of the bed experience no unbalanced motive force and are indistinguishable physically from the bulk of the bed. Liquid-phase fluidization produces only short-distance eddies or vortexes; thus there is very slow mixing in a uniform bed. But, when the particles are lighter or heavier than the bulk particle environment, there is a motive force and the off-size particles rapidly segregate.

After each of the various sizes of tracer was injected and time allowed for equilibrium distribution, radiation scans of the whole column were performed. The composite equilibrium distribution of the tracer coal after all the size fractions had been injected is shown in Fig. II-5. The segregation pattern of the different particle-size ranges is sharp. These observations show that the liquid fluidized bed is potentially a precise separating tool for particle-size classification.

The 6/8 mesh coal settled down through the bed into the throat of a conical reducer at the bottom of the column, which was connected by a 2-in. water feed line to the fluidization vessel. The water velocity was great enough at this point to keep particles out of the 2-in. line. The 14/20 mesh coal also fell through the bed and settled directly above the distribution plate at the bottom of the column. The 48/65 mesh coal rose through the bed and became situated just on top of the bulk of the 28/35 mesh bed, whose height was 13 ft. The 28/35 mesh coal was evenly distributed throughout the bed in about an hour, as expected.

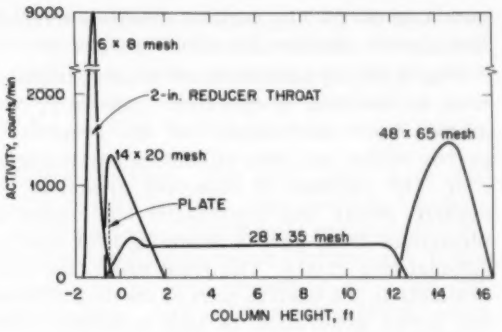

Fig. II-5 Composite radiation scan illustrating segregation of various sizes of tracer coal in a 20-ft column. Superficial velocity, 0.024 ft/sec; bed contained about 90% particles of 28/35 mesh.

EFFECT OF DENSITY ON SEPARATION OF COAL FRACTIONS

The specific goal of the second project[3] was to obtain data on the rate and sharpness of segregation of pyrites and other mineral impurities in coal-water fluidized systems as a function of particle density and size. Such data can be used in determining the rate and efficiency of cleaning coal in potential commercial installations utilizing the fluidization principle.

Hydraulic classification processes, such as water fluidization and the use of hydraulic cyclones, are of potential utility in mineral preparation in general and in coal preparation in particular for the removal of impurities. The separations generally desired in mineral preparation result in the classification of solids according to the differences in specific gravity. Hydraulic classification processes separate particles into categories that are hydraulically equivalent. This equivalence is a function of both particle size and density. The rational design of a fluidized or other hydraulic classification system therefore requires that data be obtained on the rate and sharpness of segre-

gation as affected by particle density as well as that already obtained for size segregation.

This work, in addition to its broader implication to mineral preparation generally, was aimed more specifically at the removal of pyritic sulfur and other mineral impurities from coal. The problem of removing primarily inorganic sulfur and secondarily other mineral impurities from coal is assuming ever greater national importance. The great bulk of the coals available in the eastern part of the United States for power generation is high in sulfur. Air-pollution authorities are at the same time, in the interest of national health, moving in the direction of imposing severe restrictions on the sulfur content of fuels that can be burned in power stations. Thus it will be imperative to reduce the sulfur in eastern coals in order to maintain the coal markets.

The efficient removal of pyritic sulfur and other mineral impurities from coal first requires crushing to a relatively fine particle size to liberate these minerals from the coal. This size is usually <8 mesh. The hydraulic density-classification method is one of the more promising methods potentially capable of efficiently cleaning such finely crushed coal, but few data are available to design commercial installations based on this principle.

Up to the present time, economic considerations have made the cleaning of fine coal impractical. However, the transportation of relatively fine-sized coal in the form of water slurries from mine mouth to power station has recently been introduced on a commercial scale, and wide application of this form of coal transportation is expected in the next several years. Therefore already having the coal ground fine for transport leads to more favorable economics in cleaning fine coal, and the natural integration of hydraulic cleaning with pipeline transportation now changes the situation.

Coal Feed and Radiotracers. The single run-of-mine batch of coal used in this investigation is of Pittsburgh Seam bituminous coal from the Williams Mine located in northern West Virginia. This coal contains, before cleaning, about 11% ash, 2.7% pyritic sulfur, and 4.3% total sulfur. The coal was crushed through an 8 mesh screen and then split at 48 mesh. These two screen fractions were used as feed to the fluidization unit to produce the fluidized bed into which the radiotracers were injected. They were also used in studies of density segregation in a hydroclone.

The radiotracer solids used in this work were derived from the inorganic or mineral materials separated from the coal and then neutron activated. Being physically and chemically the same as the natural materials to be cleaned from coal, they were valid tracers for following the mechanics of removal of mineral impurities in cleaning processes.

For use as tracers of known size and density characteristics, aliquots of the two broad size fractions were further screened into eight narrow particle-size fractions. From each of these, materials more dense than pure coal (1.3 g/ml) were next separated by standard float-sink methods into six density brackets. Liquids used in the float-sink preparations were mixtures of perchloroethylene and gasoline, adjusted to the desired density. The same particle-size fractions were also prepared by grinding a very rich pyrite material, whose density range of 4 to 5.0 g/ml indicated it to be virtually pure pyrite (density 5.0 g/ml). Such materials, which are called "sulfur-balls" and are readily recognized by their metal-like brilliance, can be picked by hand from the coal seam. The total of 56 size- and density-classified tracers was in size brackets of 8/14, 14/28, 28/48, 48/65, 65/100, 100/150, 150/200, and <200 mesh and in density brackets of 1.4 to 1.5, 1.5 to 1.6, 1.6 to 1.8, 1.8 to 2.2, 2.2 to 2.5, 2.5 to 2.95, and 4.0 to 5.0 g/ml.

These physically classified tracers were neutron activated in the Brookhaven reactor. Those of densities less than 2.2 g/ml (low pyrite) were irradiated for 200 hr, and those of densities above 2.2, for 70 hr. The neutron flux was 7×10^{12} neutrons/(cm^2)(sec). After a week's decay, the tracers had a specific activity of 2 to 5 μc/g, which increased with density due to the increase in metallic content. Usually 1 to 5 g of tracer was used per single tracer experiment, depending on decay time between activation and use. Counting rates of the order of 30,000 counts/min were observed through the 0.5-in.-thick steel wall of the fluidizer as the injected material passed the collimated scintillation counter. This is sufficient for very accurate tracing.

The radiation characteristics of the mixed-grain coal-pyrite radiotracers were determined. The spectrum from a virtually pure, but naturally occurring, pyrite tracer having a density

of 5 g/ml showed that ^{59}Fe was essentially the only gamma-emitting radioisotope. A spectrum from a mixed radiotracer of about 6% pyrite and the remainder coal showed that the major radioisotopes are ^{46}Sc and ^{59}Fe. The 0.89-Mev peak characteristic of ^{46}Sc is totally absent from the activated pyrite sample, which indicates that scandium is associated either with the organic coal or at least with coal minerals other than pyrite.

Fluidization Unit. The fluidization unit was similar to that used in the earlier study (Fig. II-2). The principal difference was the use of a smaller diameter section, 4 in. in diameter and 10 ft in length, below the main 6-in.-diameter by 20-ft-long fluidization section. This constricted section allowed a higher fluidizing velocity below the main column, and the higher density solids that settled out of the main bed could still be maintained in a fluidized condition and in a higher state of resolution. A drain valve was installed at the bottom of the 4-in. section for removal of dense residues so that high-gravity radioactive solids could be drained from the unit between injections of tracer solids and a sequence of injections could be made without recharging the fluidizer. The trace injection system (Fig. II-3) and the detection system were essentially the same as in the previous study.

The fluidization unit was operated as follows: An inventory of coal was charged into the unit through the top, and the coal was fluidized with water at a controlled rate that could be regulated between 0.001 and 0.05 ft/sec. Water was passed through the unit without recycling until all the fines (usually <200 mesh) were stripped out of the solids bed by the effluent water. These fines were passed overhead to waste collection. The unit was then put into closed-loop operation with recycle of the overhead water (clear) through the column by means of a pump; the closed loop minimized the dispersion of the radioactivity.

Fluidization was maintained for 30 min to ensure equilibrium in particle distribution. Then the tracer particles were injected into the bed, and the rate of travel past several predetermined positions was observed by the movable counting system used earlier (Fig. II-2). The final equilibrium position of the tracer in the column could be determined by repeated scans of the whole column.

For segregation studies, 17 kg of coal was charged to the fluidization column. In studies of 48/0 mesh beds, the superficial fluidization velocity of the water was always 0.006 ft/sec, and for the 8/48 mesh beds it was 0.016 ft/sec.

Hydroclone Unit. The unit used here for tracing pyritic particle separation in a hydroclone was a 3-in.-ID hydraulic cyclone from the Heyl-Patterson Corporation (Pittsburgh). It was installed in a loop consisting of a 500-gal slurry-mixing tank and a circulating pump (12 gal/min maximum). Coal-water slurry from the tank was pumped into the hydroclone, and the overhead (clean) and underflow (refuse) streams were piped separately back to the tank. The radiation counting or tracing equipment could be placed on either of these two offstreams for detection of the amount of tracer in the overhead or the underflow as tracer was injected into the hydroclone feed line. The ratio of the total count from the underflow stream to that of the overhead-plus-underflow streams yields directly the cleaning efficiency (E) for a particular density-size tracer. An even more sensitive procedure was to collect the two offstreams in 5-gal cans while they contained the tracer injection and to count the total radioactivity in each sample with identical counting configurations. (A typical configuration was to place the cans over a fixed scintillation counter.) This latter method was adopted for all studies. Cleaning efficiency data (the ratios of count rates from the two samples) are collected much more rapidly by such tracer methods than by methods that involve collecting, drying, and chemically analyzing samples for sulfur or pyrites. The extensive basic information thus generated on the cleaning efficiency of particles of specific size and density as a function of slurry concentration of the hydroclone feed would be prohibitively laborious to obtain by other methods.

Typical Results with Fluidized Bed. The most pertinent primary data on rates of segregation of pyritic particles in a 48/0 mesh fluidized bed of coal as obtained by tracer studies are shown in Fig. II-6. The fluidization velocity, or superficial water velocity, was 0.006 ft/sec. The radioactive pyrite was injected at a position 9.5 ft above the bottom of the fluidization column, and its passage through the fluidized bed was monitored with the counter situated 7.5 ft below the injection point. As the injected

material passed the counter, an asymmetrical distribution curve was recorded in response to the radioactivity. The time after injection at which the maximum count rate was observed yielded the peak velocities. The average velocity shown is the weighted average for all the tracer particles, calculated from the area of the count-rate response curve. The average is

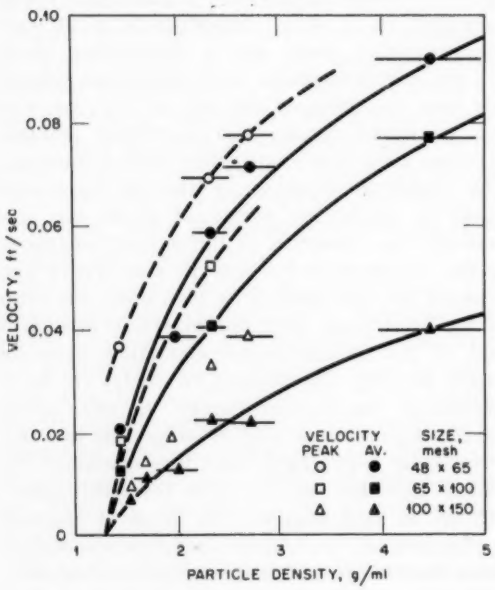

Fig. II-6 Segregating velocities of pyritic particles as a function of particle density in a fluidized bed of 48/0 mesh coal; 7.5-ft fall.

significantly less than the peak velocity due to tailing-out of the injection by turbulent mixing in the fluidized bed. These segregation velocity data clearly define the time required to remove pyritic particles of a chosen particle size and density from a full-scale fluidization unit of any dimensions for a 48/0 mesh fluidized bed.

In further examinations of the data, the average velocities as defined above were used, since they were more significant than the peak velocities determined from highly unsymmetrical tracer response curves. The peak velocities show when the largest amount of segregating material settles out of a fluidized bed.

Segregation of smaller size particles was also studied. Tracers of the small sizes, 150/200 mesh and <200 mesh, did not clearly segregate but were distributed through the bed or moved entirely up and out of the bed. Thus data of these two small sizes did not follow the pattern of Fig. II-6 and were not included in correlations. These may be viewed as the critical sizes where segregation just ceases to be practicable. For all pyritic tracers in the small size range except one, a portion flowed up while another portion moved down. This was due to the distribution of both size and density in the classification of each tracer; the finer, lighter ends of the fractions go up while the larger, heavier ends precipitate. The preparation of tracers of narrower characteristics to better define the critical segregation point (combined size and density) would be extremely tedious and time consuming. The tracers of 150/200 mesh size, and 1.4 to 1.5 and 1.5 to 1.6 g/ml density, segregate past a point 2.5 ft below the injection point but never reach a point 7.5 ft down. These particles find hydrodynamic equivalence in a stratum of large particles in a lower section of the size-segregated fluidized bed and stay there. Such particles would remain in a "middlings" cut in a fluidized cleaning process.

The upward diffusion velocities of the small pyritic particles were essentially constant for the various tracers. These particles rose through the bed at about four times the fluidization velocity, showing that there is some sort of "fluidization force" that expels the fines from the bed faster than the upflow of the fluidization medium. No explanation has been offered for this behavior, although it was also observed earlier.[2]

The data thus collected can be used to define the time to achieve a desired degree of cleaning of coal by density segregation, and a thorough evaluation of the method was made[3] by taking samples from various sections of the fluidized bed and analyzing them for ash or sulfur.

Typical Results with Hydroclone. The tracer technique yields directly the cleaning efficiency (E) for the particular operating conditions being used with the hydroclone. The cleaning efficiency as a function of particle size and density was determined for slurry concentrations of 0, 10, and 18% coal in the feed to the hydroclone. Figure II-7 gives the data for the 10% slurry concentration. Only the tracers finer than <65 mesh were studied in detail, since a few spot checks indicated that >65 mesh tracers separate to the underflow completely in 48/0 mesh slurry;

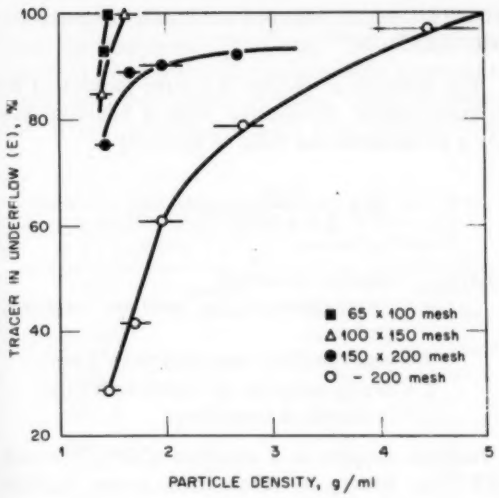

Fig. II-7 Percentage of radioactive coal particles in hydroclone underflow as a function of particle density; 10% slurry of 48/0 mesh coal. Underflow orifice, $^5/_{16}$ in.; overflow orifice, $^1/_2$ in.; pumping rate, 12.4 gal/min.

the 65/100 mesh particles are almost completely separated, even at low densities.

For 10 and 18% slurry concentrations, the results were very similar, i.e., 90% of the 150/200 mesh tracers of over 2.0 specific gravity was collected in the underflow. The rejection of <200 mesh material of lower densities was less efficient for the two slurries as opposed to water flow alone; however, this small-size low-density material did not interfere with the arbitrarily set acceptable sulfur level of 2.0%. The efficiency of rejection was greater for particles >200 mesh and for higher density particles (> 2.3 g/ml) in the size vicinity of <200 mesh for the slurries as compared with water.

Radioactive Tracers for Concentration of Ores

Gaudin and Ramdohr,[4] in work done at MIT under a DID contract, have developed an interesting device for sorting copper-bearing minerals from barren material after neutron activation of the copper in the ore. This device, together with some preliminary work on the ^{64}Cu marking of copper in copper ores by adsorption from solution, is described following a brief historical summary of earlier work on the use of radioactivity and tracers for sorting minerals.

HISTORICAL

Sorting processes have been used from earliest recorded history in connection with mining operations and mineral processing. For many centuries the eye and the hand of workmen were used, but in our present civilization this method has become uneconomical because of the high cost of labor.

The physical properties used in mechanized mass separating operations, such as specific gravity, rarely provide differences among ore lumps that parallel the metal content. As a result much waste cannot be removed in a coarse state, and relatively expensive methods, such as fine grinding, flotation, and leaching, must be used. Mass mining methods have increased and will further increase the frequency and magnitude of this economic difficulty. Applications of radioisotopes make theoretically possible several sorting processes for coarse ore lumps.

In 1946 a practical process was developed in Canada by Lapointe[17a] for sorting uranium-bearing ore from waste. It was used for several years and produced considerable amounts of uranium concentrates. In the original Lapointe ore picker, uranium ore was placed on a moving belt, and individual pieces were scanned by a G-M tube. If an individual ore lump had sufficient radioactivity to be measured by the G-M tube, it was pushed into one bin for further processing; if the ore did not contain sufficient uranium to affect the counter, the lump fell into a refuse bin. This sorter was operated on laboratory and pilot-plant scales at the Canadian Bureau of Mines laboratories in Ottawa[17b] and later on a plant scale[17c] at the Port Hope Refinery. The device was patented in the United States, Britain, and Canada,[17d] and in later work lower grade ores were sorted by substituting a scintillation counter for the G-M tube.[17e]

Following the work of Lapointe, Gaudin[18] and coworkers at MIT devised a similar method, based on the ^{9}Be$(\gamma,n)^8$Be reaction, for the concentration of beryl. The ore to be sorted was passed under an intense gamma source (Ra, ^{124}Sb, or a Van de Graaff generator) on a belt, and the neutrons generated by the reaction

$$^9\text{Be} + \gamma \rightarrow n + {}^8\text{Be}$$

were detected and used to activate a kicker device. With this apparatus, pieces of beryl as small as 1 g could be picked with certainty at rates of about five per second.

While both these devices were successful, they depended on specific properties of the material—the natural radioactivity of uranium and its daughters and the specific (γ,n) reaction of beryllium. Church[19] in 1949 attempted to generalize the method by studying the exchange of radioactive ions with minerals such as galena (PbS) and pyrite (FeS_2) with $^{35}SO_4^{2-}$ and apatite ($CaF_2 \cdot 3Ca_3P_2O_8$) with $^{32}PO_4^{3-}$. He found that the surface of the mineral had to be oxidized before exchange with the tracer would take place. This conclusion verified earlier work by Paneth,[20] who found that fresh surfaces of natural minerals were resistant to exchange but that weathered surfaces exchanged easily.

Senftle and Gaudin, in the early 1950's, made some preliminary studies of activation of ore samples by neutron irradiation. They first tried[21] irradiation of selected ores with a flux of 10^7 neutrons/(cm^2)(sec) in a Van de Graaff generator. With 2.5 sec irradiation and counting after 17 sec, minerals containing silver, aluminum, copper, and manganese showed the largest counts, as expected. In a second, more extensive, study,[22] they irradiated 150 specimens of 51 different minerals in the Brookhaven reactor and studied the resulting activities. They concluded that minerals could be separated on the basis of induced radioactivity but that, because of the effect of trace elements on total activity, each ore body would present specific individual problems. They also concluded that the neutron flux of the reactor, 10^{12} neutrons/(cm^2)(sec), was too high and that a flux of 10^9 to 10^{10} neutrons/(cm^2)(sec) would be adequate.

Halfawy and Senftle[23] made a preliminary study of the adsorption of radioactive ions of silver, zinc, lead, sodium, thallium, calcium, copper, and strontium from solution by the following eight natural minerals and rocks: galena, sphalerite, pyrite, quartz, beryl, barite, calcite, and granite. Contrary to the results of Church[19] and Paneth,[20] the metal ions were adsorbed from solution in varying degrees on different minerals without prior oxidation, and they suggested that adsorption of the proper short-lived nuclide for a particular ore could be used to tag metals prior to running an ore through a radioactive sorter.

COPPER ACTIVATION BY NEUTRON IRRADIATION[4]

The activity in curies of a pure isotope of an element after irradiation with a neutron flux for a predetermined time is given by

$$A = \frac{Nf\sigma}{3.7 \times 10^{10}\lambda}(1 - e^{-\lambda t})$$

where N = number of atoms
σ = cross-section for neutron capture, cm^2
f = neutron flux, neutrons/(cm^2)(sec)
λ = decay constant or 0.693/half-life
t = irradiation time, sec

Natural copper is a mixture of 69% ^{63}Cu and 31% ^{65}Cu, which on irradiation gives 12.8-hr ^{64}Cu and 5.1-min ^{66}Cu. The decay schemes are

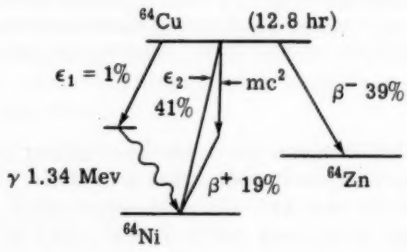

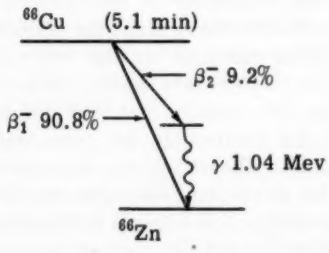

For a constant neutron flux and a preset irradiation time, the initial activities of ^{66}Cu and ^{64}Cu depend entirely on the total copper in the ore. However, not only the copper but also the other elements in the ore will be activated during the irradiation. The amounts of such interfering isotopes depend on the chemical composition of the sample. To estimate the magnitude of this effect, a representative high-grade ore sample was analyzed, and the amount of each activity for the major elements in a 20-g sample was calculated, assuming a neutron flux of 5×10^{12} neutrons/(cm^2)(sec) and 5 sec

irradiation time. The results (Table II-2) show that the isotopes ^{31}Si, ^{27}Mg, ^{24}Na, ^{51}Ti, ^{65}Mn, and ^{28}Al are formed in considerable amounts in addition to the copper isotopes. Other elements not listed contribute much less radioactivity.

Table II-2 INITIAL CALCULATED ACTIVITY IN A 20-G HIGH-GRADE ORE SAMPLE AFTER 5 SEC IN A FLUX OF 5×10^{12} NEUTRONS/(CM^2)(SEC)

Constituent	Amount present, %	Isotope found	Initial activity, mc
Al_2O_3	15.7	^{28}Al	28.20
Cu	6.12	^{64}Cu	0.33
		^{66}Cu	10.62
SiO_2	52.8	^{31}Si	1.66
MnO	0.12	^{56}Mn	0.14
Na_2O	2.1	^{24}Na	0.04
MgO	4.3	^{27}Mg	0.03
TiO_2	1.6	^{51}Ti	0.02
K_2O	2.5	^{42}K	0.0053
CaO	0.9	^{49}Ca	0.0027

Besides that of the two copper isotopes, the radiation of ^{24}Na, ^{28}Al, and ^{56}Mn will be outstanding. Silicon-31 is chiefly a β^- emitter and therefore is not measurable with the equipment used. The 1.02-Mev gamma radiation of ^{27}Mg comes so close to the 1.04-Mev gamma radiation of ^{66}Cu that it would not be practicable to differentiate between them.

Experimental. The experimental study included the following steps: Determination of optimum irradiation conditions in the reactor; analysis of the radiation spectrum after activation to distinguish the copper from other radionuclides; monitoring of overall radiation decay as a function of time; and consideration of a suitable counting technique for radiocopper.

(1) Determination of Optimum Irradiation Conditions in Reactor. The first irradiation, involving a neutron flux of 5×10^{13} neutrons/(cm^2)(sec) and an irradiation time of 5 sec, was carried out on 10 particles of rich ore containing about 5% copper and 10 particles of poor ore containing about 0.1% copper. Since the activity of the particles was found to be much too high to measure with the scintillation counter, a G-M tube was used to get an approximate idea of the overall decay rate. The half-life during the first day was between 2 and 3 hr, probably due to the presence of ^{56}Mn, but after 30 hr the activity had dropped enough to be counted with a scintillation crystal.

It was hoped that there would be a marked difference between the rich and the poor ore so that the pieces could be evaluated by total radiation measurement; however, this was not the case (Table II-3). It should be noted that some of the rich particles were much higher in activity than average. This may have been due to an exceedingly high copper content.

From these experiments it was evident that a flux of 5×10^{13} neutrons/(cm^2)(sec) was far too high. To ascertain the right flux level, a series of experiments was made with pure $CuSO_4 \cdot 5H_2O$ irradiated 60 sec. The flux ranged from 5×10^5 (^{239}Pu-Be source) to 5×10^{13} neutrons/(cm^2)(sec). The results showed that a flux of approximately 10^{10} neutrons/(cm^2)(sec) would be suitable for irradiation times of 60 sec and for small pieces of 0.1 to 5 g. Since the activity increases nearly linearly with time, higher fluxes are required for shorter irradiations. The activation characteristics of very large pieces cannot yet be predicted. It was noticed that with increasing mass the overall activity increases linearly, so that bigger pieces seem to be more favorable and need lower fluxes. However, there will be a limit to this advantage due to the absorbing effects of greater material thicknesses.

(2) Observation of Radiation Spectrum. After it was found that the overall radiation measurement did not give satisfactory results, the gamma spectrums of irradiated ore and copper sulfate samples were studied in detail. A 256-

Table II-3 RADIOACTIVITY OF INDIVIDUAL PIECES OF POOR AND RICH COPPER ORE

Activity, counts/(min)(g)			
31 hr after irradiation		51 hr after irradiation	
Poor	Rich	Poor	Rich
15,905	29,054	6,513	10,930
16,381	50,103	6,522	18,635
17,049	40,096	7,031	15,130
17,032	30,133	6,719	11,385
16,593	37,645	6,691	14,208
17,175	98,033	6,917	34,900
17,486	25,472	6,927	8,869
17,323	42,032	6,946	15,217
16,849	27,914	6,496	10,029
17,217	27,364	6,646	10,000
16,901 (av.)	34,421 (av.)	6,741 (av.)	12,711 (av.)

channel analyzer was used. The unit consisted of a 3-in. NaI(Tl) crystal, channel unit, and printer. The printed counts per channel were later transformed to graphs to show the energy distribution of the induced radiation. The equipment was calibrated with standards of ^{22}Na, ^{132}Cs, ^{60}Co, and ^{54}Mn.

The first specimens examined were the 20 ore pieces from the first irradiation experiment after activation in a flux of 5×10^{13} neutrons/(cm^2)(sec) for 5 sec and a subsequent decay for 30 hr. In both the high- and low-grade ("rock") samples, the activity of ^{24}Na remained, while copper was found only in the richer pieces. The energy of the copper radiation was 0.511 Mev, the energy of annihilation radiation of β^+ particles with ordinary electrons. The ^{64}Cu peak of 1.34 Mev was not found.

The activities that could be detected a very short time after irradiation were then determined to find out if the isotope ^{66}Cu was useful for analytical purposes. Two hundred milligrams of pure $CuSO_4 \cdot 5H_2O$ was irradiated 60 sec at a flux of 5×10^{10} neutrons/(cm^2)(sec) and the gamma spectrum was observed, beginning 4.75 min after irradiation and continuing through 42.16 min. Three peaks were found: the 0.51-Mev peak of ^{64}Cu, 1.04-Mev peak of ^{66}Cu, and a very small peak for the 1.34-Mev energy of ^{64}Cu.

In a third experiment one low- and one high-grade piece of ore were irradiated together with a reference sample of 200 mg of $CuSO_4 \cdot 5H_2O$ at 5×10^{10} neutrons/(cm^2)(sec) for 60 sec. The first measurements were made after 4.5 min for the low-grade ore and after 3 min for the high-grade. Continuous readings were then made until about 20 min after irradiation. The radioelements identified are marked on Fig. II-8, which shows the spectrums of high- and low-grade ores 13 min after irradiation. The high-grade ore shows two copper peaks, one for ^{64}Cu at 0.511 Mev and one for ^{66}Cu at 1.04 Mev, although these peaks are not markedly present in the low-grade ore. The radiations of ^{56}Mn, ^{24}Na, and ^{28}Al are present in both samples.

After a careful evaluation of the spectrums given in Fig. II-8 and similar curves made at various times after irradiation, it was concluded that ^{64}Cu is a better indicator isotope for copper than ^{66}Cu for the following reasons:

1. Greater peak height after a short waiting period, and thus better sensitivity to different copper contents

2. Longer half-life, and therefore time lapse before evaluation relatively independent of decay

3. The possibility of avoiding confusion of ^{27}Mg (1.02 Mev) with ^{66}Cu (1.04 Mev)

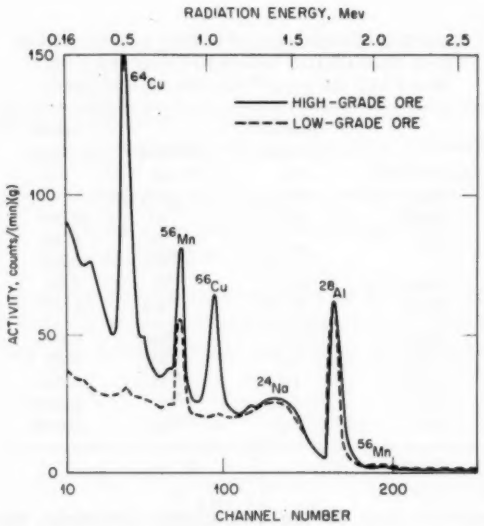

Fig. II-8 Spectrums of gamma radiation energy from 0.16 to 26 Mev emitted from high-grade ore (6% Cu) and low-grade ore (0.02% Cu). Waiting time after irradiation, 13 min.

(3) Overall Radiation Decay. For future application of the neutron-activation technique, it is necessary to know how long the irradiated ore pieces retain their radioactivity. The 20 pieces of the first experiment were counted from time to time, and the decrease in radioactivity was plotted. In the first 9 days, the activity decreased rapidly. The activity reached $1/10$ of the original value after 3 hr, $1/100$ after 50 hr, and $1/1000$ after 100 hr. After this there remained a very weak activity for a comparatively long time. This activity contained the isotope ^{59}Fe (half-life, 45 days) and another unidentified isotope with a half-life of more than 100 days. The irradiation of these ore particles was carried out for 5 sec at a flux of 5×10^{13} neutrons/(cm^2)(sec), but industrial applications will use a flux of 10^9 to 10^{10} neutrons/(cm^2)(sec), perhaps with considerably shorter irradiation times. Therefore the activity induced should drop after 2 or 3 days to near background, and the concentrates and dumps will not remain significantly radioactive.

(4) Consideration of Suitable Counting Technique for Radiocopper. Three ways of counting the induced radioactivity are possible:

1. Total radiation counting
2. Discrimination of copper radiation from other emitted radiation by gamma spectroscopy
3. Coincidence measurement of annihilation radiation

For the neutron-activation technique, the overall counting method was not successful because of the activity induced in other elements present. The second possibility proved to be successful even down to low copper contents, but it had disadvantages for industrial use. The available very high quality NaI crystals that are needed for spectroscopy are expensive, are not shockproof and moistureproof, and are not made much larger than 4 in. in diameter, and an additional discriminating electronic circuit is required. The third possibility seemed promising because:

1. Among all the induced gamma activities after neutron irradiation, there is only one annihilation-gamma emitter, namely, ^{64}Cu.
2. Large, rugged, and comparatively cheap detectors are available.
3. Coincident counting techniques give very little background radiation even for very large crystals.

SORTING DEVICE FOR COPPER ORE[4,24]

The two sorting devices mentioned in the literature[17,18] operate with a horizontal belt as the transporting unit for the mineral pieces. The advantage of this method, exact adjustability of belt speed to apparatus response, has to be compared to the disadvantages: relatively low rate of particle flow and use of mechanically moving parts in the unit (belt and rollers).

Senftle and Gaudin[21] mentioned in 1951 that ore pieces could be activated by dropping them through chutes in a reactor. The picking device described below was based on the free fall of ore particles through it. This device requires a minimum time for evaluation of each piece and therefore allows a maximum throughput.

Since the speed of a free falling particle increases from the point of release, particles should be counted as close to the release point as possible so that the counting time will be maximum. By the same token a maximum length of counter is also desirable. Maximum counter efficiency can be obtained by surrounding the path of free fall with a doughnut or tubelike detector. However, big and long counters are expensive or impossible to get, and they have the disadvantage of producing a very high background. The detection method used the β^+ decay of 12.8-hr ^{64}Cu; the β^+ interacts with an electron in the surroundings, resulting in the coincident release of two gammas of 0.51 Mev that travel in opposite directions. A plastic scintillator made of polyvinyltoluene, 10 in. in diameter and 13 in. in length with a 2.5-in. hole drilled perpendicular to the axis (Fig. II-9), was cut in half to use these special radiation properties in a coincidence counting system. This system eliminates the background nearly completely if a fast coincidence circuit is used.

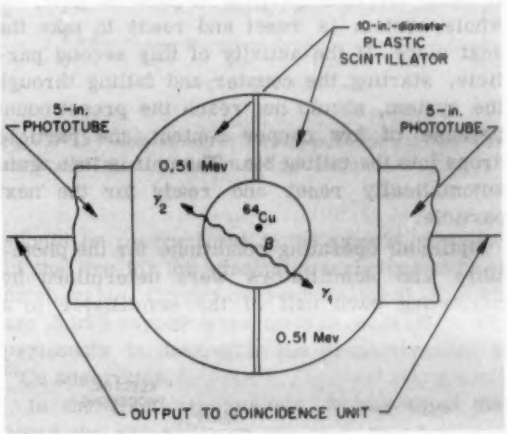

Fig. II-9 Arrangement of scintillation detectors and photomultiplier tubes for coincidence counting.

Apparatus Design. Because of these restrictions, the design of the apparatus provides for: (1) free fall of particles, (2) a long tubelike detector, and (3) coincidence counting.

The 13-in.-long scintillator stood upright on a table 30 in. high. The actual sorting gate was 15 in. from the ground to provide space for two bins. The overall path of a particle through the unit therefore was 28 in. When a particle was released 2 in. above the entrance to the counter (to provide space for a suitable releasing mechanism), the traveling time through the unit was 0.394 sec, for 0.178 sec of which it remained in the counter well (i.e., for 45% of the total time). These time-distance relations are

shown in Fig. II-10, where it can be seen that the copper content has to be evaluated in about 0.2 sec.

The separation procedure should work as follows (Fig. II-11): The previously activated particle enters the feeder and cuts the light beam to a photoelectric cell. This starts the coincidence counter, which counts the radiation of the falling particle until a preset number of coincidences is reached. This preset number is based on calculations from data about the activation, the copper content acceptance value, and counter efficiency. Having reached the preset number, the counter sends out a pulse that operates a gate. By this time the particle has left the counter and is dropped through the open gate in the concentrate bin. After a preset time, a few hundredths of a second longer than it takes the first particle to pass the gate, the whole system is reset and ready to take the next piece. If the activity of this second particle, starting the counter and falling through the system, should not reach the preset count because of low copper content, the particle drops into the tailing bin. The unit is then again automatically reset and ready for the next particle.

Optimum operating conditions for the phototubes and scintillators were determined by connecting each half of the scintillator to a

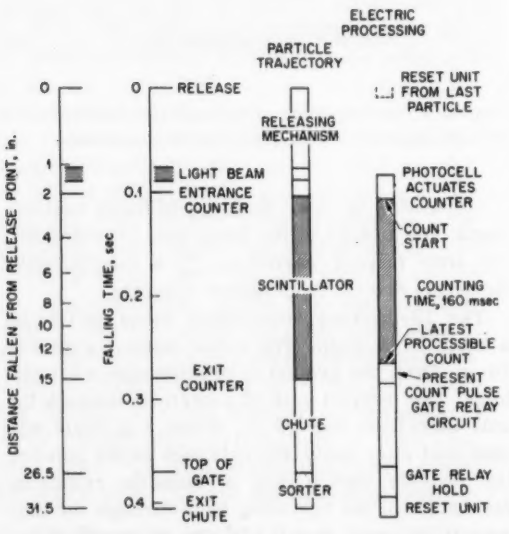

Fig. II-10 Time-distance relations between particle trajectory and electric processing in sorting device.

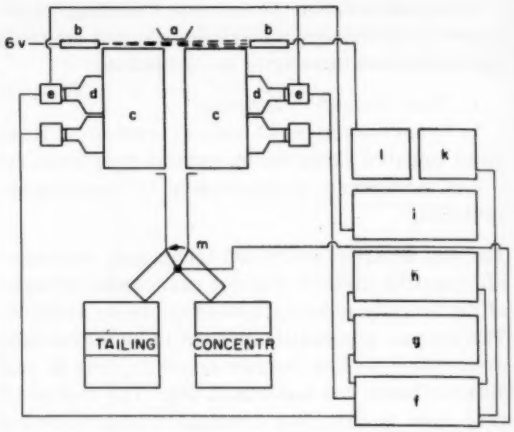

Fig. II-11 Sketch of sorting device. (*a*) Feeder. (*b*) Photoelectric eye and light source. (*c*) Plastic scintillator. (*d*) Five-inch photomultiplier tube. (*e*) Preamplifier. (*f*) Coincidence selector. (*g*) Overall activity scaler. (*h*) Coincidence scaler for preset count. (*i*) High-voltage supply. (*k*) Timer. (*l*) Photoelectric relay. (*m*) Flipping gate. (*n*) Tailing bin. (*o*) Concentrate bin.

scaler and checking the count-rate output under different conditions. Results were best with the crystal polished and coated with Glidden high-reflection paint. Then the site for the phototube was freed of paint, the phototube was attached with silicone glue, and the whole unit (crystal and tube) was covered with two layers of black electrical tape. The two halves, wrapped and sealed, were assembled, and the yield of coincidences was checked with a calibrated ^{22}Na source of 0.054 μc. At top sensitivity of 1500 volts on the tubes, 30% of the coincidences emitted were counted, which is close to the maximum amount of 44% detectable coincidences with this scintillator thickness and radiation energy. When no source or particle was in the counter, the number of random coincidences occurring from background radiation was 700 counts/min without shielding. After the counters were enclosed in 2 in. of lead, the rate dropped to 300 counts/min. If the evaluation time in the counter is 0.2 sec, then the background is about 1 count during this time.

The sensitivity of recording coincidences at various positions over the length of the scintillator with the phototubes always at the top of the scintillator was then determined. A calibrated ^{22}Na source, constantly giving off a known

number of gamma rays and annihilation coincidences, was held in various positions in the counter well, and for every position the number of coincidences was counted for 1 min. The counting rate was maximum at 6 to 9 cm from the top of the detector and decreased nearly linearly to about 23% of the maximum rate at the bottom. The maximum rate was 2700 coincidences per minute, or 10% of the total number emitted from the ^{22}Na source.

The 2-in. photomultipliers were then replaced by 5-in. tubes, which were moved down to about 5 cm from the top of the scintillator, and the experiment was repeated. The maximum counting value was at a point about 10 cm from the top of the detector. Here 19% of the total number of coincidences emitted was recorded in the scaler. Over the length of the detector, a good percentage of coincidences was measured. However, the use of two 5-in. phototubes on each scintillator instead of one should further increase this percentage.

In test operations, inactive ore particles were dropped through the activity emitted by a ^{22}Na source. Everything worked as expected. Evaluation of copper content in less than 0.025 sec was shown to be possible.

The apparatus in this form could sort particles giving off a certain number of coincidences from others that do not have the necessary activity. However, ore pieces, even if closely sized, may have different weights; therefore a substantial error can be introduced in this system.

Each piece must be weighed to correct for this uncertainty. Since the total radioactivity of each piece is roughly proportional to the weight of the piece, this activity can be used for the purpose of weighing. The unit was therefore modified so that an overall count from each piece can be obtained. In the modified design the overall count from the same phototubes that previously gave only coincidences is taken, and a predetermined number of overall pulses, say 10^4, is counted in an additional scaler (*g* in Fig. II-11). The coincidence counter is connected so that the ^{64}Cu pulses must be measured before 10^4 counts have been picked up from the ore piece. If the piece is large, it will give off these counts very quickly; if it is small, a longer time is required. By this method the overall count level should determine the counting time of copper pulses and thus give the copper content.

ACTIVATION OF COPPER ORE BY ADSORPTION

As an alternative to neutron activation of copper ore, Gaudin and Ramdohr[4] also studied the adsorption from solution of ^{64}Cu on chalcocite, a typical copper-bearing mineral. In a preliminary experiment, these workers found that chalcocite adsorbed* most of the ^{64}Cu from a solution but that quartz adsorbed almost none (Fig. II-12). The amount of copper adsorbed

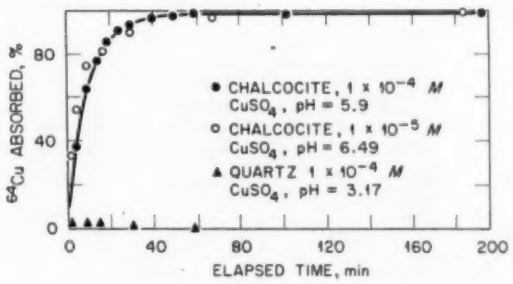

Fig. II-12 Absorption of ^{64}Cu by pure quartz and pure chalcocite after different contact times.

should be proportional to the amount of copper in the ore for the adsorption technique to be of much value. Copper ores containing 0.52, 3.11, and 5.96% copper were used in most of the experiments to determine the proportionality of ^{64}Cu adsorption.

In the first experiments, it was noted that about the same amount of copper was adsorbed on each ore sample and that the *p*H of the solution increased while it was in contact with the ore. This preliminary experiment suggested that copper was being precipitated in the pores of the ore by the alkaline reaction of the ore; therefore an experiment was done in which 0.05% sodium hexametaphosphate (Calgon) was added to the solutions to complex the copper, and the *p*H of the solutions was varied and controlled. The results of these experiments are given in Table II-4.

The ratios of specific activity were determined to be unfavorable in alkaline and slightly

*The term "adsorb" was used in the original report[4] and is retained here for consistency; however, in view of the highly specific nature of the interaction between the ^{64}Cu in solution and the copper ore, it is probable that isotopic exchange was taking place.

acid mediums. However, when the hydrogen-ion concentration was $10^{-3}M$, the average specific activity of the particles in the ores containing 5.96% copper was ~21,000 counts/(min)(g), and the average specific activity was ~900 counts/(min)(g) in those containing 0.24%. This is a ratio of specific activity between the two ores of 24.5. Since the ratio of the copper contents of the two ores is 24.8, this represents a desirable experimental condition in which the specific activity of a particle is directly proportional to its copper content. Further experiments showed that 0.05% Calgon and a hydrogen-ion concentration of $10^{-3}M$ were optimum for proportional adsorption. The time required to reach equilibrium adsorption of ^{64}Cu was ~30 min, which is quite long for a commercial process but should be satisfactory for laboratory studies.

Table II-4 RELATION BETWEEN *p*H AND THE ADSORBED ACTIVITY FOR ORES CONTAINING VARIOUS AMOUNTS OF COPPER

Cu ore		Ratio of ^{64}Cu adsorbed by ore at given *p*H to that adsorbed by ore with lowest Cu content				
Cu content, %	Cu ratio to ore with lowest Cu	*p*H = 1.22	*p*H = 2.08	*p*H = 3.03	*p*H = 5.55	*p*H = 8.30
0.24	$\frac{0.24}{0.24} = 1.00$	1.00	1.00	1.00	1.00	1.00
3.11	$\frac{3.11}{0.24} = 12.96$	29.31	17.14	11.96		2.05
5.96	$\frac{5.96}{0.24} = 24.83$	55.05	76.73	24.50	7.78	2.01

Recent Developments in Counting Methods

Studies are under way at several research institutions to improve and diversify counting methods in radioisotope applications. Two recent developments that have been reported are described below: the synthesis of exchange resins that scintillate under radiation and the construction of Geiger counters within flexible materials.

Geiger Counters in Flexible Materials

Richter and Gillespie,[25] working at Research Triangle Institute under a DID-sponsored contract, have developed Geiger counters from several flexible materials, including plastic sleeving and vacuum-cleaner hose. These flow counters, which can be coiled, wrapped, or placed in nonlinear configurations, suggest many uses. They are constructed of commercially available materials and can be made to any length. Pulse heights are smaller than those from comparable metal-wall counters but are always above 50 mv when flowing helium-butane gas is used as a counting medium. Plateaus are up to 1000 volts long with 2 to 5% slope along this span.

In some earlier work, Maze[26] painted colloidal graphite on soft glass tubing containing an axial tungsten wire. When the tube was filled with a counting gas and voltage was applied between the anode wire and graphite, the device behaved like a metal-cathode G-M counter. Since then, several external cathode counters and chambers have been constructed from pyrex and quartz.[27,28]

In the Richter-Gillespie devices, wire was slipped inside a hose or sleeving, a bare copper wire was spiraled outside, and a mixture of 98.7% helium and 1.3% butane (the Geiger gas sold by Nuclear-Chicago Corporation under its trademark Q-GAS) was allowed to flow through the tube. The counters were assembled either by joining together short segments of plastic sleeving (Fig. II-13*a*) or by starting with an adequate length of vacuum-cleaner hose (Fig. II-13*b*). The anode was maintained in an axial position during tube flexing by using polyethylene spacer disks or a flexible "skeleton" composed of disks and rods (Fig. II-13*c*). End pieces were glass T-tubes inserted in the tubing

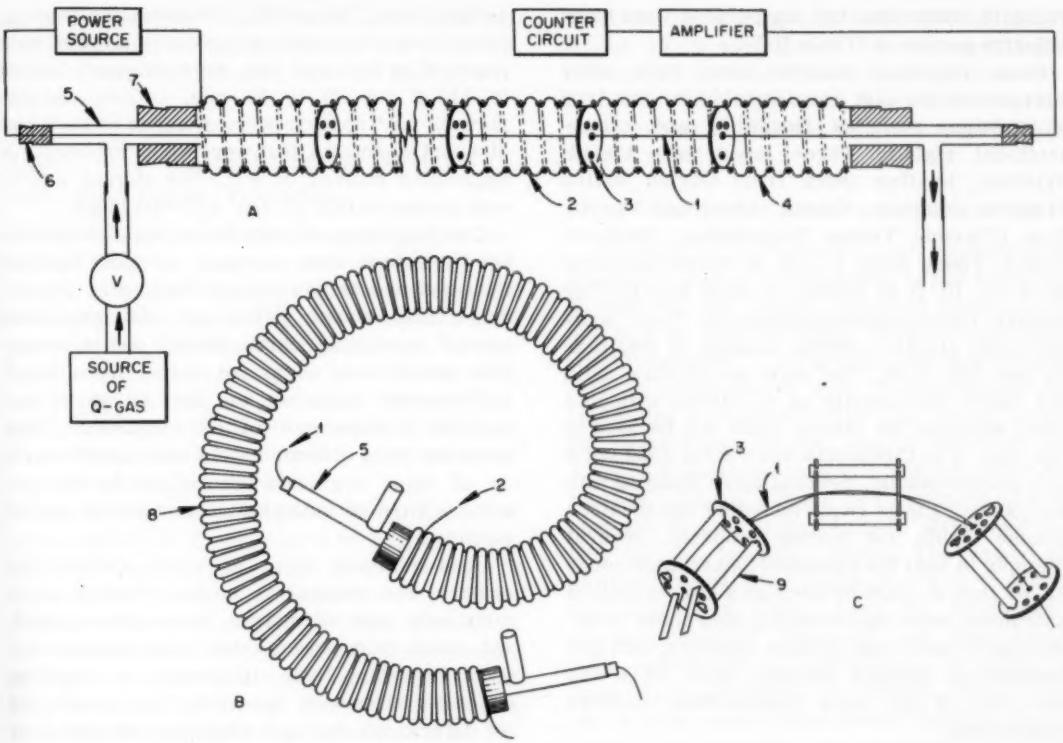

Fig. II-13 Construction of flexible-tube Geiger counters: (*a*) segmented counter; (*b*) vacuum hose counter; (*c*) cage assembly.

Explanation of Numbers

1	Anode wire	4	Overlap of segments	7	Rubber stopper
2	Cathode wire	5	T-tube end pieces	8	Vacuum-cleaner hose
3	Polyethylene disk	6	Split stopper	9	Polyethylene strips

through rubber stoppers. The anode, which entered through the T-tubes, was kept taut by slipping it through a second rubber stopper (when compressed, the stopper was gastight) at the end of the T-tubes, and in some cases by fastening a spring to each end piece. Experimental counters of plastic sleeving 3 cm by 1 m and vacuum-cleaner hose 1¼ in. by 10 ft were made and tested during this study. A 6-ft hose counter is shown in Fig. II-14.

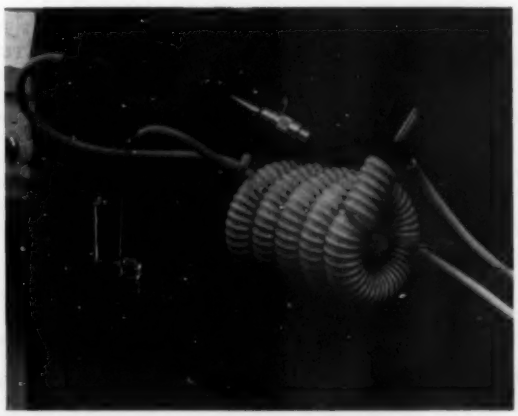

Fig. II-14 Nylaflex-constructed flexible Geiger counter. It is shown here set up as an anticoincidence coil.

EXPERIMENTAL

Two problems in making a flexible-tube counter were: (1) obtaining a conductive material for the external cathode having the desired flexibility and (2) maintaining the anode in an axial position. Among the plastic tubings investigated, all those which were found suf-

ficiently conductive for the purpose were vinyl chloride polymers (Table II-5).

Some polyvinyl chloride hoses have other characteristics that are desirable for this type of counter, such as flexibility and cross-sectional rigidity. Three types were tested: Nylaflex, Dayflex (both from Dayton Daflex Plastics Company, Dayton, Ohio) and Vac-U-Flex (Flexible Tubing Corporation, Guilford, Conn.). These were $1\frac{1}{4}$ in. in inside diameter by 6 or 10 ft in length. A 10-ft Vac-U-Flex counter, containing the polyethylene "cage" system (Fig. II-13*b*), showed a slope of less than 2% per 100 volts. The rigid metal-wire helix was used successfully as a cathode with this hose, whereas the others could not be used in this way. The thresholds were about 1300 volts with helium-butane. Several hours' flushing with the counting gas is required before the counters become stable and operate properly. Several attempts to seal the vacuum-cleaner-hose counter so that it could be used as a self-contained instrument were unsuccessful; thus these counters can be used only as flow counters, with gas continuously pumped through them. This was also true of the other flexible-tube counters constructed.

The first flexible-tube counters were made with a tungsten anode inside Tygon tubing. Glass beads were glued at 1-cm intervals on the anode, a bare copper wire was spiraled outside, and gas was allowed to flow inside. It showed a fair plateau, but some of its properties made is undesirable, and other plastics were tried (Table II-5). The most satisfactory was PVC-744, a material used in electronics as insulating "spaghetti." In later experiments, tubing was corrugated (slipped over an aluminum mandrel or threaded rod, wire-wrapped, heated to 110°C for 20 to 30 min, cooled, and removed), and spacers were attached to each end of short segments that were glued together. A segmented counter of PVC-744 showed a 500-volt plateau with a 5% per 100-volt slope.

Counting rates of both the segmented and the hose counters were as much as many hundred thousand counts per minute with little coincidence loss. Geiger pulses are not propagated beyond insulating obstructions, and a single tube therefore is composed of a series of short independent counters, any one of which can operate irrespective of its neighbors. Thus counting rates of flexible-tube instruments made up of many segments are limited by the resolving time of individual segments or scaler circuits.

Good plateaus were obtained whether the counter was straight or coiled. Various anode materials and diameters were investigated, and, aside from the expected voltage dependency upon diameter, little difference in operating characteristics was observed. The counter did not deteriorate during a counting-rate test over more than 3×10^8 counts.

The absolute efficiency of flexible-tube counters for detecting gamma rays was not determined. It is probably less than that of metal-wall counters, whose efficiency is about 1%. Attempts to increase this sensitivity were unsuccessful. Those beta particles entering the active volume of the instrument are counted. Experiments in which the counter was used as

Table II-5 TUBINGS INVESTIGATED FOR USE IN SEGMENTED COUNTERS

Tubing	Manufacturer	Conducts current
SLY-105	Illumitronic Engineering, Sunnyvale, Calif.	Yes
Tygon R3603	U. S. Stoneware Company, Tallmadge, Ohio	Yes
PVC-744	Alpha Wire Corporation, New York, N. Y.	Yes
PVC-105	Alpha Wire Corporation, New York, N. Y.	Yes
Dacron-Tygon*		Yes
Tygon R2400	U. S. Stoneware Company, Tallmadge, Ohio	No
Nalgon	Nalge Corporation, Rochester, N. Y.	No
Polyethylene		No
Silicone rubber	Bentley-Harris Manufacturing Co., Conshohocken, Pa.	No
Natural rubber		No
"Conductive" tubing	Bittner Corporation, New York, N. Y.	Yes, but no plateau obtained

*Knitted Dacron (methyl terephthalate–ethylene glycol polyester fiber, Du Pont Company) cloth tubing made gastight with Tygon paint containing colloidal graphite.

an anticoincidence device were not successful; the reduction in background of the shielded counter was only 2.5-fold, whereas 10-fold was expected.

Anion- and Cation-Exchange Resins with Scintillation Properties

Ion-exchange techniques have played an important role in analytical radiochemistry, but plastic scintillators are relative newcomers in detecting radioactivity.[29–31] Seeking a dual-purpose product, Heimbuch and coworkers,[32] working under a DID contract, have synthesized resins having both ion-exchange and scintillation properties. Their cation resin, SCR-1, and anion resin, SRA-1, now are commercially available from Tracerlab.

The resins can be used to detect alpha and beta emitters as ionic species by sorption from aqueous solution and coupling the resin to a photomultiplier tube and pulse counter. Many uses have been suggested for beads made from the resins, including monitoring of in-line process streams and rapid determination of tracers in batch-mixing studies. Their chief advantages stem from the combination of exchange and scintillation properties. Some radiochemical analyses can be shortened and simplified with this tool. The use of the resins complements other methods of radioisotope detection and counting, but they do not approach the absolute sensitivity of low-level beta or alpha counters, which detect samples with activities less than 1 dis/min. Resins can achieve this sensitivity indirectly with larger samples, however, since they concentrate the radionuclides.

In a portion of the work sponsored by Tracerlab, Heimbuch et al. performed practical experiments (1) to remove and detect ^{131}I from milk, (2) to detect ^{14}C-tagged amino acids, and (3) to measure quantitatively the radioactivity sorbed on the resin by exposure of photographic film to the resin.

Several ionic species of radionuclides, such as ^{90}Sr, ^{14}C, ^{239}Pu, and ^{36}Cl, were counted on these resins with efficiencies of from 35 to 85%. Radioisotope dilution techniques and radiochemistry with ^{90}Sr, and later with ^{60}Co, were used to measure the ion-exchange capacity of the beads. An exchange capacity of 0.1 meq per gram of beads for the cation resin was attained, but more useful pulse heights were obtained at a range of 0.01 to 0.05 meq/g (about 1% of the capacity of nonscintillating commercial resins). Anion-exchange capacities of 0.1 to 0.2 meq/g (nearly 5% of commercial capacity) were obtained with only slight reduction in pulse height.

PREPARATION OF SCINTILLATING BEADS

Attempts to sulfonate or coat commercially available plastic scintillating beads were unsuccessful. But plastic phosphor beads 0.5 to 0.7 mm in diameter were made by suspension polymerization[33–35] of polystyrene or polyvinyltoluene cross-linked with divinylbenzene and containing *p*-terphenyl. For the cation resin, the wave-band shifter usually selected was 1,4-*bis*-2-(5-phenyloxazolyl) benzene (POPOP). Ionizing sulfonic groups were introduced at or near the surface of the beads by direct sulfonation of the aromatic nuclei. The wave-band shifter for the anion resin was 9,10-diphenylanthracene, in which case the beads were chloromethylated, aminated, and then treated with methanolic trimethylamine to yield the quaternary ammonium derivative. The resulting resins were cross-linked polymers containing the exchange groups chemically bound to the surface of the beads and fluorescent compounds in solid solution.

Factors affecting scintillation pulse height, optical clarity, diameter size, and monodispersion of the beads were studied to improve pulse height obtained from the resins. Seven experiments were performed and are described in detail elsewhere:[32]

1. Comparison of polymerization initiators
2. Suspension stabilizers
3. Effect of degree of resin cross-linking
4. Comparison of various wave shifters
5. Effect of graded salt concentrations in the suspension solutions
6. Comparison of graded *p*-terphenyl concentrations
7. Effect of mineral oil on pulse height and bead quality

COUNTING EFFICIENCY OF EXCHANGE RESINS

Radionuclide ions were sorbed on scintillating resins, and activity was determined either by directly coupling a plastic cup (PC) containing beads to a photomultiplier tube with optical grease or by placing the sorption column in a

modified-well liquid scintillation counter (LSC). A pulse-height analyzer was used to measure output. After the activity of the beads had been counted, the activity of the sorbed ions could be ascertained by radiochemical analysis and, from this value, the efficiency calculated. Table II-6 shows the results of several experiments of this kind.

Cation-Exchange Resin. The efficiency of counting ^{90}Sr and ^{90}Sr-^{90}Y was determined by sorption of cations on 1-g samples of beads in 0.5- by 3.0-in. columns from 0.05*M* ethylenediaminetetraacetic acid (EDTA) at *p*H 5.5 and elution of ^{90}Sr with 6*M* HNO_3. The counting efficiency of ^{90}Sr compared favorably with the end-window tube method. The beads cannot compare with the low-background counter since the noise of the photomultiplier tube limits the sensitivity. The sorption of ^{90}Sr in the presence of magnesium and calcium was measured[36] by spiking 3 liters of tap water (containing a total of 24 meq of Ca^{2+} plus Mg^{2+}) to an activity level of 0.5 dis/(min)(ml) with ^{90}Sr, passing it through a column containing 3 g of resin with a total exchange capacity of 0.06 meq, and counting the activity on the beads. About 380 dis/min of ^{90}Sr, or 27% of the carrier-free activity, was sorbed from the water, indicating that ^{90}Sr did indeed displace Ca^{2+} and Mg^{2+} from the resin. The total count rate of 200 counts/min, obtained upon counting the beads in a Lucite cup, was 53% of the total ^{90}Sr activity sorbed.

Three alpha emitters, ^{239}Pu, ^{241}Am, and ^{210}Po, were counted like ^{90}Sr except that radiochemical analysis was not done. It appeared that mixtures of alpha emitters with an energy difference of 0.5 Mev could be resolved (Fig. II-15).

Table II-6 ISOTOPE COUNTING EFFICIENCIES WITH SCINTILLATING ION-EXCHANGE RESINS

Isotope	Maximum particle energy, Mev	Ionic species sorbed	Method of counting	Counting efficiency, %
^{14}C	0.158	CO_3^{2-}	LSC	35
^{35}S	0.167	SO_4^{2-}	LSC	39
^{36}Cl	0.714	Cl^-	LSC	85
		Cl^-	PC	50
^{131}I	0.610	I^-	LSC	74
^{90}Sr	0.540	Sr^{2+}	PC	50
^{90}Y	2.270	Y^{3+}	PC	71
^{239}Pu	5.15	$PuCl_n^{(n-4)-}$	LSC	77
		Pu^{4+}	PC	35–40
^{237}Np	4.79	$NpCl_n^{(n-5)-}$	LSC	70
^{241}Am	5.48	Am^{3+}	PC	40
^{210}Po	5.30	Po^{4+}	PC	40

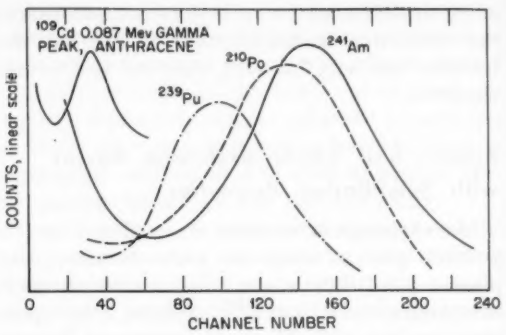

Fig. II-15 Relative alpha response curves of scintillating ion-exchange beads. (Total peak counts are not to be compared.)

Nickel-63 and ^{204}Tl were sorbed on beads, which were counted directly in a regular liquid-scintillation-counter container. Nickel-63 (beta maximum, 0.067 Mev) was counted with 12% overall efficiency in two such containers. The sorbed activity of 25,300 dis/min, as determined by radiochemical analysis and counting in a 2π flow counter, gave a net count rate of of 3170 counts/min in the liquid scintillation counter. A blank containing 1 g of beads had a background of 80 counts/min; a blank without beads also showed 80 counts/min. Thallium-204 (beta maximum, 0.760 Mev) was counted with an overall efficiency near 60%. The beads were found to have an advantage over gel or liquid scintillation solutions in that quenching agents in the sample did not affect their fluorescence. There was no resolution by the beads of gamma-ray energy with respect to a "peak" of pulses in a given channel of the analyzer, but comparisons could be made (Fig. II-16). Plastic phosphor cylinders of the same formula as the ion-exchange beads were made for between-batch testing and also for comparison within batches. Pulse heights from disks made of these cylinders were 30 to 35% of that of an anthracene crystal of equal volume when midpoints of the falling Compton edge were compared. Cesium-137 was used as the gamma source for these comparisons.

Anion-Exchange Resins. The counting efficiencies for several anionic alpha and beta emitters are listed in Table II-6. Absolute comparisons of the resin counting efficiency for

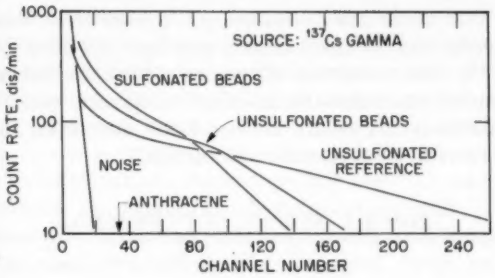

Fig. II-16 Gamma response curve for scintillating beads. The gain setting on the amplifier and voltage on the photomultiplier tube were such that the 0.087-Mev gamma ray of ^{109}Cd gave a peak at channel 33 on a 256-channel analyzer with an anthracene crystal.

the listed isotopes could not be made since more data were needed. It should be noted that the plastic-cup method was not so efficient as the liquid-scintillation-counter method. In the case of ^{36}Cl, the ratio of counting efficiencies for PC/LSC was 0.59.

Beta emitters gave a much higher photon yield per Mev of energy sorbed by the resin than did alpha emitters. This can be seen by comparing the counting efficiency of ^{36}Cl (beta maximum, 0.714 Mev) at 85% in the LSC with ^{239}Pu (alpha, 5.15 Mev) at 77% in the LSC. This is characteristic of plastic scintillators. Neptunium-237 and ^{239}Pu were counted with 70% efficiency by use of a liquid scintillation counter. This is significant because the isotopes were sorbed from concentrated HCl, and apparently the HCl had little or no quenching effect on the scintillation property of the beads. A radionuclide that forms an anionic chloride complex (e.g., Fe or Co) presumably could also be sorbed and counted on the anion resin.

PHYSICAL AND CHEMICAL PROPERTIES OF THE RESIN

Effect of Solvents. The resin has good stability toward alcohols and aromatic solvents such as benzene, toluene, or xylene. However, the aromatic compounds swell the bead and leach some of the fluor near the surface. Halogenated hydrocarbons and acetone also swell the bead. Toluene swells the resin more than do the lower alcohols and acetone, but this does not have an adverse effect on the light output. The count rates for several samples remained fairly constant for 30- to 60-day periods in toluene, as is illustrated in Table II-7. A point of caution about organic liquids is the possibility of using a compound, such as pyridine or nitrobenzene, which not only swells the bead but also quenches the fluorescence. However, even the use of trimethylamine, which is a strong liquid scintillation quencher, had little effect on pulse-height reduction during the preparation of the anion resin.

Toluene-Methanol Drying Treatment. Anion- and cation-resin samples were loaded into columns and washed alternately with toluene and absolute methanol. The resin was allowed to stand in toluene for 10 min and then rinsed with methanol. This treatment simulates the "drying" of the aqueous beads preparatory to their counting in toluene. After 10 wash cycles, the pulse height of each sample was measured. There was a slight reduction (~5%) in the pulse height of the anion resin, but none was observed in the cation resin.

Regeneration Studies. Samples of both the anion and cation resins were put through 50-cycle regeneration tests. The resin was loaded into an ion-exchange column and treated sequentially with acid and base washes. The reagents used were 5% NaOH and 5% HCl, which were used alternately with distilled-water washes after each treatment. The anion resin did not show any decrease in pulse height; however, there was a 10% reduction in the pulse height of the cation resin.

Inorganic Reagents. The anion resin was unstable to concentrated HNO_3 for 10 min at room temperature. The resulting beads were yellow to amber in color with 50% loss in pulse height. When treated with 6*M* HNO_3 in a similar manner, the pulse height of the anion resin was reduced slightly (5 to 10%). Commercial anion resins of similar chemical structure are not stable to warm solutions of 3.5*M* HNO_3. The cation resin, on the other hand, has shown con-

Table II-7 ANION-RESIN-FLUORESCENCE STABILITY IN TOLUENE

Sorbed isotope*	Counting efficiency		
	Initial %	Time elapse, days	Final %
^{36}Cl	85.6, 84.6	63	83.3, 83.2
^{239}Pu	71.4	55	77.8

*Duplicate samples were run on ^{36}Cl.

siderably more stability toward 6*M* HNO_3. A 6*M* HNO_3 wash was one of the steps used to remove Ag_2SO_4 sulfonation catalyst. Anion resin was shaken with 10% aqueous hydrogen peroxide for 90 min at 25°C. The loss in pulse height was 5% or less.

Both resins have shown good stability toward concentrated HCl and NH_4OH solutions. The resin was also stable to boiling aqueous solutions that did not contain strong oxidants. The beads are not deformed at 100°C but cannot be heated to this temperature in the presence of oxygen.

Specific Gravity. The resins have a specific gravity slightly greater than water. Beads with a diameter range of 0.3 to 0.5 mm were tested in distilled water with respect to settling rate. More than 90% of the beads settled at an average rate of 5 to 7 in./min at 25°C.

PRACTICAL APPLICATIONS

Heimbuch and coworkers explored three practical applications of scintillating resins: sorption of ^{14}C-labeled compounds from solutions, sorption of ^{131}I from milk, and quantitative determination of activity by autoradiography.

^{14}C-Tagged Compounds. Five milliliters of a solution of 1 μg of ^{14}C-tagged histamine (33,000 dis/min) was passed twice through a small column containing approximately 0.6 g of cation resin. The column was washed once with 5 ml of distilled water, and the effluent was assayed for ^{14}C activity. Results indicate that about 95% of the original activity was exchanged on the resin. The minimum counting efficiency of the ^{14}C-tagged histamine sorbed on the resin was 20%. This was 66% of the counting efficiency of the same compound in a liquid scintillation solution.

Five milliliters of a standard aqueous ^{14}C-methionine solution was passed through 1 g of H^+-form cation resin and washed with ethanol. A similar experiment was performed with anion resin in the OH^- form. Results indicate that 99% of the amino acid was sorbed by each resin. The minimum counting efficiencies for the system were 25% and 23% for toluene-immersed cation and anion resins, respectively. The counting efficiency for methionine in a liquid scintillation solution was 45%. Thus scintillating resins presumably can be used when the amino acid being determined is incompatible with the liquid scintillation solution.

Sorption and Detection of ^{131}I from Milk. Raw milk was obtained from a cow that had been fed ^{131}I. The collection efficiency of the scintillating anion-exchange resin was compared with a commercial resin, Dowex 1-X8, containing the trimethylbenzylammonium group.

Table II-8 REMOVAL OF ^{131}I FROM MILK

Resin	Volume of milk, ml	Total ^{131}I removal, dis/min	^{131}I sorbed per milliliter of milk, dis/min
Dowex 1	100 at 25°C	404	4.0
Dowex 1	100 (+ toluene) at 25°C	450	4.5
SRA	750 at 5°C	3444	4.5
SRA	740 of a 10-fold dilution at 5°C	341	0.46
SRA*	500 (+ toluene) at 5°C	2025	4.1

*Effluent was passed over Dowex 1. No significant activity (<1%) was observed, indicating that the retention efficiency of the scintillation anion resin (SRA) was equal to that of the standard Dowex 1 resin.

Three grams of 32–60 mesh scintillating resin with 0.10 meq/g exchange capacity was compared with 2.5 g of 100–200 mesh commercial resin with a capacity of 3.2 meq/g. The flow rate of milk through the columns was maintained at about 2 ml/(cm^2)(min). The resins were first put in the chloride form with HCl and then washed with distilled water until nearly neutral effluents were obtained. Nothing was added to the milk except toluene, which was used as a preservative for half the samples. It was found that the scintillating resin, with less than one-tenth the exchange capacity of the commercial resin, removed the iodine from milk with equal efficiency. Furthermore, over seven times the volume of milk was passed through the fluorescent resin as through the commercial resin. Activated resin samples were compared by transferring them to a 15- by 75-mm test tube and counting them in a gamma well counter (NaI crystal). Retention of ^{131}I was better than 90%, even when diluted milk with a specific activity of only 0.45 dis/(min)(ml) was used. It should be noted that the maximum permissible concentration of ^{131}I in milk is 200 μμc/liter or 0.44 dis/(min)(ml). It was concluded that the anion resin could serve adequately as an analytical tool for ^{131}I in aqueous solutions. Experimental results are summarized in Table II-8.

Photographic Film Sensor. One of the current problems for accurate low-level counting is the necessity for expensive and complicated equipment. The possibility of using scintillating ion-exchange resins coupled with photographic film as a nonelectronic detection device was investigated. Plutonium-239 and ^{36}Cl were sorbed on resin in 1.5-dram glass vials. A sensitive film was wrapped directly around the vial and exposed to the activated resin for various periods of time. The exposure times (24 hr) and activities required [50,000 dis/(min)(g)] to produce quantitative results render this system impractical at this time.

POTENTIAL APPLICATIONS

Heimbuch et al. envisaged several applications in analysis and research for scintillating ion-exchange resins. The concentration by evaporation of solutes from large quantities of dilute solutions can be eliminated in some cases, and the use of the beads in leak detection with alpha or beta tracers is possible. Monitoring of in-line process streams where the beads can be used to detect tracers can be considered. The beads can be placed in a loop and viewed with a photomultiplier tube for detection of function (or malfunction) of a process. An extension of this principle can be applied to the monitoring of ion-exchange and chromatographic columns. With the insertion of a scintillating resin "sandwich" at a specific position in the column, the detection of a radiotracer could indicate the resolution of a desired constituent, exhaustion of the column capacity, or the time to collect a given fraction.

Since the resins are not affected by oxygen or many of the quenchers present in biological samples, they complement liquid scintillators when there is sample incompatibility and quenching.

Because of the ease of sample preparation with these resins, radiochemistry may be shortened for some isotopes that can be sorbed and counted directly on the bead. The difficulty of electroplating certain alpha emitters can be circumvented for samples emitting about 20 dis/min or more. The property of ion exchange also allows for the preparation of a "weightless" sample so that self-sorption of emitted particle energy is not a problem.

The resin sample allows for immediate counting; carrier yield can be determined later. This would be important where daughter growth complicates counting and calculations. Rapid sample preparation is important for short-lived alpha and beta emitters needing fast decontamination and counting times. Aqueous solutions containing unknown levels of activity can be screened with an economy of time, labor, and materials.

The resin method is also an alternative counting technique to that of gas counting. The gas apparatus is complex, and the methods can become tedious for sample preparation. Both ^{14}C and CO_2 and ^{35}S and SO_2 are determined by gas counting techniques. It has been demonstrated that the anion resin will efficiently sorb and count ^{14}C as carbonate and ^{35}S as sulfate. Inorganic and organic phosphates tagged with ^{32}P can be counted efficiently on the anion resin and thus are potentially useful in research with nucleic acids, phospholipids, and carbohydrates. Other possible applications are in space and air-pollution work.

Radio-Snow Gages: A Review of the Literature

By James L. Smith and Donald W. Willen*

In 1950, information about the use of radioactive sources began to appear in the literature of both snow and soil scientists. Since the Gerdel pilot study[37] in 1950, more than 20 papers have been published concerning the use of radioactive sources as tools for measuring snowpack water content, this research having been carried on in seven different nations. All but three of these papers describe fixed-location snow gages used for measurement of total water equivalent in a snowpack. Agashkin[38] and Sternzat and Sapozhnikov[39] reported on semiportable units, but these units are essentially the same as the fixed equipment cited below. Ten of the cited papers report on the development and testing of portable equipment for measuring soil water content and soil density, and three papers are concerned with use of these portable

*California Cooperative Snow Research Project, conducted by the Pacific Southwest Forest and Range Experiment Station, Forest Service, U. S. Department of Agriculture, in cooperation with the State of California, Department of Water Resources.

units for measuring water content and snow density at various depths in a snowpack profile.

Fixed-Location Snow Gages

Gerdel's pioneering research set the stage for experiments using isotopes to measure snow water content. He reported the development of a radiotelemetering snow-gage system that used the principle of water absorption of gamma emissions. Since gamma rays are about 100 times more penetrating than beta and 10,000 times more penetrating than alpha, he felt that only gamma rays have sufficient energy to penetrate a deep snowpack. He described the theoretical approach to the problem as: "The measured intensity of the radiation which passes through snow... may be expressed in terms of water equivalent of the snowpack regardless of its density or variations of density within it."

Preliminary experiments of Gerdel et al.[37] in the spring of 1948 at the Central Sierra Snow Laboratory in California involved gamma emission from 20 mc of radiozinc installed beneath a 40-in. snowpack of 50% density, i.e., 20 in. equivalent water. A G-M tube and a survey meter connected to a recording potentiometer produced a strip chart that recorded snow depletion for 1 week. Gerdel remarked that this was probably the first record of snowmelt ever obtained without disturbing the snowpack by sample removal.

During the 1948–1949 snow season, a ^{60}Co source was installed flush with the soil surface, and a G-M tube was suspended 15 ft above it. Pulses received by the G-M tubes were transmitted by radio to the laboratory headquarters. A ^{90}Sr source was used in subsequent experiments during the summer of 1949.

Calibration experiments were conducted with snows of different densities and with a water tank installed between the radioisotope and the G-M tube. Equations and calibration curves are given in Gerdel's article.

SOURCES

Cobalt-60 has been the most popular source with all investigators because of its high specific activity, relatively long half-life (5.3 years), and simple radiations (1.17 and 1.33 Mev). However, other sources have also been used.[37,40] Radioactive cobalt sources used have varied in size from 30 to 80 mc.[37,41–43]

EQUIPMENT INSTALLATION

Equipment installations and measuring techniques have varied in these studies. Gerdel et al.[37] placed the radioactive source at the soil surface, as did Agashkin,[38] Doremus,[44] Hildebrand,[45] Martinec,[42] Robinson,[43] and Sternzat and Sapozhnikov.[39] Higashi and Itagaki[46,47] placed the source above the ground with the G-M counter tube at the soil surface. He felt that the counter temperature remained more constant under the snow cover than in the open and that background radiation was reduced or eliminated since the snowpack tended to absorb it. Duncan and Warnick,[40] Fischmeister,[41] and Itagaki[48] also used this arrangement. Itagaki used ethyl formate as a quenching agent in the G-M tube because the more usual alcohol quench was not satisfactory at temperatures below 0°C.

The distance[46] between the radioactive source and the counter has usually been 10 to 15 ft. Occasionally, however, deep snow has covered the whole apparatus and bent or displaced it so that the source-counter relation has been changed, resulting in an inaccurate count.

Currently the most widely accepted model is the radioactive snow gage used by the U. S. Army Corps of Engineers. It is described by Robinson[43] as a lead-shielded collimator, containing 80 mc of ^{60}Co, which is buried in the ground; a scintillation detector is mounted on an H-frame structure 15 ft above the collimator. The detector consists of a 1.5-in.-diameter thallium-activated NaI crystal and a photomultiplier tube. Shims are mounted over the collimator to compensate for source decay. The system is designed for use with a maximum snow depth of 50 in. water equivalent. The apparatus operated satisfactorily over an entire winter, but adjustment was difficult to make, and temperature variation of the detector caused variations in counting rates.

Duncan and Warnick[40] described a telemetering system for use with the snow gage and reported results from tests using butyl rubber pillows, metal diaphragms, snow capacitors, and a neutron probe for measuring snow water equivalents.

CALIBRATION

Several systems of calibration have been used. For continuous checking, Gerdel et al.[37] and Itagaki[48] placed a small sample of shielded

^{90}Sr in the housing of the G-M tube and removed the shield by remote control during the check. For calibrating the snow gage, hand-packed snow piles[37] and known depths of water[37,40] have been most popular. Duncan and Warnick[40] obtained better calibration by allowing a 15-min pause between readings of 1 min or less, thereby limiting drift. Later they used a swimming pool in place of a water barrel, thus approximating an absorber of infinite size and more closely resembling the conditions of a continuous snowpack. This test showed that the calibration curve should be a straight line (on semilog paper) over the entire calibration range, rather than curving off at high water levels. Another test indicated that the pulse-height discriminator in the scintillation system should be set to pass only those pulses in the photopeak range. Energies below the photopeaks produced considerable differences in the counting rate between water and snow of equal water equivalent.

Various depths of water equivalent measured by the radioactive snow-gage method are given by the authors. Agashkin[38] measured depths of water equivalent ranging from 33.5 in. to presumably near zero, since he gives rates of melt covering periods of several days. Gerdel et al.[37] found that measurements up to 45 in. of water equivalent could be obtained with less than 5% error. The system developed by Itagaki[48] is limited to a water equivalent of 23.5 in. Kuz'min[49] found that snow with a water equivalent less than 2 in. produced a relative error beyond the allowable limit. Martinec[42] measured snow 96.5 in. deep with a water content of 52 in. and snow densities ranging from 11 to 60%. The system used by Robinson[43] is designed for a 50-in. maximum depth of snow water equivalent.

Martinec[42] determined that the absorption coefficient for water was constant for all snow layers up to a water equivalent of 52 in. This coefficient is similar to that obtained by Gerdel et al.[37] and is close to the theoretical value. Martinec concluded that it was possible to express intensity of radiation in terms of snow water content regardless of the density of the snowpack.

The application of nuclear radiation techniques to most of hydrometeorology is outlined by Danilin.[50] He describes the nature of radioactive isotopes, their measurement, and their use in measuring water in its various forms — soil moisture, snow water content, and ground water table.

In addition to measuring the water equivalent of snowpacks, two investigators have related the melting of the snowpack to other factors. Agashkin[38] compared snowmelt in a forest clearing, a spruce forest, a mixed forest, a clover field, and a wasteland. Martinec[51] successfully used his radioactive snow gage for snowmelt studies relating ablation rate to a degree-day factor, in which the degree-day factor indexes water-content depletion of the snowpack caused by a mean 1° rise in temperature above freezing during a 24-hr period.

Portable Neutron and Gamma Probes

Three of the papers cited[52a,53,54] report the use of portable radioactive probes and scalers to measure snow water content and snow density at various depths within a snowpack profile. The investigators worked with commercially available radioactive probes of types commonly used to measure soil moisture and soil density.

Belcher, Cuykendall, and Sack[55] reported the measurement of soil moisture and density by neutron and gamma-ray scattering the same year that Gerdel reported his pilot study in snow measurement with a gamma source. This was followed in 1952 by reports on soil moisture determination by neutron scattering by Gardner and Kirkham,[56] and Carlton et al.,[57] and in rapid succession by several other workers.[58–66]

In 1962 Danfors, Fleetwood, and Schytt in Sweden[53] reported results from the use of a commercially available neutron probe (Nuclear-Chicago Corp. P-19 probe) in determining the snow density of various portions of a glacier. Access holes were drilled, and measurements were made between 0.3 and 30 m below the surface. The snow density was also determined gravimetrically. Good agreement was obtained between neutron-probe and gravimetric snow-density determinations. The authors found a considerable spread of some of the individual values around the linear relation existing between the snow density and the counting rate. They noted that no systematic investigation of the factors causing this variation had been made.

In the same year Gay[54] reported success in the use of Nuclear-Chicago neutron (P-19) and gamma (P-20) probes to measure snow water content and snow density. This work was per-

formed in 1958–1962 in the Sierra Nevada Range of California.

Gay's work was based on the premise that hydrologists must study the water content and density changes of the snowpack throughout an accumulation and melt season. Since gravimetric methods destroy the sampling site, a systematic method was needed for study of the profile of a pack *in situ*. Gay felt that the neutron and gamma probes offered the opportunity to study the snowpack profile without disturbing it, that changes in density could be detected, and that ice-layer formation and free water ponded within a pack could be observed.

INSTRUMENTATION

To study the water content, Gay[54] used a probe (Nuclear-Chicago P-19) with a 5-mc radium-beryllium source, which emits fast neutrons, and a boron trifluoride gas detector tube sensitive only to slow neutrons. An access tube is inserted into the snowpack or soil, and the probe is lowered to the desired depths. The fast neutrons emitted interact with the surrounding mass and lose energy (velocity); a portion backscatters to the detector. These backscattered neutrons have been slowed, largely by collision with the hydrogen atoms in the soil and incorporated water or almost totally by the hydrogen atoms in snowpack water. Water in the pack or the soil is then related to the rate of returning neutrons as indicated by the counting equipment.

The density measurement is based on an interaction of gamma rays with electrons in the material surrounding the radioactive source. Gay used the commercially available Nuclear-Chicago P-20 probe with a ^{137}Cs source. The probe is positioned in an access tube, and gamma rays are scattered by collision with electrons. In soils and similar material, the number of electrons per unit volume determines the scattering ability. An increase in density, to a certain point, thus increases the probability for scattering. Some of these scattered rays return to the detector and are counted. The counting rate is proportional to density for low-density materials. However, when density increases beyond a certain point, absorption becomes a greater factor than backscattering, and the counting rate decreases. The counting rate is inversely proportional to soil density in the range 48.5 to 150 lb/cu ft.

CALIBRATION

Gay calibrated both the neutron and gamma probes gravimetrically with snow samples taken with a SIPRE* 500-cm^3 density sampling tube (Figs. II-17 and II-18). Such samples normally show a variation of 4 to 5% from the mean of a number of samples.

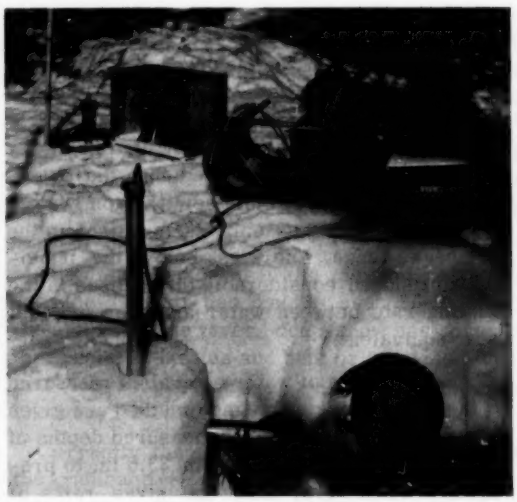

Fig. II-17 Taking a gravimetric SIPRE sample for the calibration of snow density gage.

Gamma Probe. The counts per minute observed with the gamma probe and densities determined with SIPRE snow samples were closely related, with an error of about 5% from a smooth line drawn through the density data.

The counting rate was found to increase in proportion to snow density to 31.2 lb/cu ft (50% snow density) because more of the gamma rays are reflected into the detector as the snow density increases.

Although Gay did not sample snow of densities above 50%, he claimed that a point in density is finally reached at which more gamma rays are attenuated and absorbed than reflected. At this point the counting rate decreases with further increase in density.

Continuation of this work[52a] in 1962 resulted in improved calibration of the gamma and neu-

*U. S. Army Snow, Ice, and Permafrost Research Establishment, now the U. S. Army Cold Regions Research and Engineering Laboratory, Hanover, N. H.

Fig. II-18 Pit excavation with SIPRE density samplers in place.

tron probes by averaging counting rates determined both 6 in. above and 6 in. below the measurement point. This decreased the variability of the counting rate about the calibration line of the gamma probe by 22 to 50% of the unexplained variance.

Neutron Probe. Neutron-probe counting rates plotted against snow density determined gravimetrically (SIPRE tubes) show a wide variation around a mean line (Fig. II-19).[54] Rates were found to be lower for snow than for an equivalent amount of water in the soil. Gay explained this phenomenon thus:

> The apparent low count rates in snow may be caused by changes in either the moderating effect of hydrogen atoms bound into ice crystals or in the manner in which the slowed neutrons are reflected into the detector tube. The scatter occurs in snowpack measurements near 40% snow density when appreciable quantities of melt water may be present in the snowpack. The presence of this free water greatly increases the count rate. A change of count rate due to change in state of water from liquid to solid was indicated by counts in ice and in water in a container 11.75 in. dia and 13 in. deep. The count rate in ice of 0.917 density was 12% lower than that expected.

No improvement was obtained in the prediction of density and water content from the neutron probe by using counting rates determined 6 in. above and 6 in. below the point of measurement for depths 12 in. and lower. At the 6-in. depth, counting above and below accounted for 75% of the variance observed about the calibration line.

Further studies conducted in the winter of 1963–1964 improved calibration of both gamma and neutron probes. Willen and Smith[52b] gravimetrically calibrated the probes against both SIPRE samples and a sample approximately the same size as the sphere-of-influence of the probes (a cylinder 12 in. in height and 12 in. in diameter). The larger sample greatly reduced the 4 to 5% variability inherent in SIPRE samples. Calibration of the top 12-in. layer was improved for the gamma probe by separation of the source and detector.

ICE-LAYER DETECTION

The density (gamma) probe was tested for its ability to locate ice lenses and layers of varying density within a snowpack profile.[54] Gamma

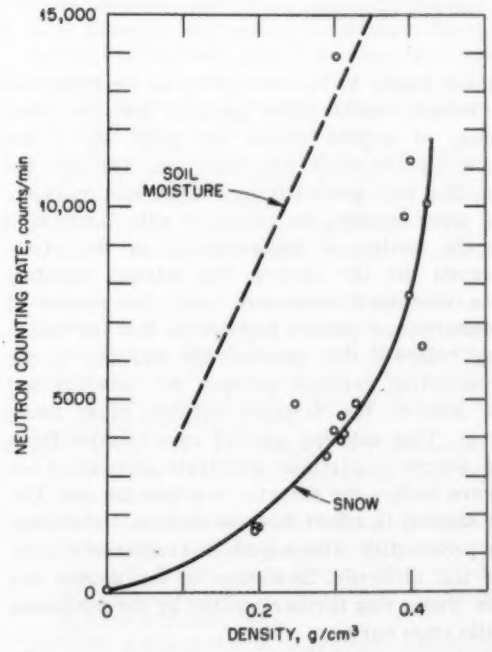

Fig. II-19 Relation of neutron counting rate to snow density determined with SIPRE sampler and neutron soil-moisture probe.

counting rates were determined at 1-in. intervals and related to profile characteristics (Fig. II-20). The incremental change in counting rate began to increase as the center of the measurement of the probe left the snow-air interface. It decreased as the measurement

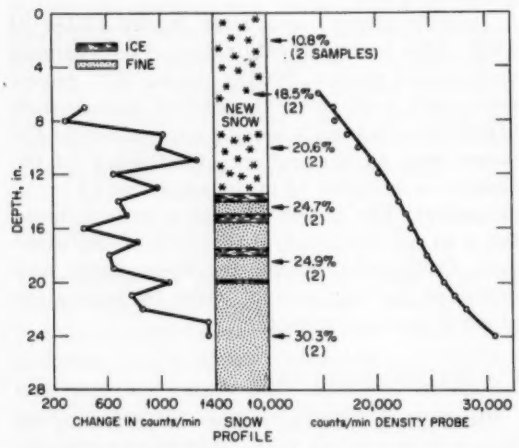

Fig. II-20 Change in gamma counting rate with change in snow density (depth) and occurrence of ice layers in a snowpack.

center began to be affected by an ice layer and increased again after passing the ice lens. Thus, at depths below the point where the snow-air interface was effective, although the counting rate generally increased with increasing snow density, the change in rate diminished as the center of measurement of the probe entered the ice layers. The gamma counting rate remained depressed until the center of measurement passed beyond the last ice layer. Gay believed this phenomenon was due to the geometrical relation between the detector and the source, the distance between these being 10 in. This allowed gamma rays emitted from the source to partially penetrate underlying ice layers before the detector reached the ice. The ice layers, in effect, became shields, decreasing the probability of backscattered radiation reaching the detector. Detection of ice lenses and free water was further limited by the nonlinear calibration curve.

Anderson et al.[52a] found that an ice lens 1.25 in. thick increased the neutron counts (neutron probe) 30% but that gamma counting rates were affected only slightly. The neutron probe appeared to offer promise for detection of such layers, and the gamma probe offered the most promise for density measurement of snow with included ice.

SPHERE OF INFLUENCE OF GAMMA PROBE

Gay studied the size of the sphere-of-influence of the gamma probe by progressively decreasing the diameter of a column of snow surrounding the source-detector probe (Fig. II-21). A counting rate of 95% of that in an undisturbed snowpack was produced in a 25% density snow column with a 13-in. radius and in a 37% density snow column of 16 in. radius. Contrary to expectation, the denser snow required a larger column than the less dense snow to produce the 95% counting rate. Gay suspected that snow structure factors, such as

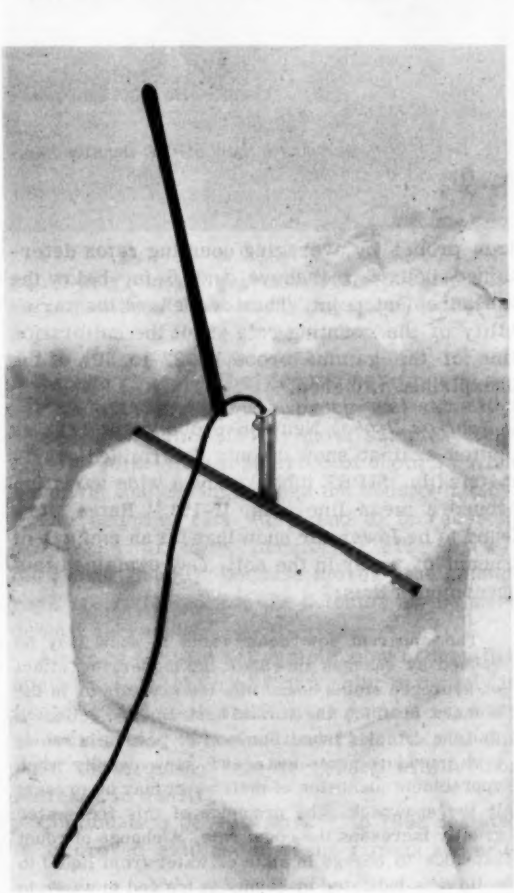

Fig. II-21 Sphere-of-influence studies with density probe.

crystal size and orientation, affected the gamma attenuation enough to cause this difference.

INTERFACE EFFECTS

The effect of the snow-air interface was found to be critical, preventing gamma determination of density in the top 8 in. of snow. Proximity to the soil seemed to have little effect. Anderson et al.[52a] felt that this difference was related to the similarity of the water content of both soil and snow.

Further tests on snow-air interface effects showed that the length of access tube extending above the snow affected counting rates for all depths through 18 in. The effects of the access tube length were large through the 9-in. level, becoming insignificant at the 12-in. level.

AVERAGE SNOWPACK DENSITY DETERMINATION BY GAMMA PROBE

Gay found that "the gamma probe consistently underestimated the average snowpack density, because of loss of counts to the air as the probe nears the surface and because the nonlinear shape of the calibration curve "weights' the low density strata." He concluded, however, that the density (gamma) probe provided "a useful measure of snowpack density profiles within the range 20-40%." It integrates a large volume for each measurement and is therefore limited for detecting free water and ice lenses. The neutron probe did not provide a satisfactory measure of profile density in these studies.

References

Radioactive Tracer Uses in the Mining Industry

1. *a.* *Isotopes Radiation Technol.*, 1(3): 226-44 (Spring 1964).
   b. G. J. Rotariu, Use of Radioisotopes in the Foreign Coal Industry, *Isotopes Radiation Technol.*, 1(3): 264-8 (Spring 1964).
2. P. M. Yavorsky and E. Gorin, Utilization of Radioactive Isotopes in Coal Process Research, Final Report, Task I, USAEC Report NYO-2597, Consolidation Coal Co., April 1960; P. M. Yavorsky and E. Gorin, Studies of Fluidized Particle Mechanics with Radioactive Coal Tracers, *Trans. Am. Nucl. Soc.*, 3(1): 197-9 (1960).
3. P. M. Yavorsky and E. Gorin, Utilization of Radioactive Isotopes in Coal Process Research, Final Report—III, USAEC Report NYO-9852, Consolidation Coal Co., May 1962.
4. A. M. Gaudin and H. Ramdohr, Final Report on Radioisotopes for Coarse Ore Concentration, USAEC Report TID-19015, Massachusetts Institute of Technology, January 1962.
5. H. J. Rose, Potential Applications of Radioisotopes to the Mining, Preparation, Transportation, Storage, Handling, and Use of Coal, USAEC Report NYO-2859, Bituminous Coal Research, Inc., November 1960.
6. R. A. Semmler, J. E. Brugger, and F. F. Rieke, Gamma-Scattering Density Meters: Analysis and Design with Applications to Coal and Soil, USAEC Report TID-14178, Laboratories for Applied Sciences, University of Chicago, December 1961.
7. R. A. Semmler, Gamma Scattering Density Meters: Field Trials in Coal, *ibid.*, Suppl. 1, March 1963.
8. *Isotopes Radiation Technol.*, 1(2): 167-8 (Winter 1963–1964).
9. U. S. Atomic Energy Commission, Isotope Development Program, Contract Scope Statements, USAEC Report TID-4202, September 1963, p. 80.
10. *Isotopes Radiation Technol.*, 1(1): 22 (Fall 1963).
11. U. S. Atomic Energy Commission, Isotopes Technology Development Program, Fifth Annual Contractors Meeting, December 2–3, 1963, Washington, D. C., USAEC Report TID-7681, February 1964, pp. 46-9.
12. D. E. Hull and R. R. Bowles, New Use for Radioactive Tracers, Measuring Catalyst Flow Rates in Cat Crackers, *Oil Gas J.*, 51(46): 295-9 (1953).
13. A. J. Kinsella, Jr., and J. J. Mitchell, Better Catalyst-loss Studies, *Petrol. Process.*, 10: 1718-23 (1955).
14. V. P. Guinn, Tracing Catalysts in Refinery Crackers, *Nucleonics*, 14(5): 69-72 (1956).
15. D. E. Hull, Radiotracer Studies of Flow Patterns in Industrial Plants, *Intern. J. Appl. Radiation Isotopes*, 1: 305-13 (1957).
16. *a.* R. L. Heath, Gamma Ray Spectrum Catalog, USAEC Report IDO-16408, Phillips Petroleum Co., July 1957.
    b. S. Kinsman (Ed.), Radiological Health Handbook, U. S. Department of Health, Education, and Welfare, Report PB-121784, January 1957.
    c. D. J. Hughes and J. A. Harvey, Neutron Cross Sections, USAEC Report BNL-325, Brookhaven National Laboratory, 1955.
17. *a.* L. A. Kaufman, The Radiogenic Concentration of Uranium Ores, *Can. Mining Met. Bull.*, 43: 450-3 (1950).
    b. C. M. Lapointe and R. D. Wilmot, Electronic Concentration of Radioactive Ores with the Lapointe Picker Belt, Report NP-3827(TR-95/52), Department of Mines and Technical Surveys (Canada), 1952.
    c. C. M. Lapointe and R. D. Wilmot, Electronic Concentration of Ores with the Lapointe Picker Belt, Report NP-4384(Memo No. 123), Department of Mines and Technical Surveys (Canada), 1952.

d. C. M. Lapointe, Apparatus for Sorting Radioactive Ore, U. S. Patent 2,617,526, Nov. 11, 1952, assigned to Eldorado Mining and Refining Ltd. and USAEC. (This device is also covered by Canadian Patent 467,482 and British Patent 658,574.)

e. A. H. Bettens and C. Lapointe, Electronic Concentration of Low Grade Ores with Lapointe Picker, Report NP-5508(TR-123/54), Department of Mines and Technical Surveys (Canada), 1954.

18. A. M. Gaudin, J. Dasher, J. H. Pannell, and W. L. Freyberger, Use of an Induced Nuclear Reaction for the Concentration of Beryl, *Trans. AIME*, 187: 495-8 (1950).
19. T. G. Church, Formation of Radioactive Surface Films on Minerals, Canadian Report CRC-407, National Research Council of Canada, 1949.
20. F. Paneth, *Radio-Elements as Indicators and Other Selected Topics in Inorganic Chemistry*, Cornell University Press, Ithaca, N. Y., 1928, p. 67.
21. F. E. Senftle and A. M. Gaudin, Concentration of Ores by Induced Activities, *Nucleonics*, 8(5): 53-9 (1951).
22. A. M. Gaudin, F. E. Senftle, and W. L. Freyberger, How Induced Radioactivity May Help Separate Minerals, *Eng. Mining J.*, 153(11): 95-9, 174, 196 (1952).
23. M. Halfawy and F. E. Senftle, Adsorption of Radionuclides on Minerals for Ore Benefication Purposes, *Z. Physik. Chem. (Frankfurt), New Series*, 12: 196-205 (1957).
24. A. M. Gaudin and H. F. Ramdohr, Induced Radioactivity for Coarse Copper Ore Concentration, *Can. Met. Quart.*, 1(2): 178-85 (1962).

Recent Developments in Counting Methods

25. H. G. Richter and A. S. Gillespie, Jr., Flexible Geiger Counters, USAEC Report ORO-482, Research Triangle Institute, 1961; H. G. Richter and L. F. Ballard, Construction and Operating Characteristics of Flexible Geiger Counters, in *Nuclear Electronics*, Vol. I, Proc. Conf. Belgrade, 1961, pp. 339-44, International Atomic Energy Agency, Vienna, 1962; H. G. Richter and A. S. Gillespie, Flexible Geiger Counter, U. S. Patent No. 3,110,835, Nov. 12, 1963.
26. R. Maze, Compteurs à paroi de verre et à cathode externe, *J. Phys. Radium*, 7(8): 164-6 (1946).
27. A. L. Cockroft and J. M. Valentine, The Properties of Proportional Tubes and Ion Chambers with Glass Envelopes and External Graphite Electrodes, *J. Sci. Instr.*, 27: 262-3 (1950).
28. A. Moljk, R. W. P. Drever, and S. C. Curran, Operation of Proportional Counters at High Temperatures, *Rev. Sci. Instr.*, 26: 1034-7 (1951).
29. H. Kallmann and M. Furst, Fluorescence of Solutions Bombarded with High Energy Radiation (Energy Transport in Liquids), *Phys. Rev.*, 79: 857-70 (1950).
30. M. G. Schorr and F. L. Torney, Solid Noncrystalline Scintillation Phosphors, *Phys. Rev.*, 80: 474 (1950).
31. W. L. Buck and R. K. Swank, Preparation and Performance of Efficient Plastic Scintillators, *Nucleonics*, 11(11): 48-52 (1953).
32. A. H. Heimbuch, Scintillating Ion Exchange Resins, *Trans. Am. Nucl. Soc.*, 4: 251-2 (1961); A. H. Heimbuch and H. Y. Gee, Development of a Cation Exchange Resin with Scintillating Properties, USAEC Report NYO-9138, Tracerlab, 1962; A. H. Heimbuch, H. Y. Gee, H. Bould, and W. Schwarz, A Scintillating Anion Exchange Resin, USAEC Report NYO-10405, Tracerlab, 1963; A. H. Heimbuch and W. J. Schwarz, A New Technique for the Detection of Radioactive Biochemicals by Scintillating Ion Exchange Resins, *Atompraxis*, 10: 70-4 (1964); Fluorescent Ion Exchange Resins, American Chemical Society, 144th National Meeting, April 1963, p. 6B (abstract).
33. W. P. Hohenstein and H. Mark, Polymerization of Olefins and Diolefins in Suspension and Emulsion, Part I, *J. Polymer Sci.*, 1: 127-45 (1946).
34. F. H. Winslow and W. Matreyek, Particle Size in Suspension Polymerization, *Ind. Eng. Chem.*, 43: 1108-12 (1951).
35. F. D. Brooks, Organic Scintillators, in *Progress in Nuclear Physics*, Vol. V, O. R. Frisch (Ed.), Pergamon, New York, 1956.
36. L. B. Farabee, Procedure for the Radiochemical Analysis of Sr and Ba in Human Urine, USAEC Report ORNL-1932, Oak Ridge National Laboratory, 1955.

Radio-Snow Gages: A Review of the Literature

37. R. W. Gerdel, B. L. Hansen, and W. C. Cassidy, The Use of Radioisotopes for the Measurement of the Water Equivalent of a Snowpack, *Am. Geophys. Union Trans.*, 31(3): 449-53 (1950).
38. Yu. N. Agashkin, Investigation on Snow Melting Using the Method of Radioactive Isotopes, *Izv. Akad. Nauk SSSR, Ser. Geograf.*, No. 4: 117-21 (1960). (Translation: SIPRE* Report No. 12, January 1961, 18603.)
39. M. S. Sternzat and A. A. Sapozhnikov, Measurement of the Water Content of Snow with Radioactive Isotopes, in *Meteorologicheskie Pribory, Gidromet. Izdat. Leningrad*, pp. 114-7, 1959. (Translation: SIPRE* Report No. 12, January 1961, 18136.)
40. D. L. Duncan and C. C. Warnick, Instrumentation for Hydrologic Measurements at the Univ. of Idaho, in *Proc. 31st Western Snow Conf.*, pp. 67-73,

*U. S. Army Snow, Ice, and Permafrost Research Establishment, now U. S. Army Cold Regions Research and Engineering Laboratory, Hanover, N. H.

1963, Colorado State University, Fort Collins, Colo. (Obtained from W. D. Simons, Chairman, Western Snow Conf., P. O. Box 1352, Tacoma 1, Wash.)

41. V. Fischmeister, Determination of Water Value of a Snowcover with Radioactive Materials (in German), *Oesterr. Wasserwirtsch.*, 8: 86-93 (April 1956).
42. J. Martinec, Measurement of Snow-Water Content with the Use of Radiocobalt, in *Proc. Intern. Union Geodesy Geophys. Assoc. Sci. Hydrol., Toronto, September 1957,* Publ. 46, Vol. 4, Snow and Ice, pp. 88-91, 1958.
43. C. Robinson, Gamma Radiation Gauges: Snowpack Water Content, *Elec. World,* 154(17): 82-3 (1960).
44. J. A. Doremus, Telemetering System for Radioactive Snow Gage, *Electronics,* 24(2): 88-91 (1951).
45. C. E. Hildebrand, Development and Test Performance of Radioisotope-Radiotelemetering Snow-Gage Equipment, Civil Works Investigation Project CS 1-170, U. S. Army Corps of Engineers, San Francisco, 1956.
46. A. Higashi and K. Itagaki, A Radioactive Snow Gage for Practical Use, I, *J. Appl. Phys. (Japan),* 25(3): 93-8 (1956).
47. A. Higashi, Snow Survey in Hokkaido, Japan, in *Proc. Intern. Union Geodesy Geophys. Assoc. Sci. Hydrol., Toronto, September 1957,* Publ. 46, Vol. 4, Snow and Ice, pp. 22-39, 1958.
48. K. Itagaki, An Improved Radio Snow Gage for Practical Use, *J. Geophys. Res.*, 64(3): 375-83 (1959).
49. P. P. Kuz'min, Experimental Investigation on the Water Yield from Snow by Means of Radioactive Cobalt, *Tr. Gos. Cirol. Inst. Vyp.*, 65: 30-49 (1958). (Translation: SIPRE* Report No. 12, January 1961, 18729.)
50. A. I. Danilin, *The Use of Nuclear Radiation in Hydrometeorology,* Gidromet. Izdat., Leningrad, 1957. (Translation: No. 60-19973, Special Library Association Translation Center, Chicago.)
51. J. Martinec, The Degree-Day Factor for Snowmelt-Runoff Forecasting, in *Proc. Intern. Union Geodesy Geophys. Assoc. Sci. Hydrol., Helsinki, 1960,* Publ. 51, pp. 468-77, 1960.
52. *a.* H. W. Anderson, P. M. McDonald, and L. W. Gay, Use of Radioactive Sources in Measuring Characteristics of Snowpacks, U. S. Forest Service Research Note PSW-11, Pacific Southwest Forest and Range Experiment Station, Berkeley, Calif., 1963.
    b. D. W. Willen and J. L. Smith, The Use of Radioactive Isotopes To Characterize the Hydrologic Performance of Mountain Snowpacks, unpublished report on file at Pacific Southwest Forest and Range Experiment Station, Berkeley, Calif., 1964.
53. E. Danfors, A. Fleetwood, and V. Schytt, Application of the Neutron Scattering Method for Measuring Snow Density, *Geografiska Annaler,* 44: 409-11 (1962).
54. L. W. Gay, Measuring Snowpack Profiles with Radioactive Sources, *Proc. 30th Western Snow Conf.*, pp. 14-9, 1962, Colorado State University, Fort Collins, Colo. (Obtained from W. D. Simons, Chairman, Western Snow Conf., P. O. Box 1352, Tacoma 1, Wash.)
55. D. J. Belcher, T. R. Cuykendall, and H. S. Sack, The Measurement of Soil Moisture and Density by Neutron and Gamma Ray Scattering, Technical Development Report 127, Civil Aeronautics Administration, Washington, D. C., 1950.
56. W. Gardner and D. Kirkham, Determination of Soil Moisture by Neutron Scattering, *Soil Sci.*, 73: 391-401 (1952).
57. P. F. Carlton, D. J. Belcher, T. R. Cuykendall, and H. S. Sack, Modifications and Tests of Radioactive Probes for Measuring Soil Moisture and Density, Technical Development Report 194, Civil Aeronautics Administration, Washington, D. C., 1953.
58. J. W. Holmes, Calibration and Field Use of the Neutron Scattering Method of Measuring Soil Water Content, *Australian J. Appl. Sci.*, 7: 45-58 (1956).
59. J. W. Holmes and A. F. Jenkinson, Techniques for Using the Neutron Moisture Meter, *J. Agr. Eng. Res.*, 4(2): 100-9 (1959).
60. A. H. Knight and T. W. Wright, Soil Moisture Determination by Neutron Scattering, in *Proc. 2nd Radioisotope Conf., Oxford, England, 1954,* Vol. 2, pp. 111-22, 1954.
61. M. Kursin, Use of Radioactive Substances for Measuring Flow of Liquids (in Russian), *Gidrotekhnika Melioratsiya,* 6: 33-6 (1956).
62. L. H. Stolzy and G. A. Cahoon, Field-Calibrated Portable Neutron Rate Meter for Measuring Soil Moisture in Citrus Orchards, *Soil Sci. Soc. Am. Proc.*, 21: 571-5 (1957).
63. J. F. Stone, D. Kirkham, and A. A. Read, Soil-Moisture Determination by a Portable Neutron-Scattering Moisture Meter, *Soil Sci. Soc. Am. Proc.*, 19: 419-23 (1955).
64. J. F. Stone, R. F. Shaw, and D. Kirkham, Statistical Parameters and Reproducibility of the Neutron Method of Measuring Soil Moisture, *Soil Sci. Soc. Am. Proc.*, 24: 435-8 (1960).
65. C. H. M. Van Bavel, Measurement of Soil Moisture Content by the Neutron Method, Report ARS-41-24, U. S. Department of Agriculture, Agricultural Research Service, Washington, D. C., 1958.
66. C. H. M. Van Bavel, N. Underwood, and R. W. Swanson, Soil Moisture Measurement by Neutron Moderation, *Soil Sci.*, 82: 29-41 (1956).

*U. S. Army Snow, Ice, and Permafrost Research Establishment, now U. S. Army Cold Regions Research and Engineering Laboratory, Hanover, N. H.

Section

III

Power Reactor Technology

Food Irradiation

Effect of Gamma Irradiation on Shasta Strawberries Under Marketing Conditions

By E. C. Maxie, N. F. Sommer, and Henry L. Rae*

The work discussed here† was done to evaluate, under simulated and actual shipping and marketing conditions, the effectiveness of gamma irradiation in retarding decay derived from field infections; the respiratory response of strawberries to low doses of gamma rays and the resulting increase in refrigeration requirement; the effects of gamma irradiation on the ascorbic acid content of Shasta strawberries; and the susceptibility of irradiated strawberries to transit injury.

Postharvest losses of strawberry fruit have been estimated[1] to be 25% of production in the United States. Powelson[2] found evidence that 90% of the strawberries lost to decay along the Pacific Coast were infected with *Botrytis cinerea* Pers., and his data indicate that much postharvest decay results from infections originating in the field before harvest. Often, floral parts are invaded first, and the receptacle is infected by fungal growth from these aging structures. Since infections within the tissues of strawberries are inaccessible to fungicidal dusts and sprays, a noninjurious agent able to penetrate the fruit tissues would be advantageous in controlling decay of strawberry fruits.

Ionizing radiation has shown[3] some promise in controlling decay in Shasta strawberries. However, irradiation has been reported to cause significant destruction of ascorbic acid in strawberries,[4] although De Zeeuw[5] and Romani et al.[6] reported that radiation in the pasteurization range does not cause a nutritionally significant loss. De Zeeuw did not indicate the time interval between irradiation and analyses in his experiments, but Romani et al. held their fruit for no more than 4 days prior to analysis. This time interval is considerably less than many marketing periods for California strawberries. In studies on the effects of gamma irradiation on the flavor and texture of the Shasta and Lassen varieties of strawberries held under simulated transit conditions, Johnson[7] found no major adverse effects on aroma, flavor, or texture with doses of 0.200 Mrad or less.

Experimental Work

Data obtained in a series of experiments indicated that a gamma irradiation of 0.200 Mrad can significantly decrease the subsequent amount of *B. cinerea* rot in strawberry fruits during a simulated transit and marketing sequence. Shasta strawberries that were unusually sound at harvest were gamma-irradiated with 0.100 to 0.300 Mrad and then stored 6 days at 5°C. The amount of fruit that was marketable on the day that it would have reached the terminal market increased from 85% with no irradiation to 98% with 0.300 Mrad (Table III-1). Even when the berries were in poor condition at harvest, the percentage that was marketable was higher for the irradiated fruit. Most of the fruit judged "soft" showed mushy areas on the surface. With a dose of 0.300 Mrad, even in the fruit that was originally of good quality, the

*University of California, Davis, Calif.

†Originally reported in "Radiation Technology in Conjunction with Postharvest Procedures as a Means of Extending the Shelf-life of Fruits and Vegetables," USAEC Report SAN-2001, Annual Report, University of California, Davis, Jan. 30, 1963.

percentage of soft fruits increased sharply; and, in the poor-quality fruit, a few berries collapsed completely, a reaction typical of Shasta strawberries subjected to very high levels of gamma irradiation.

Five percent of Salinas strawberries may show actively growing lesions from *B. cinerea* infection at harvest. In transit, these decaying berries infect adjacent fruit, with the intertwining mycelia producing a "nest" of rotting berries. When one severely decayed fruit was placed in the center of the fruit mass in each basket just prior to treatment, gamma irradiation significantly inhibited "nesting" during a low-temperature simulated transit period (Table III-2).

Table III-1 EFFECT* OF LEVEL OF GAMMA IRRADIATION ON SHASTA STRAWBERRIES HELD UNDER SIMULATED TRANSIT AND MARKETING CONDITIONS AFTER IRRADIATION

Irradiation, Mrad	Amount of fruit in each class,† %					
	Initially high quality			Initially low quality		
	Sound	Soft	Decayed	Sound	Soft	Decayed
Stored 6 Days at 50°C						
0	85.2		14.9	37.2	35.2	27.4
0.100	93.3		6.7	46.0	39.3	14.6
0.200	99.0		1.0	51.0	38.0	11.0
0.300	98.0		2.2	38.3	51.7	10.0
Stored 5 Days at 50°C and Then Held 48 Hr at 20°C						
0	19.6	3.2	77.2			
0.100	60.3	12.2	27.5			
0.200	69.5	10.6	19.9			
0.300	72.8	27.2	0.0			

*Values corrected for field decay at harvest. Both "sound" and "soft" fruit were marketable.

†Fruit that was initially of "high" quality contained 5% soft and 3% decayed berries; "low" contained 25% soft and 3% decayed.

Table III-2 EFFECT OF GAMMA IRRADIATION ON DECAY OF SHASTA STRAWBERRIES WITH ONE SEVERELY DECAYED FRUIT PLACED IN EACH BASKET PRIOR TO TREATMENT

Dose, Mrads	Amount of decayed fruit, %
Fruit Stored 10 Days at 5°C	
0	57.0
0.100	17.4
0.200	13.3
0.300	3.1
0.400	6.6

EFFECT OF IRRADIATION ON BERRIES IN WHICH COOLING WAS DELAYED

Strawberries should be precooled immediately after harvest because the fruit softens rapidly at field temperatures, development of active lesions is rapid at warm temperatures, and berries subjected to a delay in cooling lose their characteristic luster, with a concomitant loss in customer appeal. Berries that had been gamma-irradiated after a 6-hr delay in cooling and then stored 8 days at 5°C were only 5% decayed, but, in the controls, decay was 29% (Table III-3). A delay in cooling had no effect on the amount of decay in either control or irradiated fruit. However, all fruit held 3 hr prior to cooling showed a loss in luster, a condition that became objectionable in fruits held 6 hr before cooling.

The decrease in decay in the irradiated berries is the result chiefly of a delay in lesion development rather than of inactivation of all fungal cells within the lesion. Irradiation of warm fruit may be effective provided the fruit is moved quickly from the field to the irradiator and then cooled immediately.

When the respiration rate of irradiated Shasta strawberries was measured at 5°C, berries subjected to 0.200 Mrad showed a 45% increase in carbon dioxide evolution [23.4 to 34 mg/(kg)(hr)] 24 hr after treatment. By 48 hr after

Table III-3 EFFECT OF 0.200 MRAD GAMMA IRRADIATION ON SHASTA STRAWBERRIES ON WHICH COOLING WAS DELAYED

Delay in cooling, hr	Amount of fruit in each class, %					
	No irradiation			0.200 Mrad irradiation		
	Sound	Soft	Decayed	Sound	Soft	Decayed
	Fruit Stored 8 Days at 5°C					
0	22	28	50	67	27	6
3	26	24	50	51	34	9
6	6	15	79	52	37	11

treatment, the respiration rate of the irradiated berries was only 12% above that of the control lots. Thus at 5°C the refrigeration requirement per ton of strawberries per 24 hr to remove the heat of respiration would increase from about 5148 to 7040 Btu during the first day. Thereafter the irradiated fruit would require but little added refrigeration for the removal of respiratory heat.

ASCORBIC ACID CONTENT OF IRRADIATED BERRIES

The ascorbic acid contents of Shasta strawberries held for simulated transit periods were not decreased by a nutritionally significant amount by 0.100 and 0.200 Mrad gamma irradiation (Table III-4).

Table III-4 EFFECT OF GAMMA IRRADIATION ON ASCORBIC ACID CONTENT OF SHASTA STRAWBERRIES

Dose, Mrads	Ascorbic acid, mg per 100 g of original weight	
	2 days after irradiation	11 days after irradiation
0	65.7	66.0
0.100	64.0	69.9
0.200	59.2	58.8

SHIPMENT OF IRRADIATED BERRIES

In a test shipment of irradiated strawberries from Salinas, Calif., to Chicago, Ill., with 6 days having elapsed between harvest and arrival, there were no immediately apparent differences in fruits irradiated with 0 to 0.200 Mrad. Fruits irradiated with 0.250 and 0.300 Mrad showed a somewhat higher percentage of soft fruits. Fruits irradiated with 0.350 Mrad showed severe radiation injury, with many berries collapsed from loss of texture. However, when the berries were allowed to stand 18 hr at ambient temperature (18 to 24°C) after removal from the cars, the irradiated fruits were in decidedly better condition than the unirradiated. Those that received 0, 0.150, 0.200, and 0.250 Mrad showed 19, 10, 7, and 4% decayed berries, respectively (Table III-5).

Selection of Optimum Radiation Dose

The choice of the optimum radiation dose for strawberries is difficult. Radiation may be viewed as a stress condition, and the physiological status of strawberry fruits would be expected to influence the level of radiation required to cause injury to the berries. Strawberries grown at abnormally low temperatures or under a heavy nitrogen regime are more

Table III-5 EFFECT OF GAMMA IRRADIATION ON SHASTA STRAWBERRIES IN A TEST SHIPMENT FROM SALINAS, CALIF., TO CHICAGO, Ill.

Dose, Mrads	Amount of fruit in each class, %					
	On arrival in Chicago			Held 18 hr at 18 to 24°C following removal from railroad car		
	Sound	Soft	Decayed	Sound	Soft	Decayed
0	87	5	8	75	5	19
0.150	87	8	5	79	11	10
0.200	88	8	4	84	9	7
0.250	74	21	5	76	20	4
0.300	66	29	5	65	30	5
0.350	6	90	4	5	90	5

prone to physiological disorders than those grown under usual conditions. In the early spring of 1963, we found excessive softening in strawberries subjected to 0.250 Mrad. Later in the summer this dose produced no major symptoms of injury. We chose 0.200 Mrad as the tentative maximum permissible dose for the Shasta variety because we have seen no adverse effect from this treatment under a variety of conditions.

The principal benefit that might be derived from gamma irradiation of strawberries is retardation of decay during a normal transit and storage period. We have held some irradiated strawberries as long as 45 days without visible decay. After 21 days, however, the berries lost their characteristic appearance, aroma, and flavor. This occurs as a result of normal physiological and biochemical processes within the fruit. Thus we do not foresee any dramatic extension in shelf-life of strawberries from gamma irradiation. Irradiated strawberries can be expected to have less decay upon arrival at the market if handled properly. This could mean a retail period of 2 to 4 days longer than for unirradiated fruit under American marketing procedures. This extension of retail period and decrease in decayed fruit during transit could be a significant advance in presenting high-quality fruit to the consumer. In our opinion, commercial test shipments of irradiated strawberries are needed to test the irradiation process under the varied conditions existing in the American marketing procedures.

Materials and Methods

Shasta strawberries were obtained directly from the fields of Salinas Strawberries, Inc., at Salinas, Calif., immediately cooled to 37°F by the forced-air principle,[8] and trucked to Davis, Calif., under forced-air refrigeration. The individual crates were covered with shrinkable plastic and irradiated in the Mark II food irradiator[9] with the fruit temperature at 3 to 5°C and with air moving through the chamber at a rate of 6500 ml/min. The plastic cover was removed, and the fruit was stored at 5°C and a relative humidity of 93%. Fruits destined for the test shipment were handled as above and then trucked back to Salinas for loading into a refrigerated Railway Express car.

Ascorbic acid was determined by the method of Loeffler and Ponting.[10] Respiration rates were determined by the method of Claypool and Keefer.[11] Refrigeration requirements for removing the heat of respiration were calculated by the method of Wright et al.[12] Dosimetry was as described by Romani et al.[13]

At the end of the simulated and actual transit tests, the berries were sorted into sound, soft, and decayed fruit, and the results were expressed as percentage of the total.

Summary

Gamma irradiation of Shasta strawberry fruits at doses of 0.200 Mrad significantly decreased the amount of decayed berries without apparent ill effects under actual and simulated marketing conditions, provided the berries were cooled immediately after harvest and kept cool. Field infections by the principal pathogen, *Botrytis cinerea* Pers., are not completely inactivated, the beneficial effect of irradiation being inhibition of lesion development. Normal physiological and biochemical processes cause the loss of characteristic appearance, aroma, and flavor after approximately 21 days in cold storage.

References

1. U. S. Department of Agriculture, Agricultural Research Service, Washington D. C., Report ARS-20-1, p. 190, 1954.
2. R. L. Powelson, Initiation of Strawberry Fruit Rot Caused by *Botrytis cinerea*, *Phytopathology*, 50: 491-4 (1960).
3. K. E. Nelson, E. C. Maxie, and W. Eukel, Some Studies in the Use of Ionizing Radiation To Control *Botrytis* Rot in Table Grapes and Strawberries, *Phytopathology*, 49: 475-80 (1959).
4. I. D. Clarke, Possible Applications of Ionizing Radiations in the Fruit, Vegetable, and Related Industries, *Intern. J. Appl. Radiation Isotopes*, 6: 175-81 (1959).
5. D. De Zeeuw, Experiments on the Preservation of Fresh Fruits by Irradiation, *Food Irradiation*, 1(3): A5-7 (1961).
6. R. J. Romani, J. van Kooy, and B. J. Robinson, Gamma Irradiation of Fruit: Preliminary Physiological Studies, *Food Irradiation*, 2: A11-3 (1961).
7. C. J. Johnson, Physical and Sensory Tests on Fresh Strawberries Subjected to Gamma Irradiation, M.S. thesis, University of California, Davis, 1964.
8. R. Guillou, Coolers for Fruits and Vegetables, *Calif. Univ. Agr. Expt. Sta. Bull.* 773 (1960).

9. R. J. Romani, E. C. Maxie, C. O. Hesse, and N. F. Sommer, ^{60}Co Gamma-ray Irradiator Opens New Doors to Biological Research at Davis, *Calif. Agr.*, 16: 1-4 (1962).
10. H. J. Loeffler and J. D. Ponting, Ascorbic Acid. Rapid Determination in Fresh, Frozen, or Dehydrated Fruits and Vegetables, *Ind. Eng. Chem. Anal. Ed.*, 14: 846-9 (1942).
11. L. L. Claypool and R. M. Keefer, A Colorimetric Method for CO_2 Determination in Respiration Studies, *Proc. Am. Soc. Hort. Sci.*, 40: 177-86 (1942).
12. R. C. Wright, D. H. Rose, and T. M. Whiteman, The Commercial Storage of Fruits, Vegetables, and Florist and Nursery Stocks, U. S. Department of Agriculture Handbook 66, 77 pp., 1954.
13. R. J. Romani, B. J. Robinson, H. L. Rae, E. C. Maxie, and N. F. Sommer, Fruit Irradiation: Physical Methods, *Radiation Botany*, 3: 345-50 (1963).

Section

IV

Isotopes and Radiation Technology

Source Development

More than 30 radioisotopes have been mentioned in recent years for use as radiation sources in medical and industrial radiography. In an earlier issue of *Isotopes and Radiation Technology*,[1] Pressly briefly reviewed gamma-emitting and bremsstrahlung sources and described work at Oak Ridge National Laboratory (ORNL) on the preparation and use of ^{55}Fe and ^{147}Pm. Krabbenhoft and Green[2] summarized work on 13 isotopes used in medical radiography and reported on experiments with four of them and ^{177}Lu. Pool and Spangenberg[3] at the Gatlinburg conference this year added four more isotopes—^{155}Eu, ^{159}Dy, ^{175}Hf, and ^{181}W—to the growing list. Their criterions were availability, ease of production, half-life, suitability of emission spectrums, and specific activity of the material in which the radionuclide is contained. A recent text[4] lists nine other industrially important sources but points out that ^{60}Co, ^{192}Ir, ^{170}Tm, and ^{137}Cs are used in most commercial radiography work involving isotopes. In work sponsored by the Division of Isotopes Development (DID), ^{85}Kr has been studied as a potential radiographic source.[5] Others have also been reported.[6–11] Table IV-1 itemizes the isotopes mentioned in the reports noted above.

There is a continuing need for small, lightweight, easy-to-use, and safe radiographic equipment for medical purposes in many areas of the world. Isotopic sources are ideal supplements to conventional X-ray equipment for use in hospital and operating rooms, emergency and civil defense situations, disaster areas, zoos, farms, and military installations.[6] In industry, where isotopic radiographic sources are becoming commonplace, the lack of inexpensive low-energy (0.02 to 0.1 Mev) X-ray sources has limited their utilization in many areas.[5] Although standard X-ray machines satisfy the needs of most industrial and medical applications, these machines have some limitations. Their large physical size limits their use where geometric requirements cannot be met—for example, in inside-out radiography of small tubular structures and 4π radiography. Furthermore, they require either external power or batteries.

Progress is being made in industrial and medical applications of radioisotopes in radiography. For example, Green and Krabbenhoft[7] and Allen et al.[8] recently reported at an American Nuclear Society meeting on a sealed radioisotope source applied to a tuberculosis survey system for chest radiography. They used ^{169}Yb in equipment that can be set up in minutes, weighs about 225 lb, and fits in the trunk of an automobile. In a series of DID programs, workers at Tracerlab[5,9] and Illinois Institute of Technology Research Institute (IITRI)[10,11] studied three fission-product beta emitters—^{147}Pm, ^{90}Sr, and ^{85}Kr—as potentially useful industrial radiographic sources. At ORNL both ^{125}I and ^{241}Am sources have been tested,[12,13] and in Stockholm[14,15] as well as in this country,[16,17] ^{125}I is still being developed for radiography. Henrikson et al.[15] recommend that a ^{125}I X-ray unit always be kept in stock for ready use, for example, in forensic dental studies at the scene of a crime or at an archeological site.

Various factors affect sensitivity[4a,b] (Fig. IV-1) in radiography, and comparison of isotopes for radiographic use is often difficult because experimental conditions vary from one study to the next. A group in England recently studied these factors exhaustively,[4b] but comparative work with isotopes and these factors has not been done. A wide variety of specimens, films, techniques, and exposure times used is included in a table in Krabbenhoft and Green's review.[2] Pool and Spangenberg,[3] at the Department of Physics and College of Dentistry at Ohio State University, have been attempting to

Table IV-1 ISOTOPES APPLIED TO RADIOGRAPHY

Isotope	Method of production	Half-life	Principal use*	Reference
^{241}Am	$^{239}Pu(n,\gamma)^{240}Pu$ $^{240}Pu(n,\gamma)^{241}Pu$ $^{241}Pu \xrightarrow[13.2\ years]{\beta^-} {}^{241}Am$	470 years	I, M; see ^{147}Pm	2, 4*a*, 11, 13
^{195}Au	$^{194}Pt(p,n)^{195}Au$	185 days	I, M, feasible[29]	11, 29
^{109}Cd	$^{108}Cd(n,\gamma)^{109}Cd$	1.3 years	Impractical	11
^{60}Co	$^{59}Co(n,\gamma)^{60}Co$	5.2 years	I, commonly used	4*a*
^{131}Cs	$^{130}Ba(n,\gamma)^{131}Ba$ $^{131}Ba \xrightarrow{\beta} {}^{131}Cs$	9.7 days	M, among top 11 of 48 evaluated[3]	2, 3
^{134}Cs	$^{133}Cs(n,\gamma)^{134}Cs$	2.3 years	I, one of 12 named; suitable, but cost per curie unfavorable	4*a*; 4*c*
^{137}Cs	Fission	33 years	I, commonly used	4*a*
$^{139}Ce(?)$†	– –	– –	M, mentioned only	2
^{144}Ce	Fission	285 days	M, among top 11 of 48 evaluated[3]	2, 3, 4*a*
^{159}Dy	$^{158}Dy(n,\gamma)^{159}Dy$	144 days	M, among top 11 of 48 evaluated	3
^{155}Eu	Fission; $^{154}Sm(n,\gamma)^{155}Sm$ $^{155}Sm \xrightarrow{\beta} {}^{155}Eu$	1.7 years	I, one of 12 named[4]; M, among top 11 of 48 evaluated[3]	3, 4*a*
^{55}Fe	$^{54}Fe(n,\gamma)^{55}Fe$	2.9 years	No use mentioned; pictures comparable to low-voltage X-ray machine	1
^{153}Gd	$^{152}Gd(n,\gamma)^{153}Gd$	230 years	M, poor[2]; among top 11 of 48 evaluated[3]	2, 3, 6
^{175}Hf	$^{174}Hf(n,\gamma)^{175}$	70 days	M, among top 11 of 48 evaluated	3
^{125}I	$^{124}Xe(n,\gamma)^{125}Xe$ $^{125}Xe \xrightarrow[18\ hr]{EC} {}^{125}I$	57.4 days	M; see ^{147}Pm and text	2, 3, 11
^{129}I	Fission	1.6×10^7 years	Impractical	11
^{192}Ir	$^{191}Ir(n,\gamma)^{192}Ir$	74 days	I, commonly used	4*a*, 23
^{85}Kr	Fission	10 years	I, M; β^- excited source	5, 9
^{140}La	$^{139}La(n,\gamma)^{140}La$	40 hr	I, one of 12 named	4*a*
^{177}Lu	$^{176}Lu(n,\gamma)^{177}Lu$	7 days	M, good potential	2, 6
^{24}Na	$^{23}Na(n,\gamma)^{24}Na$	15 hr	I, one of 12 named	4*a*
^{109}Pd	$^{108}Pd(n,\gamma)^{109}Pd$	13.6 hr	Impractical	11
^{147}Pm	$^{147}Nd \xrightarrow[11.06\ days]{\beta} {}^{147}Pm$	2.5 years	I, M; β excited source; outweighs ^{241}Am, ^{125}I (Ref. 11); well-suited for portable use	1, 10, 11
^{210}Po	Naturally radioactive	138.38 days	Mentioned	4*a*
^{226}Ra	Naturally radioactive	1600 years	I, one of 12 named	4*a*
^{90}Sr	Fission	28 years	I (Ref. 10); M (Ref. 2); β^- excited source	2, 10
^{145}Sm	$^{144}Sm(n,\gamma)^{145}Sm$	340 days	M, among top 11 of 48 evaluated[3]	2, 3, 6
^{153}Sm	$^{152}Sm(n,\gamma)^{153}Sm$	47 hr	I, one of 12 named[4]; M, good[2]; impractical[11]	2, 4*a*, 6, 11
^{182}Ta	$^{181}Ta(n,\gamma)^{182}Ta$	111 days	I, one of 12 named	4*a*
^{170}Tm	$^{169}Tm(n,\gamma)^{170}Tm$	129 days	I, one of 12 named[4]; M, poor[2]; impractical[11]	2, 3, 4*a*, 6, 11
^{181}W	$^{180}W(n,\gamma)^{181}W$ or $^{181}Ta(p,n)^{181}W$	126 days	M, among top 11 of 48 evaluated	3
^{133}Xe	Fission	5.27 days	M, short-exposure work mentioned[2]; impractical[11]	2, 11
^{169}Yb	$^{168}Yb(n,\gamma)^{169}Yb$	32 days	M, best[2]; chest radiography	2, 6

*I, industrial; M, medical use.

†Unclear whether an isotope of cerium or cesium was used.

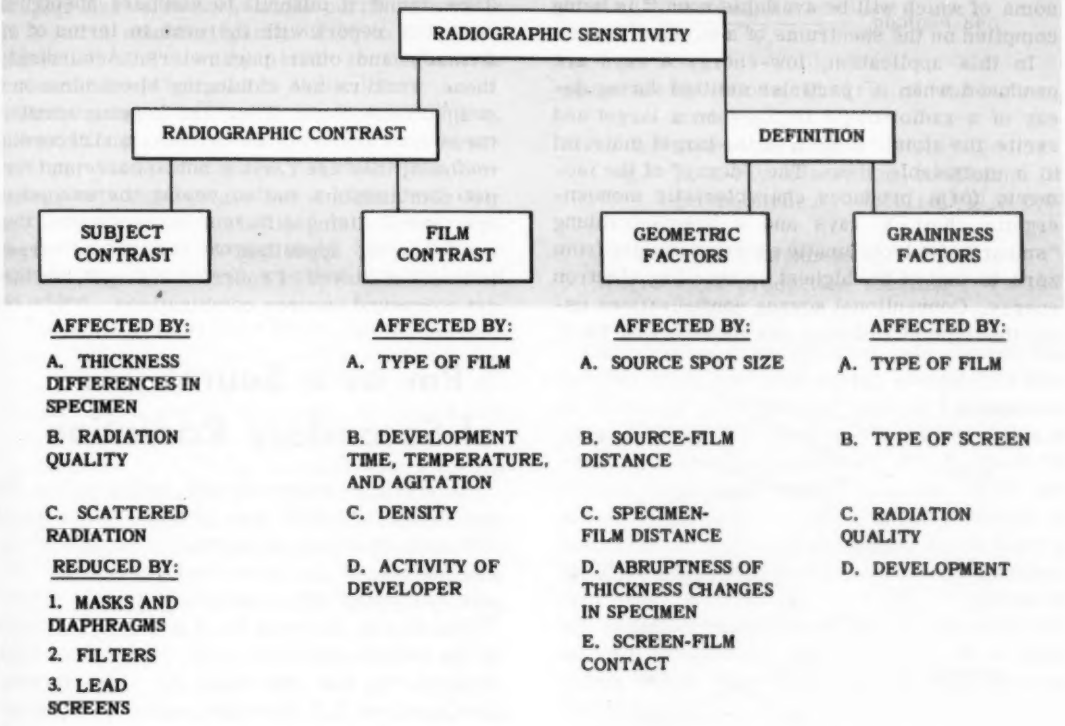

Fig. IV-1 Factors affecting radiographic sensitivity. See also Ref. 4*b* and Table IV-1.

find a base for comparison of the usefulness in isotopic radiography of a number of radionuclides. In their words:

> ... (a) the spectral shapes of the radiations from conventional x-ray machines operated at various kilovoltage dial settings were obtained by the use of a NaI crystal and a multichannel pulse height analyzer, (b) Hurter-Driffield [i.e., exposure–film density] curves from various films exposed to radiations from radioactive sources and x-ray machines were made, and (c) 48 promising radionuclides were selected and closely examined for spectral suitability using a multichannel analyzer.

They found that to obtain a radiograph with an exposure time of a few seconds from the radiations of any one of 11 "premium" radionuclides, radiosource strengths of about 1 curie were required—a strength that limits the use of radioisotopes for clinical visualization of tissue. On the other hand, they noted that with the use of image converter tubes smaller sources (a few millicuries) would be possible. Hence they consider these 11 radionuclides to have a bright future in this application.

Krabbenhoft and Green[2] evaluated ^{170}Tm and four other isotopes not used previously for clinical radiography. They made 145 exposures using ^{169}Yb, with emphasis on chest radiography, and studied the effects of type of grid, variability of exposure time, and short source-film distance. A portable chest radiography device for tuberculosis surveys is now using this isotope,[7,8] and, although exposures are only slightly longer than those with X-ray equipment, they are short enough to allow as many patient exposures per day as with X rays. They consider the air-skin dose to be 2 or 3 mr, which is about the dose received in 1 week by the patient from radiation in his natural environment. Secondary radiation is also low, and the operator receives only a fraction of the weekly dose from background.

Beta-Ray-Excited Sources for Radiography

Beta-emitting isotopes are becoming useful as radiographic sources. Basic information,

some of which will be available soon,[18] is being compiled on the spectrums of a number of them.

In this application, low-energy X rays are produced when β^- particles emitted during decay of a radioisotope impinge on a target and excite the atomic K shell of the target material to a metastable state. The "decay" of the isomeric form produces characteristic monoenergetic (Kα) X rays and a bremsstrahlung "smear" of polychromatic energies ranging from zero to that of the highest bombarding electron energy. Conventional source configurations using this type of radiation are shown in Fig. IV-2.

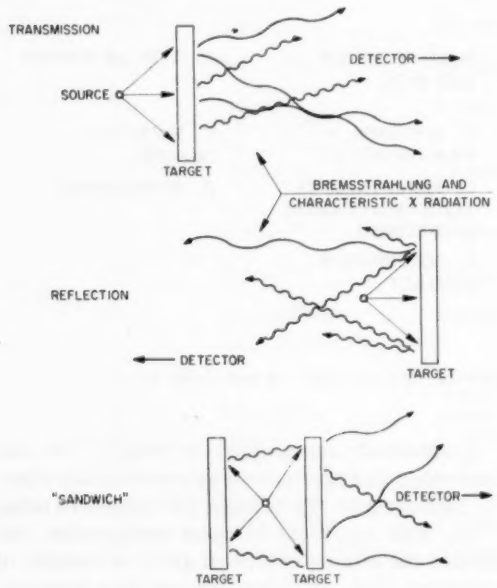

Fig. IV-2 Bremsstrahlung source configurations.[5]

The bremsstrahlung component can be decreased by selection of source parameters, thus allowing the monoenergetic X-ray beam to become a significant portion of the total (characteristic plus continuous) photon flux. The radiation source thus produced is suitable for radiography of low-mass objects because its narrow spectral spread is in the low-energy range needed for radiographic contrast and detail.

During extended research at the Edsel B. Ford Institute, Preuss and coworkers[18] noted that much of the literature describing experimental spectral determinations was concerned with a limited number of beta emitters and an equally restricted number of target materials. They found it difficult to compare spectrums from one report with the next in terms of efficiency and other parameters. Accordingly, these workers are cataloging spectrums on a comparative basis. They are keeping constant the source assembly and detection and recording methods; they are varying beta-source and target combinations and surveying the secondary spectrums. Using different radioisotopes, they are studying apposition of source and target, intimate mixtures of source and target, and target compound–source combinations.

^{147}Pm as a Source of Secondary Radiation

At IITRI a source-target configuration for secondary radiation was coupled with several different detection systems.[11] For this study, 250 curies of 2.6-year fission-product ^{147}Pm was fabricated into a pellet. With this "pure" ^{147}Pm source, in which the X rays are produced in the isotope itself and in the chemical carriers present, the flux was about 5.5×10^5 photons/(cm^2)(sec) at 1 ft from the source. The spectrum was relatively monoenergetic, peaking at 0.04 Mev.

Radiographs of both medical samples and representative low-atomic-number materials were made with this source with standard and Polaroid X-ray films with and without intensifier screens. Although this photon flux was too small for satisfactory results when currently available image-intensifier systems were used, radiographs made with about 1-min exposure showed sufficient detail that gross defects in the objects could be determined.

Source Requirements and Design

To make a source that would be useful in nondestructive testing for radiographic or fluoroscopic applications, Ezop[11] tried to satisfy three general requirements: (1) a small focal spot for good definition, (2) a photon energy (radiation quality) appropriate for the object under test to give good subject contrast and definition, and (3) a photon flux (intensity) large enough to satisfy exposure time or intensity limits.

Again the source material chosen was ^{147}Pm. Its beta radiations have a maximum energy of 0.23 Mev and a range of 50 mg/cm^2 in aluminum, and it has no gamma radiation. The oxide,

Pm_2O_3, has a radiochemical purity exceeding 99% and a chemical purity of 90 to 95%, with samarium and neodymium as impurities. Promethium-147 decays to stable ^{147}Sm.

Previous studies[10] had shown that, with ^{147}Pm, X-ray (Kα photon) yields are a few tenths percent per beta particle and that, with other low-energy beta emitters, output is higher with intimate mixtures of source and target than with discrete source and target units. Since ^{147}Pm is both source and target, no other material need be added.

The source fabricated for this program contained 366 mg of $^{147}Pm_2O_3$ compressed and sintered into a pellet approximately 7 mm in diameter and 2 mm in thickness. The pellet was encapsulated in an aluminum container 0.5 in. in diameter by 0.75 in. in length with a 15-mil aluminum end window and placed in a stainless-steel and Hevimet housing with a movable shutter. (Detailed drawings are given in the report.[11]) The overall size of the source was about 2 by 2 in. The shutter was controlled with a 3-ft-long camera cable release. Dose-rate measurements with the shutter closed were less than 7 mr/hr with a 3-in.-diameter thin-walled ionization chamber in contact with the source housing and approximately 135 mr/hr at 1 ft below the end window with the shutter open.

Spectrum and Output

The energy spectrum of the emerging photons was measured with a 1.5- by 1-in. thin-window NaI(Tl)-crystal scintillation detector and multichannel pulse-height analyzer. Because of the intensity of the source, a source-to-detector distance of 30 ft was necessary to avoid spectral distortion in the analyzer. The spectrum obtained has a pronounced peak in the region around 0.04 Mev (Fig. IV-3). This peak results primarily from emission of the 0.0385-Mev Kα X rays of promethium following K-shell ionization and is superimposed upon a bremsstrahlung continuum. The photon spectrum is more nearly monoenergetic than the outputs of conventional X-ray machines.

The source-target mixture used consisted of the ^{147}Pm source, with promethium and its daughter samarium acting as the target materials. The secondary photon yield of this configuration is the integrated product of the photon production function multiplied by a self-absorption function. The X-ray output, N_x, from this source is given by

$$N_x \approx \frac{AaN(w_k)(1 - e^{\mu_x t})}{\mu_x} \text{ photons/sec}$$

where A = specific activity of the source, curies/g
a = source area, cm^2
μ_x = K X-ray absorption coefficient (in promethium $\mu_x = 4.66$ cm^2/g at 0.04 Mev)
t = source thickness, g/cm^2
$N(w_k)$ = total production function ($\sim 4 \times 10^{-3}$ photon per beta)

Calculations from spectral data showed that the flux of photons with energy around 0.04 Mev is $\sim 5.5 \times 10^5$ photons/(cm^2)(sec) at 1 ft from the source. From the equation, the expected flux is $\sim 8.1 \times 10^5$ photons/(cm^2)(sec) at 1 ft. Since the 15-mil aluminum window absorbs ~5.5% and since ~10% of the K-shell vacancy results in emission of Auger electrons and not K X rays, the expected flux is reduced to $\sim 7 \times 10^5$ photons/(cm^2)(sec) at 1 ft. The total flux of photons of all energies calculated from the spectral data is $\sim 8 \times 10^5$ photons/(cm^2)(sec) at 1 ft. A mid-range value was chosen for the fluorescence contribution.

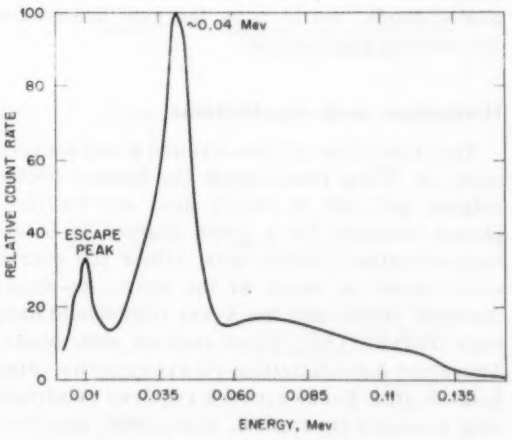

Fig. IV-3 Promethium-147 energy spectrum.

Results of Experimental Applications

The ^{147}Pm source output was essentially monochromatic, and experimental applications centered around inspection of low-atomic-number or thin materials, e.g., medical and dental radiography and fluoroscopy as well as

radiographic inspection of components used in the missile, aircraft, and electronic industries. In a later study at ORNL,[1] a human hand and various metal and plastic objects were radiographed with good results.

Table IV-2 summarizes the results of the radiographs made by Ezop[11] with ^{147}Pm and gives one comparison with an exposure from a conventional hospital X-ray machine.

A survey of image intensification equipment indicated that the minimum X-ray requirement is 3 to 6 mr/min at the face of the image-intensifier tubes for usable results. Since the experimental source delivers approximately 2 mr/min at 1 ft with no object absorbing the photon beam, the output of this source is too weak for satisfactory use with current models. Increasing the effective source output by increasing the source area or decreasing the source-to-detector distance would provide a sufficient flux at the face of the image tube, but penumbra effects would distort the image and wash out any fine detail. However, Ezop[11] noted that image-intensifying systems now under development may allow the use of low-activity input sources, and such devices as image-intensifier spark tubes,[19] which allow photographic recordings of single electrons from the photocathode, would have the gain needed for low-energy applications.

Limitations and Applications

The limitations of beta-excited X-ray sources such as ^{147}Pm result from the limited photon outputs per unit of source area and the fixed photon energies for a given source. To obtain high-definition radiographs, either the source area should be small or the source-to-object distance large, and the X-ray film should have high definition, which implies slow speed. Therefore high-definition radiography using beta-excited X-ray sources requires relatively long exposure times, and, conversely, short exposure times result in loss of definition. The fixed photon energies from any given source also limit its use to certain classes of materials; for example, the low-energy (0.04-Mev) photons from ^{147}Pm are most applicable to low-atomic-number or thin materials.

Because of general characteristics mentioned above, certain nondestructive-testing uses of beta-excited X-ray sources, ^{147}Pm in particular, seem practical. An X-ray system consisting of an isotopic source and a mechanical Polaroid film unit requires no darkrooms, chemicals, or power supplies. Loading of the cassette, exposure, and development require less than 5 min, and results are available for immediate evaluation.

Pressly at ORNL recently made a series of radiographs that illustrate the potential application of ^{147}Pm sources in nondestructive testing. The object chosen was an Amperex 6960 vacuum tube, one end of which is encased permanently in an alloy- or silver-coated copper wall. Figure IV-4 shows two exposures of this tube made with a 970-curie $^{147}Pm_2O_3$ source. Its coil and thin wires are visible in Fig. IV-4*b*, but actually all the details shown in this picture were seen when the 9-min radiograph (Fig. IV-4*a*) was placed on a light table or held up to an ordinary light source. The radiographs also demonstrate that degrees of density can be visualized by manipulating exposure time. Pressly noted that, with a 3000 X Polaroid *positive-negative* film, improved image visualization might permit exposures shorter than 9 min for similar materials. This film is not now available.

In the medical field such a unit could provide on-the-spot radiographic inspection to determine the location of possible bone fractures or of foreign matter lodged in body tissue. Although the results would not contain as much detail as radiographs made by conventional techniques, they could provide emergency diagnostic information. For military applications, especially in combat zones, such examinations may be the only ones available. Possible civilian applications might include on-the-spot radiographs of persons injured in accidents or routine examinations where access to an X-ray laboratory is impractical or would cause a hardship to the patient.

The number of practical potential industrial uses of beta-excited X-ray sources probably exceeds the medical ones because exposure-time requirements are not so critical. In general, high-definition radiographs should be possible because there is no relative motion among source, object, and film to wash out fine detail. Field inspections, especially those involving limited accessibility, and routine nondestructive tests where geometric problems necessitate small and/or irregularly placed X-ray sources appear feasible with isotopic devices. Inside-out radiography of a pipe is an example of such a use. Other specific applications could include

Table IV-2 EXPERIMENTAL RADIOGRAPHY OF HUMAN AND INDUSTRIAL MATERIALS*

Source	Film†	Object	Source-film distance	Exposure time	Results
Hospital machine	Kodak Royal Blue Medical	Skeleton hand	Not stated	Not stated	Good diagnostic value
^{147}Pm	Same film with screen A	Same	1 ft	30 sec	Fine structure visible; not so sharp as machine
	Same	Same	2 ft	140 sec	Quality improved slightly over 30 sec
	Same	Lower forearm and hand	1 ft	50 sec	Gross defects clearly visible
	Same film with screen B	Chipped finger bone	Same	60 sec	Bone chip visible; overexposed
	Same	Foot	Same	Same	Bone fine structure visible
Collimated ^{147}Pm	Same	Jawbone and teeth	2 in. (source inside, film on teeth)	10, 15 sec	Teeth visible; no evaluation
	Kodak No-Screen	Same	Same	Few minutes	Fine structure detail improved over 10, 15 sec exposure
^{147}Pm	Polaroid radiographic type 3000 X	Skeleton hand	1 ft	1 min	No fine structure visible
	Same	Hand	9 in.	40 sec	Limited to locating fractures and foreign bodies in bone structure
	Same	Foot	1 ft	1 min	Same
	Kodak Royal Blue Medical with screen B	Copper, aluminum materials	1 ft	1 min	Various resolutions achieved; no evaluation
	Polaroid radiographic type 3000 X	Same	6 in.	20 sec	Internal void in aluminum connector visible
Ordinary photograph	Unspecified	Radiotransmitter	Unspecified	Unspecified	Object nearly invisible
^{147}Pm	Polaroid radiographic type 3000 X	Same	1 ft	5 min	Components visible
	Kodak Royal Blue Medical with screen B	Same	Same	1 min	Same
	Same	Potted circuits	Same	Same	Components visible; visual inspection would require destruction
	Same film with screen A	Same	Same	Same	Same
	Polaroid radiographic type 3000 X	Dosimeter and switch	Same	Same	Same
	Kodak Royal Blue Medical with screen B	Cast turbine blade	Same	30 min	No evaluation; blade visible

*Compiled from data and radiographs shown in a report by Ezop[11] of IITRI.

†Screen A, Patterson Lightning Special Intensifying Screen; screen B, Patterson HiSpeed Screen. In the Polaroid exposures the results are printed positive.

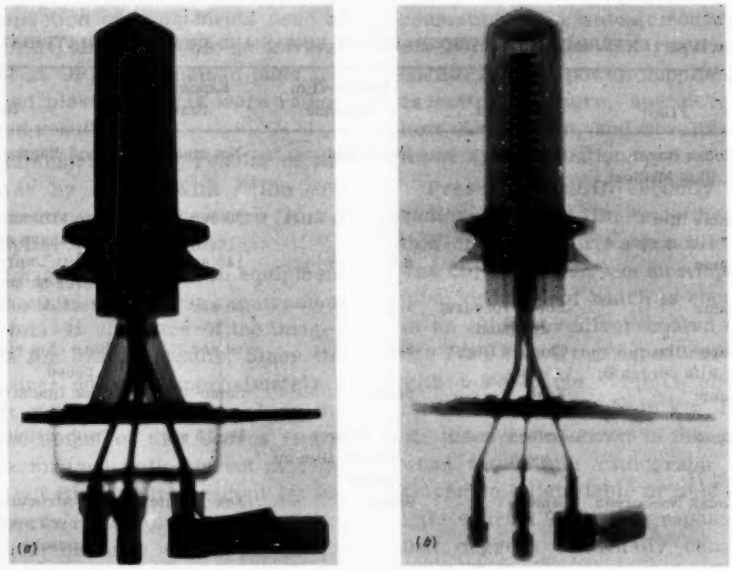

Fig. IV-4 Radiographs of vacuum tube with ^{147}Pm source with exposure times of (*a*) 9 min and (*b*) 36 min. Picker X-ray Polaroid T60-824 equipment was used, the Amperex 6960 tube being placed on the cassette and the source positioned 41 cm from the film. Source: 970 curies of ^{147}Pm (455 curies per gram of $^{147}Pm_2O_3$), of which 57.4% was $^{147}Pm_2O_3$, and the remainder, $^{147}Sm_2O_3$. Polaroid 3000 X positive film. Readings with ionization chamber type dosimeter were 600 mr/hr at the surface of the film and 20 mr/hr at 1 ft perpendicular to the beam.

radiographic tests on encased electronic circuits; thin welds, such as those found in tubing and airframe construction; and inspection of thin-sheet and low-atomic-number materials used in missile, aircraft, and allied industries.

Nondestructive tests such as critical absorptiometry, thickness gaging, and quantitative and qualitative analysis by fluorescence excitation are also possible with beta-excited X-ray sources.[10]

Economics of ^{147}Pm Source*

At a price of $12 per curie for the 95% chemically pure ^{147}Pm (specific activity 600 curies per gram of promethium) used in Ezop's study, the cost of an X-ray source similar to the experimental one described above would be approximately $3000. If a ^{147}Pm source should be fabricated from material having a specific activity of 920 curies per gram of promethium and a thickness of 650 mg/cm^2 ($\sim 3/\mu_x$), it would have a flux of $\sim 6.2 \times 10^5$ photons/(cm^2)(sec) at 1 ft. This would be a 12.5% increase in output at an 8% lower cost. A high-specific-activity source with a $2/\mu_x$ thickness would have the same output as the experimental source with a 40% lower cost.

Ezop[11] noted that costs also could be lowered by reprocessing the source material after, say, a period of one half-life, the source material being returned for credit on a new source; users of reactor fuel elements operate in this manner. He also concluded, from calculations of expected photon yields and other characteristics, that ^{147}Pm outweighs both ^{241}Am and ^{125}I in usefulness as a radiography source.

*Generally speaking, costs given for isotopic radiographic sources are those of the isotope, and do not necessarily represent total cost, including encapsulation and other charges. In the case of ^{147}Pm, the stated price included a purification step to remove ^{152}Eu and ^{154}Eu.

^{85}Kr for Beta-Excited Radiation

A variation of the beta-excited X-ray radiographic method[20] has been developed[5,9] with

^{85}Kr. In addition to being readily available and relatively inexpensive, this radioisotope is biologically inert. Advances in "packaging" of ^{85}Kr have allowed its use in solid form,[21] the krypton being trapped by molecular bonds in hydroquinone to form a clathrate. Specific activities have been obtained by this method which correspond to many atmospheres of gaseous ^{85}Kr of the same volume.

Bersin et al.[5] studied the use of clathrates in radiorelease applications, tracing, radiography, X-ray analysis, therapy, and X-ray measurement. McCue[9] later published an account of the work on radiography alone. Krypton gas has also been used as a beta source for bremsstrahlung and characteristic radiation by other researchers.[10,22]

Nuclear-Chicago Corp. constructed two sources for DID-sponsored work at IITRI,[10] one containing about 25 mc, and a second, 500 mc of gaseous ^{85}Kr. The cylindrical containers were thin electrolytic nickel tubes 0.25 in. in diameter and 4 in. in length with wall thicknesses of about 0.0015 in. The 25-mc source was used for a study of spectral distribution of X rays produced in different geometries and with various target materials. The 500-mc source was used in experimental applications. Filosofo[10] pointed out that, with the source material of about 80 mc/cm^3 available at present, even in a relatively high-pressure beta source contained in a capsule made of proper target materials the total beta activity and X-ray output were still below those obtainable for the same size source with ^{90}Sr and ^{147}Pm, two radioisotopes he also tested. High-activity X-ray sources using ^{85}Kr also are limited by the presence of a 0.54-Mev gamma component. For every curie of ^{85}Kr, this component will give an exposure of about 10 mr/hr at 1 ft; thus effective shielding for biological protection is needed if a large amount of this isotope is used. Filosofo concluded that the main field of application of the gaseous source could be thickness gaging by absorption and fluorescence radiation measurements.

McCue,[9] a coworker of Bersin at Tracerlab, stated that low-energy X-ray sources using beta excitation from ^{85}Kr clathrate to produce X-ray fluorescence of a target material can be successfully used for the radiography of low-mass objects. An inherent advantage of the ^{85}Kr clathrate over gaseous ^{85}Kr is the simplicity of containing relatively high source strengths in small volumes. A 500-mc gaseous source requires a pressure of 8.75 atm, while 1 g of solid clathrate has the same activity at atmospheric pressure. The theoretical upper limit is 3 curies per gram of clathrate* when 5% enriched ^{85}Kr is used.[5]

Four source-target configurations were studied at Tracerlab in exploring ^{85}Kr clathrates for radiography.

Mixture Configuration

Bersin and coworkers[5] selected seven target materials to give a range of Kα energies between 0.01 and 0.1 Mev:

Target compound	Kα, Mev
KCl	0.012
Ag_2CO_3	0.022
$BaCl_2$	0.032
Sm_2O_3	0.04
W	0.069
$PbCl_2$	0.074
U_3O_8	0.097

Clathrate with a specific activity of 0.5 mc/g was mixed with 25 to 75 wt.% target material. Data were obtained by scintillation spectrometry with a 1.5- by 1-in. NaI(Tl) crystal, phototube, and 20-channel analyzer. Source-target mixtures were inserted in a Lucite-lined counting well.

By analysis of the source data obtained by varying the target material, target concentration, angular geometry, beam filtration, and layer thickness, these investigators formulated the following concepts on clathrate-target mixtures. Data were compared on the basis of spectral purity and intensity of Kα flux.

Target Atomic Number. In general, increasing the target atomic number increased the Kα flux output. A notable exception was U_3O_8, which produced less Kα flux per millicurie than one of the lower atomic number targets, probably because of the excessive screening by the many oxygen atoms and the scattering of Kα and β^- radiation. The relative spectral

*McCue[9] claims a potential capability of 4 curies per gram of clathrate and states that an equivalent gaseous pressure would have to be 70 atm to contain the same activity. A concentration of 0.5 curie per gram of clathrate is now possible.[5]

purity for U_3O_8 also was decreased, probably for the same reasons. The sharpness, or spectral "purity," of the Kα peaks was taken here as the ratio of the counts in the Kα channel (5.5 kev wide) to the counts in the spectrum band between Kα and Kα + 50 kev. Deterioration of spectrometer resolution with decreasing energy was considered in tabulating the results (Table IV-3). Accuracies of measurement were ±15%.

Table IV-3 EFFECT OF TARGET ATOMIC NUMBER ON Kα FLUX AND PURITY

Mixtures of 50 wt.% target-clathrate and an angular geometry of 45° used

Target material	Target atomic number	Relative Kα flux	Spectral purity*
U_3O_8	92	0.80	0.260
$PbCl_2$	82	1.0	0.290
W	74	0.65	0.280
Sm_2O_3	62	0.60	0.265
$BaCl_2$	56	0.55	0.130
Ag_2CO_3	47	0.23	0.075

*See text.

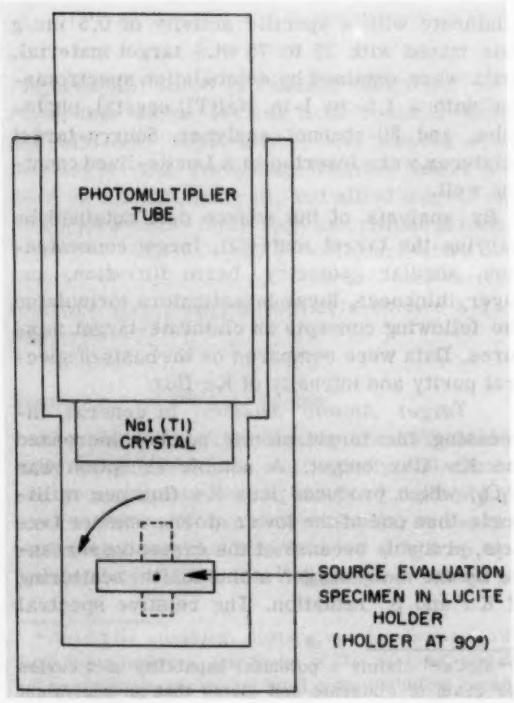

Fig. IV-5 Experimental arrangement for ^{85}Kr source-target evaluation.

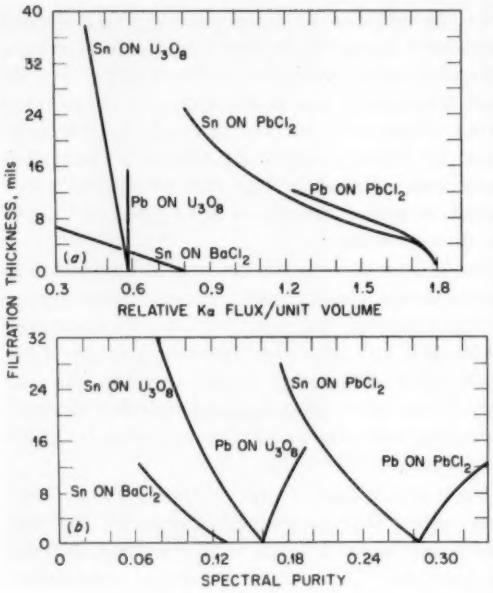

Fig. IV-6 Effect of lead and tin filtration on (*a*) flux and (*b*) spectral purity. For these experiments, 50 wt.% concentrations of target-clathrate mixtures were used.

Target Concentration. The Kα energy production per unit volume passed through a maximum at 40 to 50 wt.% target concentration. On a unit radioactivity basis, where the total volume increased with increasing target concentration, the Kα production was a continually increasing function of target concentration.

Angular Geometry. The experimental arrangement is shown in Fig. IV-5. Variation of the angular orientation of the rectangular slab of target-clathrate mixture significantly affected the Kα production and spectral purity. An optimum value of slab orientation was about 45°, since purity at that angle was only slightly decreased from maximum, and Kα detection was down less than half.

Beam Filtration. The influence of various thicknesses of lead and tin filtration on the spectral purity and flux was investigated for $PbCl_2$, $BaCl_2$, and U_3O_8 mixtures (Fig. IV-6). Tin filtration not only decreased the Kα flux but also decreased the purity. Lead filtration increased the purity substantially for both U_3O_8 and $PbCl_2$ mixtures but obliterated the low-energy barium Kα line from the $BaCl_2$ mixture.

Layer Thickness. Lead chloride mixtures (50 wt.% clathrate) with slab depths ranging from

$\frac{1}{16}$ to $\frac{1}{2}$ in. were evaluated at 45° geometry. Purity increased with thickness over the range investigated, and the Kα flux per millicurie appeared fairly constant. The net effect is one of improved performance with increasing thickness up to at least $\frac{1}{2}$ in.

Transmission Configuration

Bersin and coworkers measured the lead Kα production and purity primarily for comparison with earlier results obtained by IITRI workers using gaseous ^{85}Kr sources.[22]

A 0.005-in. target was optimum for maximum Kα flux in both studies. Integrating the differential spectrum for total counts in the energy band 0.06 to 0.09 Mev and computing the total number of β^- particles striking the target, they found a conversion efficiency (Kα photons per β^- particle impinging × 100) of 0.75%.

Some error was introduced into this determination because of geometric approximations and beta-range estimates for the mixture density. These were not thought to exceed ±25%, however, and agreement with measurements by others using gaseous ^{85}Kr was within 25%.

A similar conversion-efficiency calculation for the $PbCl_2$ and clathrate mixture was complicated by the geometric arrangement of target and β^- sources. On the assumption that all beta particles emitted interact eventually with a lead atom, a conservative conversion efficiency for Kα of lead per β^- is 2.5%; an empirical determination of this conversion efficiency based on the Kα peak intensity with the ^{85}Kr 0.540-Mev gamma yielded a Kα of lead per β^- total conversion efficiency of 6.06%.

Reflection Configuration

With the transmission source (discussed above) in a reflection configuration obtained by inverting the holder, spectrums were obtained for two different backing thicknesses. These showed an abundance of bremsstrahlung below the Kα 0.074-Mev emission. The Kα flux for this arrangement was approximately 20% greater than that obtained in transmission, but purities were about the same.

Sandwich Configuration

A source fabricated with ^{85}Kr with lead-foil backing was tested in a transmission configuration, and spectrums were obtained for varying thicknesses of reflector and filter. Variation of the backing thickness produced no significant changes over the range investigated, a result confirming earlier findings. Increasing the transmission–foil thickness decreased the Kα flux accordingly, but the spectral purity remained essentially constant. At best, spectral purity does not appear significantly higher for sandwich configurations, and Kα flux is found to be slightly less (about 5%) compared with mixture configurations of equal strength.

Specific Applications

Sources were constructed as cubes of Lucite containing the clathrate-target mixtures in their centers. Radiographs were made by use of sources with a clathrate specific activity of 0.15 mc/mg of beta activity, or about 6 μc/mg of characteristic radiation activity (assuming a 4% conversion efficiency).

Eastman Kodak type KK industrial X-ray film was selected for radiographs of several objects, including sealed relays and a Geiger tube. Actual source Kα intensities ranged from 0.20 to 0.35 mc. In these radiographs the details of peas in a pod, contacts, springs, and relays are visible (see Fig. IV-7, for example).

In addition to the "cube" sources, two high-flux "monoenergetic" sources were designed with optimum concentration, geometry, and filtration parameters derived during the preliminary investigation. One such source (Fig. IV-8) was constructed by coating uranium-foil cones with U_3O_8-^{85}Kr clathrate "paint." The uranium foil served several functions by providing low-energy X-ray filtration, additional reflection and transmission, and bremsstrahlung production and by increasing the Kα flux. Clathrate and U_3O_8 were mixed in 50 wt.% concentrations, liquified with toluene solvent and Lucite binder, and applied as a coating to the uranium-foil cones. When assembled coaxially, the cones formed a single unit with layers of uranium foil and mixture.

The spectrum resulting from this source design is shown in Fig. IV-9, together with a spectrum from a 50 wt.% mixture of U_3O_8 and ^{85}Kr clathrate. Bersin et al.[5] claimed that a 30% improvement in spectral resolution was obtained with this special source design. The conversion efficiency for this source has been measured to be 2.8%, while the conventional mixture yields 3.3%. McCue said that radio-

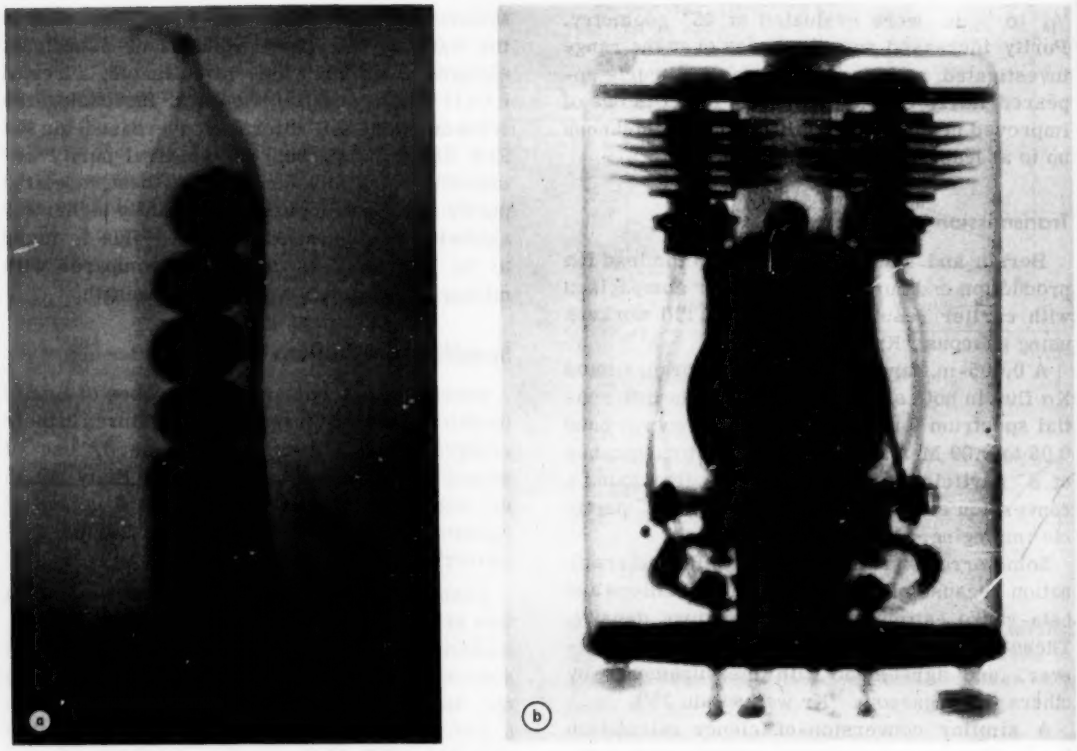

Fig. IV-7 Radiographs obtained by use of krypton clathrate-target mixtures as sources of secondary radiation. (*a*) Pea pod: source-subject distance, 6 in.; exposure time, 2.85 min/in. per 10 mc of source Kα radiation. (*b*) Leach No. 973 sealed relay: 1 ft; 0.71. Eastman Kodak type KK industrial X-ray film was used, and source intensities ranged from 0.2 to 0.35 mc. (Courtesy of J. C. McCue; see Ref. 9.)

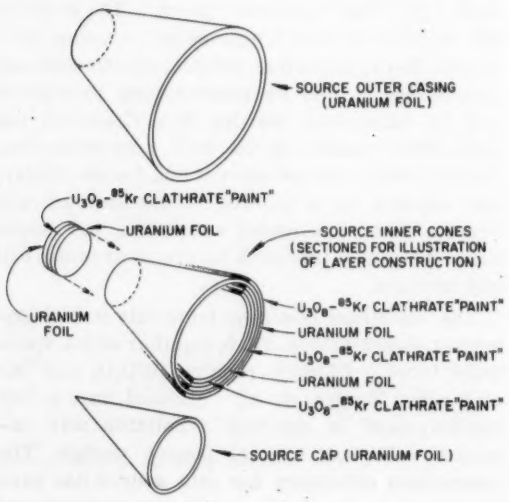

Fig. IV-8 Sketch of cone source construction.

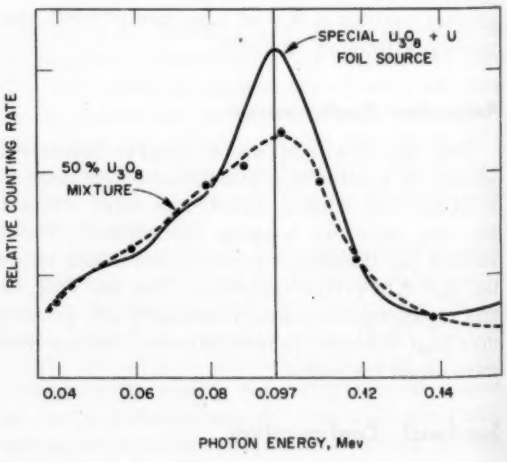

Fig. IV-9 Comparative spectrums of special design source and conventional mixture.

graphs would be at least as good, and probably better, with the special design as with the U_3O_8-^{85}Kr clathrate mixture.

Other Isotopes for Radiography

Despite the potential usefulness of beta-excited X-ray sources for radiography, isotopes that emit effective gamma radiation are the best-established sources for this application at the moment. Fundamentals of gamma radiography, practical aspects such as exposures, and interpretations of radiographs are given in a 1961 handbook.[23] This handbook emphasizes ^{192}Ir, but the principles and methods described are applicable to other isotopes such as ^{60}Co and ^{170}Tm.

A promising area of development is in work with the low-energy gamma emitters ^{55}Fe and ^{125}I. Resolution of very small differences in densities is possible by use of these isotopes.[1,12] Table IV-4 and the following paragraphs summarize some of this work.

In experiments at ORNL, Russell[12] prepared two ^{125}I sources for study and evaluation. Two curies of ^{125}I and 0.5 mg of normal ^{127}I were precipitated together as silver iodide, and the dried salt was placed in a stainless-steel capsule (Fig. IV-10) with a 1-mil-thick 2-mm-diameter stainless-steel window that was sealed by welding. The radiation through the window of the source was 450 mr/hr at 16 in. from the center of the source.

Iodine and silver both absorb some of the radiation emitted by the ^{125}I; therefore, in preparation of the second source, the efficiency was increased by using $Na^{125}I$ instead of $Ag^{125}I$. The ^{125}I was distilled from a small volume into 1.0 ml of 0.0001*N* sodium hydroxide solution. This solution was evaporated to dryness in an aluminum cup 0.090 in. in inside diameter by 0.070 in. in depth and welded closed in an aluminum capsule 0.375 in. in length by 0.140 in. in diameter and having a 0.010-in.-thick aluminum

Table IV-4 SOME EXPERIMENTS WITH GAMMA-EMITTING ISOTOPIC SOURCES AND MACHINES IN RADIOGRAPHY

Source	Object	Source-film distance, cm	Film	Time	Calculated exposure times for larger source	Reference
1.96 curie ^{125}I	Guinea pig	~25	Du Pont Cronar	1.5 hr	Not given	24
	Hand	~33	Polaroid 3000 X	3 min	Not given	12
4 mc ^{125}I	Cadaver hand	50	Ansco No-screen X-ray	20 hr	1 min with 5 curies; 3 sec with 100 curies	16
12 mc ^{125}I	Teeth	6	Kodak Kodirex	12 min	8 sec with 1 curie	14
	Teeth	7	Kodak Ultra-speed Dental	7 min	40 sec with 1 curie	14
	Cadaver hand	20	Cea Singul-x	1 hr	40 sec with 1 curie	14
	Teeth	6	No-screen*	12 min	Not given	15
0.25 mc ^{125}I	Vacuum tubes; fuses	~20	Medical X-ray*	17 hr	30 sec with 500 mc	17
85-kvp Picker X-ray machine	Vacuum tubes; fuses	~61	Medical X-ray*	7 sec 15 ma	Not given	17
50 mc ^{55}Fe	Pansies; leaves	~10	Polaroid 3000 X	4.5 hr	Not given	1
8-kvp X-ray machine	Roses	87	Eastman type "M"	~2–3 min 30 ma	Not given	25
10-kvp X-ray machine	Diatomaceous earth	~114	Eastman High Resolution plates	42 min 30 ma	Not given	26
320 mc ^{241}Am	Hand; mechanical pencil	25	Ilford High Contrast Industrial	10 min	Not given	13
320 mc ^{241}Am	Simulated luggage container	25	Royal Blue Medical	10 min	Not given	13
^{169}Yb, ^{153}Gd, ^{152}Sm, ^{170}Tm, ^{177}Lu	Variety of clinical exposures	Varies	Varies	Varies	Varies	2
Other beta-gamma emitters	Variety of clinical exposures	Varies	Varies	Varies	Varies	Reviewed in 2, 28

*No manufacturer given.

window. This capsule was placed inside another aluminum source holder having a wall thickness of 0.020 in. The radiation from this capsule was 260 mr/hr at 16 in. The capsule was placed in a modified GMR model 110 radiographic exposure device,* or "camera." A 5-mil stainless-steel window in the radiographic exposure device decreased the radiation to 160 mr/hr at 16 in. A radiograph of a guinea pig made with this source is shown in an earlier issue of this review,[24] and further evaluation was being done at two laboratories at the time of this writing.

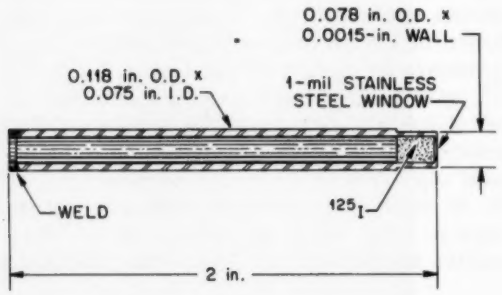

Fig. IV-10 Stainless-steel capsule for ^{125}I source.

A source described by Beronius et al.[14] was found useful for roentgen diagnostics and for forensic odontology. The active material for this source was supplied as carrier-free iodide in an alkaline sulfite solution. Inactive sodium iodide was added as carrier, and the halide was electrolytically (anodically) deposited on the hemispherical end face of a 0.5-mm-thick silver wire. The amount of iodide deposited was calculated from measurements of the activity of the solution before and after electrolysis. The activity of ^{125}I deposited was 12 mc, and it was calculated that the total amount of iodine in the deposit would correspond to 200 mc if carrier-free ^{125}I had been used. These investigators claim it is possible to make a source of ~1 curie with a diameter of 0.5 mm by this technique.

An exposure mechanism with exchangeable apertures and a total length of 3 cm was constructed. A gold alloy was used as shielding material. This apparatus makes possible intraoral mounting and prevents any significant dosages in unwanted directions. The small dimensions of the radiation source permit good resolution in the radiographs even when distances between the source and the subject are short.

Usable radiographs of a dry skull and a cadaver hand were also made with this device. Further work with this source and image intensifiers indicated that sources of higher activities could be of outstanding value during surgical operations.

Henrikson et al.[15] used the same source with exchangeable collimators to reduce secondary radiation. They noted that in odontological forensic identification the removal of the head, parts of the jaws, or extraction of some teeth for closer examination is often a necessary, time-consuming, and unattractive procedure. For instance, if there is characteristic root-filling, this will be destroyed if the tooth is extracted. Radiography of root-filled teeth is a better technique, since individual characteristics of root-fillings of cadavers in many cases have been decisive links in identification when radiographs of such fillings were compared with those taken during life.

The forensic odontologist, using a portable ^{125}I X-ray unit, can give information on lines of fractures, which sometimes show that violence came from a certain direction. This information may be valuable if the state of the body is such that changing the position of the skull will result in a dislocation of bone defects and lines of fractures. Dislocations of this kind can lead to an incorrect deduction or can make a conclusion impossible.

A criminal case is mentioned[15] in which identification was made with the use of a ^{125}I radiograph:

> A 25-year-old woman disappeared in Stockholm without trace on the night of 16th December, 1961. By chance she was found in a small wood on 8th March, 1962 (after the passage of 83 days), dead and covered with snow. The body was frozen fast to the ground. The head was surrounded by ice and lay in a slight depression in the ground. Neither the leader of the Homicide Squad, the forensic pathologist, nor the forensic odontologist could make any investigation *in situ* without taking the risk of destroying clues that had not yet been uncovered .... The ground immediately around and under the body was carefully loosened and, without moving it in any way, the body was then transported on its frozen bed of approximately 1,000 kg of earth and pine needles to the State Laboratory of Forensic Medicine in Stockholm. There the body was slowly

*Provided by General Motors Corporation Research Laboratories.

thawed at 16°C for five days, after which the forensic pathologist, the police, and the forensic odontologist could commence their closer investigations.

The dental identification, which was made even though part of the face had been destroyed, confirmed absolutely the identity of the woman by a comparison of the ^{125}I radiographs with X-ray plates of her previous dental treatments, and no fracture lines on the teeth or jaws indicative of violence could be discovered by "panorama" pictures. (In the panorama technique with a portable source, the source is placed inside the mouth and the film outside.)

Gruverman and Schivley,[17] using a similar source, extended these diagnostic and dental studies to industrially significant items. Their exposure device has an outer shield consisting of a steel-encased 3-mm lead cover that is screwed over an inner shield. They claim that the shield is capable of attenuating ^{125}I radiations by a factor of 10^{20}. A cable-trigger device is used to control the exposure. When the trigger is depressed, the source, which is plated on the end of a silver wire and encapsulated in plastic, moves forward, parting the leaves of the inner shield, and is thus exposed. The inner shield consists primarily of 0.5 mm of gold; it attenuates the ^{125}I radiation by a factor of about 10^4. Thus adequate protection for curie-level sources could be achieved with a shield weighing less than 500 g. (The source diameter in this instance is 0.5 mm.) These workers conclude that fully shielded models, even at curie level, would weigh less than 1 kg, including shielding.

Pressly,[1] using a ^{55}Fe source, obtained radiographs comparable to those made with a low-voltage X-ray machine.[25,26] His work was discussed in an earlier issue of this review.

Americium-241 gamma sources[13] have been prepared from AmF_3, $Am_2(C_2O_4)_3$, and AmO_2. Spectrums are shown for two of these compounds in Fig. IV-11; the spectrum for AmO_2 is similar to that for $Am_2C_2O_4$. An AmO_2 source encapsulated in stainless steel showed no distortion of the source window or leakage after 1 year. Satisfactory radiographs were obtained with these sources, and, in addition, they were used in absorptiometry studies.

As mentioned earlier in the present report, Krabbenhoft and Green[2] evaluated ^{153}Gd, ^{153}Sm, ^{170}Tm, ^{177}Lu, and ^{169}Yb and found the last to be most practical. Details of source preparation

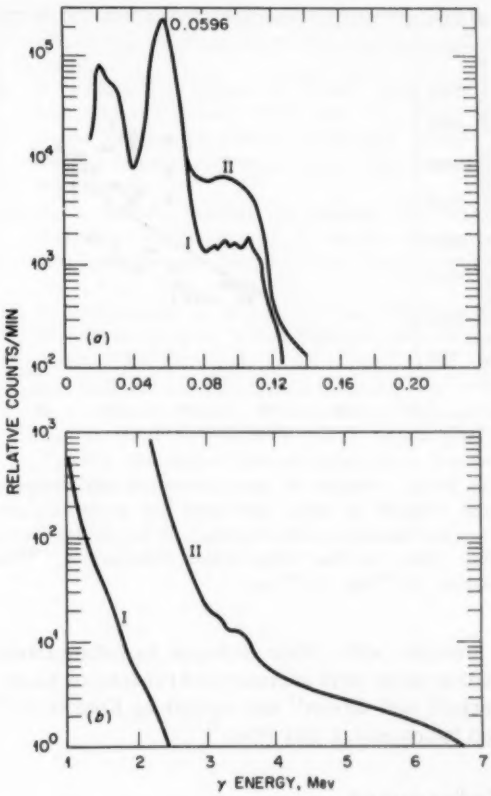

Fig. IV-11 Gamma spectrums of ^{241}Am sources. I, $Am_2C_2O_4$; II, AmF_3; curves were normalized to equal 0.0596-Mev peak heights. (*a*) Low-energy range: no absorber was used; source distance, 1 m. (*b*) High-energy range: counting geometry changed.

were not given. A radiographic exposure device was constructed with tungsten alloy for shielding, and exposures as short as 0.1 sec were timed. The device weighed 26 lb. The unit, *mrhm* (milliroentgens per hour at 1 m) times *seconds*, was chosen to denote exposure. By use of such data as are given in Fig. IV-12, exposure times could be calculated. Exposure time with a known source strength and for a given chest thickness is determined by dividing the exposure in *mrhm* times *seconds* by the source strength in *mrhm*. These workers made 177 clinical exposures with these radioisotopes, the majority of them with ^{169}Yb. A portable chest-radiography system has been developed,[7,8] and ^{169}Yb recently was shown to be valuable for radiography of thin sections of steel and aluminum.[27]

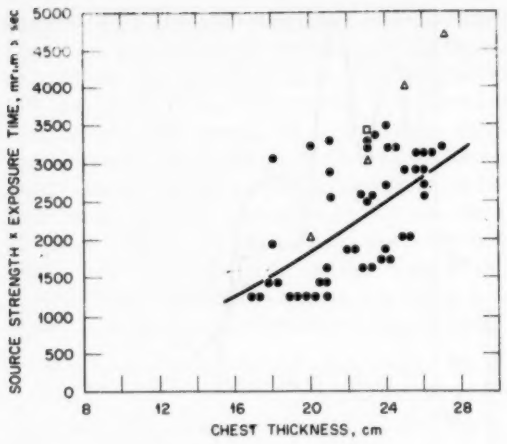

Fig. IV-12 Product of source strength and exposure time related to chest thickness for three isotopic sources. Source-to-film distance, 36 in.; Kodak Royal Blue film; Du Pont High-Speed Screens. ●, ^{169}Yb source. □, ^{153}Sm. △, ^{177}Lu.

Results with other isotopes in beta-gamma radiography were summarized recently by Krabbenhoft and Green[13] and earlier by Kohl et al.[4a] and Spangenberg and Pool.[28]

References

1. R. S. Pressly, Radioisotope Sources for Radiography, *Isotopes Radiation Technol.*, 1(2): 174-7 (Winter 1963–1964).
2. K. L. Krabbenhoft and F. L. Green, Some New Portable Radioactive Sources for Diagnostic Radiography, *Am. J. Roentgenol. Radium Therapy Nuclear Med.*, 90(6): 1123-42 (1963).
3. M. L. Pool and H. D. Spangenberg, Jr., Potentials of Isotopic Radiography (abstract), in Second Annual Oak Ridge Radioisotope Conference, April 19–22, 1964, USAEC Report TID-7689.
4. *a*. Jerome Kohl, R. D. Zentner, and H. R. Lukens, *Radioisotope Applications Engineering*, pp. 355-61, D. Van Nostrand Co., Princeton, N. J., 1961.
   b. G. M. Ardran, H. E. Crooks, and B. J. O'Loughlin, Image Quality and the Speed of Systems in Medical Radiography, British Report AERE-R-4533, February 1964.
   c. J. W. Dutli and D. E. Elliott, The Application of Cesium-134 to Industrial Radiography, *Nondestructive Testing*, 14(2): 24-7 (1956).
5. Richard Bersin, F. J. Brousaides, David Chleck, C. O. Hommel, and J. C. McCue, The Study of Inverse Radioactive Tracer Techniques and Applications of Radioactive Quinol Clathrates, USAEC Report NYO-2764, Tracerlab, Inc., July 1960.
6. Walter H. Lange, J. L. Greene, F. L. Green, and G. P. Graham, Advances in Isotope Radiography, *X-Ray Technician*, 34(4): 197-206 (1963).
7. F. L. Green and K. L. Krabbenhoft, A Tuberculosis Survey System Using a Portable Radioactive Source for Chest Radiography, *Trans. Am. Nucl. Soc.*, 7(1): 206-7 (1964).
8. J. H. Allen, G. P. Graham, W. F. Hawkins, and F. L. Green, Portable Chest Radiography Equipment with Radioactive Source for Tuberculosis Surveys, *Trans. Am. Nucl. Soc.*, 7(1): 206-7 (1964).
9. J. C. McCue, Soft Gamma Radiography with Minimum Hazard Radioisotope, *Nondestructive Testing*, 20: 383-6 (1962).
10. I. Filosofo, Isotopic Sources of Secondary Radiation, USAEC Report ARF 1122-27, Armour Research Foundation of Illinois Institute of Technology, February 1961; similar material in I. Filosofo, L. Reiffel, C. A. Stone, and L. Voyvodic, Design and Characteristics of Beta-Excited X-Ray Sources, in *Radioisotopes in the Physical Sciences and Industry, Proc. Conf., Copenhagen, 1960*, Vol. II, pp. 3-21, International Atomic Energy Agency, Vienna, 1962.
11. J. J. Ezop, Study of the Capability of Isotopic Source of Secondary Radiation, USAEC Report IITRI-1209-9, Illinois Institute of Technology Research Institute, February 1963.
12. H. T. Russell, Production of ^{125}I and Fabrication of ^{125}I X-Ray Sources, USAEC Report ORNL-TM-562, Oak Ridge National Laboratory, July 1963.
13. J. E. Strain and G. W. Leddicotte, The Preparation, Properties, and Uses of Americium-241, Alpha-, Gamma-, and Neutron Sources, USAEC Report ORNL-3335, Oak Ridge National Laboratory, August 1962.
14. P. Beronius, S. Forberg, C.-O. Henrikson, and R. Söremark, The Use of Iodine-125 as an X-Ray Source in Roentgen Diagnostics, *Intern. J. Appl. Radiation Isotopes*, 13: 253-4 (1962).
15. C.-O. Henrikson, R. Söremark, and K. O. Frykholm, The Use of an Iodine-125 X-Ray Unit in Forensic Odontology, *Odontologisk Revy*, 13(2): 130-8 (1962).
16. W. G. Myers, On a New Source of X-Rays, *Ohio State Med. J.*, 58(7): 772-3 (1962).
17. I. J. Gruverman and J. K. Schivley, Iodine-125 Makes a Better Low-Energy Gamma Radiography Source, *Nucleonics*, 21(5): 96-7 (1963).
18. L. E. Preuss, H. Collins, and E. R. Wilson, A Report on Compilation of Some Beta-Excited Spectra (abstract), in Second Annual Oak Ridge Radioisotope Conference, April 19–22, 1964, USAEC Report TID-7689.
19. B. Zacharov, Image Intensifier Spark Tube, *Rev. Sci. Instr.*, 33(12): 1461-2 (1962).
20. J. G. Kereiakes and A. T. Krebs, Optimum X-Ray Yields in Beta-Excited X-Ray Sources, in *Proc.*

U. N. Intern. Conf. Peaceful Uses At. Energy, 1958, 2nd Geneva, 20: 234-7, United Nations, New York, 1958.

21. D. J. Chleck, F. J. Brousaides, C. Hommel, W. Sullivan, L. Fishbein, and C. Ziegler, Yearly Report on the Development of Radiochemical Analyzers for Nonradioactive Gases and Study of Radioactive Clathrates, USAEC Report AECU-4493, Tracerlab, Inc., July 1, 1959.
22. L. Voyvodic, Isotopic Sources of Secondary Radiation, Interim Technical Report No. 2, March 1 – July 1, 1959, USAEC Report ARF-1122-13, Armour Research Foundation of Illinois Institute of Technology, August 1959.
23. *The AECL Iridium-192 Radiography Handbook*, Technical Bulletin IR-1, Atomic Energy of Canada Limited, Commercial Products Division, Ottawa, Canada, June 1961.
24. *Isotopes Radiation Technol.*, 1(2): 144 (Winter 1963–1964).
25. R. W. McClung, Techniques for Low-Voltage Radiography, *Nondestructive Testing*, 20: 248-53 (1962).
26. R. W. McClung, Studies in Contact Microradiography, USAEC Report ORNL-3511, Oak Ridge National Laboratory, October 1963; *ibid.*, Studies in Contact Microradiography, *Mater. Res. Std.*, 4(2): 66-9 (1964).
27. H. A. Burley, Nuclear Techniques for Product Improvement, Society of Automotive Engineers Meeting, Detroit, March–April 1964, Preprint 828A, 8 pp. (Conf.-464-1).
28. H. D. Spangenberg and M. L. Pool, Production of Roentgenograms by X-Ray Radiation from Radioactive X-Ray Emitters, *J. Am. Dental Assoc.*, 47: 624 (1953).
29. H. T. Russell, Reactor Production of ^{109}Cd and Its Use as an X-Ray Source, USAEC Report ORNL-TM-805, Oak Ridge National Laboratory, September 1964.

Section

V

Isotopes and Radiation Technology

Safety

Shielding Requirements for Isotopic Power Sources

By E. D. Arnold*

A handbook[1] showing shielding requirements for isotopic power sources has been prepared. Radioisotopic power sources used in terrestrial, marine, and space applications must be shielded or isolated to prevent dangerous radiation to personnel handling the sources, damage to instrument systems associated with their use, or interference with measurements that use radiation detection instruments. The handbook, which also lists radiation properties of the isotopes studied, is intended primarily for use by design engineers in preparing preliminary source designs. The handbook reference list contains 37 titles.[2–38]

Since one set of conditions cannot apply to all possible uses of a given source, calculations were made for a wide variety of conditions. From the data given in the handbook, it should be possible to determine shielding-material or separation-distance requirements for the isotopes studied for any set of established conditions. The results are presented as graphs of dose rate vs. shield thickness in order to make the report as general as possible. Shield weights were not plotted as a function of dose rate since a particular type of shield (cylinder, contoured cylinder, shadow, or sphere) and the radiation limitations based on application would have to be decided on before the actual weights could be calculated. Calculation of the shield weight is easy once the thickness is known and the type of shield has been selected.

*Oak Ridge National Laboratory.

Isotopes Studied

Radiation-intensity calculations were made for shielded and unshielded isotopic power sources fabricated from 17 different isotopes:

Isotope	Physical form	Isotope	Physical form
^{60}Co	Metal	^{210}Po	Metal matrix with void space for gas collection
^{85}Kr	Liquefied gas	^{232}U	Oxide
^{90}Sr	Oxide and titanate	^{228}Th	Oxide matrix with void space for gas collection
^{95}Zr-^{95}Nb	Oxide	^{238}Pu	Oxide
^{106}Ru	Metal	^{242}Cm	Oxide matrix with void space for gas collection
^{137}Cs	Glass	^{244}Cm	Oxide
^{144}Ce	Oxide		
^{147}Pm	Oxide		
^{170}Tm	Oxide		
^{171}Tm	Oxide		
^{204}Tl	Metal		

The sources made from most of these radioisotopes are intended primarily for power applications, but several isotopes, including ^{137}Cs, ^{95}Zr-^{95}Nb, ^{60}Co, ^{85}Kr, and ^{106}Ru, also show promise as sources of high-energy gamma radiation for use, for example, in sterilization or for initiation of chemical reactions.

In a previous study,[2] which was a part of this overall study of shielding requirements and which determined radiation and shielding requirements for the more promising isotopes (^{90}Sr, ^{137}Cs, ^{144}Ce, ^{147}Pm, ^{210}Po, ^{238}Pu, ^{242}Cm, and ^{244}Cm), it was established that shield weights ranging from 20 lb for ^{238}Pu to over 500 lb for ^{137}Cs would be required for 10,000-thermal-watt sources when used in an instrumented space mission. That study also indicated that weight penalties can be avoided if separation distance, rather than shielding, is relied on for protection. Separation distances ranging from 2 ft for ^{238}Pu to 40 ft for ^{137}Cs give protection equivalent to the shield weights quoted.

The fission products—^{90}Sr, ^{137}Cs, ^{144}Ce, and ^{147}Pm—have special appeal because they are produced in large quantities from nuclear reactor operation.

Among the isotopes that may be produced by irradiation of special target materials (^{60}Co, ^{204}Tl, ^{232}U, ^{238}Pu, ^{242}Cm, and ^{244}Cm), ^{60}Co, although easy to produce, requires a special design for the heat-source generator because much of its emitted energy is penetrating gamma radiation. Therefore ^{60}Co may be limited in its use as a power source but, for the same reason, would have special interest as a radiation source.

Plutonium-238 is most generally favored as a heat source because of its long half-life and the fact that it can be used with almost no special shielding. However, its biological hazard encourages the search for a competitive material.

Curium-244 is expected to become available at a reasonable cost whenever plutonium assumes a significant place as a recycled fuel in thermal reactors for power production.

Promethium-147, although its half-life is shorter than the other very promising isotopes, can be considered realistically for some uses as a substitute for ^{238}Pu. Energy, cost, low shielding requirements, and minimum biological hazard are all factors favorable to ^{147}Pm when nearly pure.

The strong points for ^{232}U (and its daughter ^{228}Th) are high power densities and unusually long life at nearly constant heat output.

Other characteristics of radioisotopes that will be factors in the choice of one for a particular use are the relative biological effects and the type of radiation emitted. Those which are almost pure alpha emitters and also have a low neutron production rate, such as ^{238}Pu and ^{210}Po, or low-energy pure-beta emitters, such as ^{147}Pm, require the least shielding, which is a significant advantage where direct-contact fabrication and minimum shield weight are of interest.

Reliability of the Data

The results, which are presented in the handbook as graphs, are thought to be within 50% of the expected radiation value, based on the assumptions used and on the accuracy of the input source strengths and of the permanent data tables of the computer code. The dose rates are probably overestimated rather than underestimated. An error of ±50% in radiation level would correspond to an error of ±0.175 "tenth thickness" (thickness of shielding necessary to attenuate radiation dose rate by a factor of 10).

The results are only as accurate as the knowledge of the neutron, gamma, beta, and/or bremsstrahlung spectrums. This is especially true for sources whose spectrums lie entirely in the lower energy (less than 0.5 Mev) range. Conversely, the calculated radiation intensities from sources that have high-energy gamma spectrums of high or well-known yield are probably accurate. This is especially true for ^{60}Co, ^{95}Zr-^{95}Nb, ^{137}Cs, ^{144}Ce, ^{210}Po, ^{228}Th, and ^{232}U. Calculated radiation intensities of sources that have only low-energy bremsstrahlung or gamma radiation are as accurate as the estimates of their spectrums and of the self-absorption within the source itself. For bremsstrahlung sources the calculated dose rates and/or shield thicknesses are more accurate for high-energy spectrums (within the accuracy of the actual spectrum calculation) than for the low-energy ones.

It should be emphasized that in many cases the total energy production rate of a given isotope is much greater than the recoverable heat rate in the source itself. This is especially true for isotopes that produce considerable gamma radiation. For these isotopes an external heat recovery unit (partial shield) can be provided to convert the gamma energy to heat. This may even be so for the high-energy beta emitters that produce bremsstrahlung energy equivalent to a few percent of the average beta energy. Here the economics of providing an external heat recovery unit for a few percent of the total energy must be considered.

Therefore, where minimization of shield weight is of utmost importance, a final experimental determination of the shield thickness, and even a source mockup (especially for the lower energy gamma or bremsstrahlung sources), may be necessary before the final source and shield design are selected. Such experimental verification is, of course, always required before a license to install and operate a source can be obtained.

Allowable Radiation Levels and Biological Hazards

Gamma dose rates were calculated in rads (or millirads) per hour, with human tissue as-

sumed to be the absorption medium. Neutron dose rates were plotted in terms of milliroentgens equivalent physical (mrep) per hour since the data were expressed this way in most of the literature. In addition, in discussions of manned satellites and allowable radiation exposure to man, doses in roentgens equivalent man (rem) must also be considered.

The shielding or separation-distance requirements for isotopic power sources are determined from the following maximum allowable radiation levels:

1. *Man.* The maximum permissible radiation dose rates established by the National Committee on Radiation Protection for occupational personnel exposure are assumed to apply to those working around isotopic sources and preparing them for a launch. The recommended maximum allowable doses, integrated over a 13-week period, without reference to instantaneous dose rate, are 3 rads of gamma and 0.3 rad of fast neutrons for whole-body exposure and 25 rads of gamma and 2.5 rads of neutrons for hand and arm exposures.

2. *Transistorized Instruments.* Data on the effects of radiation on instrument systems are available in reports of the REIC series from the Radiation Effects Information Center at Battelle Memorial Institute, Columbus, Ohio, and in the proceedings of a recent symposium Allowable radiation doses vary widely with the type of radiation and type of instrument system. Maximum allowable doses [10^7 rads of gamma, 10^4 rads of fast neutrons ($\sim 10^{12}$ neutrons/cm^2), and 10^4 rads of solar protons ($\sim 10^{12}$ protons/cm^2)] were chosen on the basis that they probably would not cause significant radiation damage in typical transistorized instrument systems. Some damage has been observed at doses 10 times greater, and there is significant damage at doses 100 times greater.

3. *Radiation Detection Instruments.* Radiation detection instruments (including scintillation counters, G-M counters, and ionization chambers) are often used to measure radiation background in space or on or near the moon or planets, or physical properties such as density and composition. Thus power sources emitting radiation of a type and energy similar to that being measured must be shielded or separated from the radiation detection instruments to prevent interference with measurements. For some measurements the radiation level due to the power source may have to be as low as 0.01 mrad/hr in the vicinity of the instrument.

In providing shielding or separation distance to satisfy the above maximum levels, the natural radiation levels at various points in space (Table V-1) must be taken into account. These are often high enough, especially for humans, to require shielding of the payload itself. The shield thickness or separation distance from the isotopic supply can then be correspondingly smaller.

Table V-1 RADIATION LEVELS IN SPACE

Radiation source	Radiation levels, rads/hr	
	No shield	10 g/cm^2 shield
Van Allen belts		
Electrons	10^3-10^5	~ 0
Bremsstrahlung	1–100	1–30
Protons	10–100	1–10
Solar-flare protons (typical)	10–100	1–10
Galactic cosmic rays	$\sim 10^{-3}$	$\sim 10^{-3}$

Method for Calculating Radiation Levels

The gamma and/or bremsstrahlung radiation level and shielding requirements were calculated with the Shielding Design Calculation (SDC) code.[6] Sources were assumed to be right-circular cylinders with heights equal to diameters and clad with 0.2 cm (corresponding to 0.54 g/cm^2) of aluminum (Fig. V-1). The outer surface of the source was assumed to be 1 cm from the inner face of the shield for all shielded sources. The dose point was assumed to be 100 cm from the center of shielded sources and was varied from 50 to 1000 cm from the centers of unshielded sources.

Self-attenuation within the sources is determined in the SDC code by calculating self-absorption factors or exponents (self-absorption distances), the common practice in hand calculations as described in the shielding literature.[7–11]

Radiation Production in Decay Processes

Calculations were made on beta, gamma, and neutron emissions, with special emphasis on processes which, though often ignored, are important in accurate determinations of shielding requirements. These processes include beta

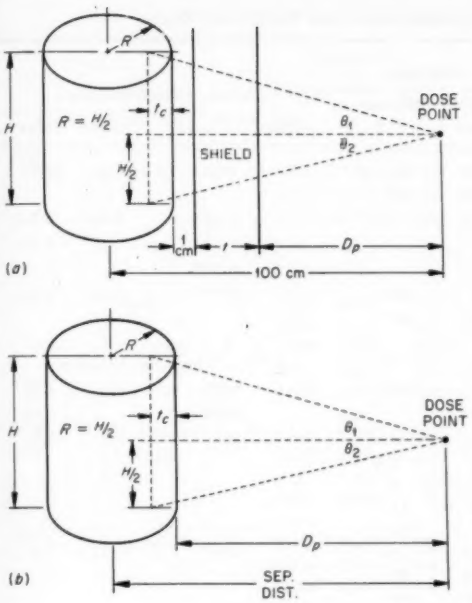

Fig. V-1 Space relations between source, shield, and dose point used for calculations in the handbook. (*a*) Shielded source. (*b*) Unshielded source.

spectrum analyses to permit accurate evaluation of average beta energies, bremsstrahlung production in beta decay, decay gamma production, internal conversion in gamma decay, other sources of gamma rays, and neutron production.

Radiation Characteristics and Shielding Requirements

Radiation characteristics and shielding requirements were studied for each of the 17 isotopes as an individual entity. Nuclear data were tabulated for the various isotopes considered (Table V-2).

The results of the calculations are presented as graphs of gamma-radiation intensity (millirads/hour at 1 m) as a function of (*a*) thickness of iron, lead, and uranium shielding and of water shielding for sources that also emit neutrons; (*b*) neutron-radiation intensity (millireps per hour at 1 m) as a function of water thickness for shielded neutron-emitting sources; or (*c*) gamma-radiation intensity as a function of distance from the center of unshielded sources. Radiation intensities for sources of all 17 materials in the range 100 to 20,000 thermal watts are presented.

The type of information given in the handbook for ^{60}Co is shown below (Table V-3 and Figs. V-2 through V-4). Similar information is given in the handbook for all the other isotopes studied.

Cobalt-60 is produced in substantial quantities for use as a gamma source. In portable radiographic devices it has largely replaced radium. Its half-life is fairly long, 5.3 years, and its biological toxicity is lower than that of most other possible isotopic source materials (^{90}Sr and all the alpha emitters). The fact that inactive normal cobalt can be encapsulated and then irradiated to the desired activity without further processing is a distinct advantage, which is specific to this isotope. The characteristics of its radiation are unfortunate for the present applications because of the major component of high-energy gammas that must be absorbed to yield appreciable heat. Of the isotopes considered in this report, only ^{60}Co and ^{95}Zr-^{95}Nb require a special design for the heat generator, apart from also requiring heavy shielding. For applications where weight is an important consideration, ^{60}Co is therefore at a disadvantage. Furthermore, its intense and energetic gamma activity inhibits its use as a typical or representative heat source for use in demonstration devices. Like all isotopes that have a substantial portion of their heat in

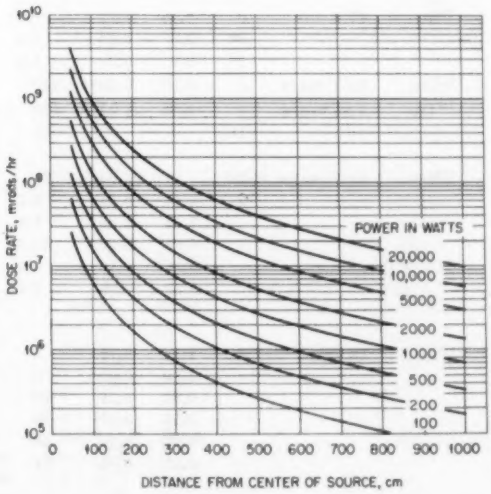

Fig. V-2 Gamma dose rates from unshielded ^{60}Co power sources as a function of distance from source center. Specific activity of source, 200 curies per gram of cobalt.

Table V-2 NUCLEAR DATA FOR ISOTOPES CONSIDERED FOR POWER SOURCES

Nuclide	Half-life	Particles: Type	Energy, Mev: Max.	Energy, Mev: Av.	Abundance, %	Photons: E, Mev	Photons: Abundance, %	Power, watts/kilocurie: Alpha	Beta	Gamma	Total
^{60}Co	5.27 years	β	0.312	0.095	100	1.172	100		0.56	14.80	15.36
						1.333	100				
^{85}Kr	10.3 years	β	0.672	0.253	100	0.517	0.7		1.498	0.024	1.522
^{90}Sr	28 years	β^*	0.545	0.20	100				1.184		1.184
^{90}Y	64.2 hr	β^*	2.27	0.944	100				5.588		5.588
^{95}Zr	65 days	β^*	0.89	0.34	2	0.76	55		0.73	4.33	5.06
		β^*	0.40	0.122	43	0.72	43				
		β^*	0.36	0.109	55						
^{95m}Nb	90 hr	IT				0.21	2		Included in above		
^{95}Nb	35 days	β	0.16	0.044	100	0.76	100		0.26	4.5	4.76
^{106}Ru	1.0 year	β	0.04	0.009	100				0.05		0.05
^{106}Rh	30 sec	β	3.54	1.52	79	2.42	0.3		8.4	1.2	9.6
			3.03	1.30	7	1.55	0.5				
			2.40	0.98	11	1.04	2				
			1.99	0.79	2	0.62	11				
			1.42	0.40	1	0.51	20				
^{134}Cs	2.2 years	β	0.68	0.22	9	0.473	2		0.87	10.13	11.0
			0.65	0.20	58	0.567	22				
			0.41	0.122	4	0.605	100				
			0.08	0.02	27	0.796	91				
						0.801	18				
						1.038	0.9				
						1.168	3				
						1.367	5				
^{137}Cs	26.6 years	β^*	1.18	0.42	8				1.23		1.23
		β^*	0.52	0.19	92						
^{137m}Ba	2.6 min	IT			92	0.662	83.5			3.61	3.61
^{144}Ce	285 days	β	0.31	0.090	65	0.134	17		0.44	0.20	0.64
			0.22	0.060	5	0.10	2				
			0.17	0.045	30	0.08	2				
						0.04	17				
^{144}Pr	17.5 min	β	2.98	1.21	97.7	2.2	0.8		7.08	0.19	7.27
		β^*	2.3	0.89	1.3	1.5	0.25				
		β^*	0.8	0.28	1.0	0.7	1.6				
^{147}Pm	2.67 years	β	0.23	0.067	100	0.121	< 0.1		0.397		0.397
^{146}Pm	1.94 years	β	0.78	0.27	35				0.50		
		EC			65	0.45	65			4.62	5.12
						0.75	65				
^{152}Eu	12.7 years	EC		0.04	73	0.122	10.9		0.17 (EC)		
		β	1.46	0.53	5.7	0.245	5.0		0.42	4.05	4.64
			1.05	0.36	1.6	0.344	18.5				
			0.68	0.22	13.8	0.780	8.4				
			0.36	0.10	3.5	0.965	10.1				
			0.22	0.06	2.4	1.087	8.4				
						1.113	9.3				
						1.409	16.8				
^{154}Eu	16 years	β	1.84	0.70	7	0.123	35		1.17	6.99	8.16
			1.60	0.60	3	0.593	4				
			0.83	0.28	20	0.725	21				
			0.55	0.17	30	0.875	13				
			0.25	0.07	28	0.998	14				
			0.15	0.04	12	1.007	17				
						1.277	42				
^{148}Pm	42 days	β	2.5	0.99	6	0.10	8		1.49	11.28	12.77
			2.0	0.72	1	0.19	5				
			1.2	0.42	3	0.29	12				
			1.07	0.37	5	0.41	16				
			0.76	0.25	19	0.43	11				

Table V-2 (Continued)

Nuclide	Half-life	Particles: Type	Particles: Energy, Mev: Max.	Particles: Energy, Mev: Av.	Particles: Abundance, %	Photons: E, Mev	Photons: Abundance, %	Power, watts/kilocurie: Alpha	Power, watts/kilocurie: Beta	Power, watts/kilocurie: Gamma	Power, watts/kilocurie: Total
^{148}Pm	42 days	β	0.64	0.21	11	0.55	92				
			0.57	0.18	15	0.63	90				
			0.47	0.14	40	0.73	36				
						0.91	19				
						1.01	20				
						1.46	2				
^{170}Tm	127 days	β	0.968	0.33	76	0.084	3.4		1.91	0.02	1.93
			0.884	0.30	24						
^{171}Tm	1.94 years	β	0.097	0.029	98	0.0667	2		0.17	0.008	0.178
			0.03	0.01	2						
^{204}Tl	3.9 years	β*	0.764	0.27	98				1.57		
		EC		0.38	2	0.071(x)	2		0.045	0.008	1.623
^{210}Po	138.4 days	α	5.305	5.305	100	0.803	1.2×10^{-3}	31.41			31.41
^{232}U	74 years	α	5.318	5.318	68	0.0579	0.21	31.37			31.37
			5.261	5.261	31.68	0.131	0.075				
			5.134	5.134	0.32	0.268	4×10^{-3}				
						0.326	4×10^{-3}				
^{228}Th	1.91 years	α	5.421	5.421	71	0.0845	1.6	31.95		0.008	31.96
			5.338	5.338	28						
			5.208	5.208	0.4						
			5.173	5.173	0.2						
			5.137	5.137	0.03						
^{224}Ra	3.64 days	α	5.681	5.681	95	0.2411	3.7	33.56		0.053	33.61
			5.445	5.445	5						
^{220}Rn	51.5 sec	α	6.282	6.282	100	0.542	0.03	37.19		0.001	37.19
^{216}Po	0.158 sec	α	6.775	6.775	100			40.11			40.11
^{212}Pb	10.64 hr	β	0.580	0.19	16	0.115	3		0.71	1.07	1.78
			0.340	0.11	80	0.239	74				
			0.160	0.05	4	0.415	0.01				
^{212}Bi	60.5 min	β	2.25	0.95	63.8	0.72	19		3.59	4.38	7.97
						0.83	19				
		α	6.09	6.09	9.85	1.03	6	12.97		0.06	13.03
			6.05	6.05	25.3	1.34	5				21.00
			5.77	5.77	0.6	1.61	7				
			5.622	5.622	0.05	1.81	7				
			5.603	5.603	0.4	2.20	3.5				
						0.04	25				
						Others	Weak				
^{208}Tl	3.1 min	β	1.795	0.67	50	0.277	10		3.40	19.95	23.35
			1.518	0.55	21	0.510	25				
			1.284	0.45	25	0.582	80		1.23†	7.22†	8.45†
			1.032	0.30	4	0.859	15				
						2.620	100				
^{212}Po	0.30 μsec	α	8.78	8.78	100			51.98			51.98
								33.16†			33.16†
Total of all daughters in equilibrium with ^{232}U											238.63
^{238}Pu	89.8 years	α	5.495	5.495	72	0.0435	0.038	32.46			32.46
			5.452	5.452	28	0.099	8×10^{-3}				
						0.150	1×10^{-3}				
						0.203	4×10^{-4}				
						0.76	5×10^{-5}				
						0.875	2×10^{-5}				
^{242}Cm	163 days	α	6.11	6.11	73.7	0.044	0.039	36.10			36.10
		~	6.066	6.066	26.3	0.1018	3.5×10^{-3}				
						0.1576	2.3×10^{-4}				
^{244}Cm	18.4 years	α	5.801	5.801	76.7	0.043	2.1×10^{-2}	34.28			34.28
			5.759	5.759	23.3	0.1	1.5×10^{-3}				
						0.15	1.3×10^{-3}				

*Unique first forbidden transition.
†When existing as a ^{232}U or ^{228}Th daughter.

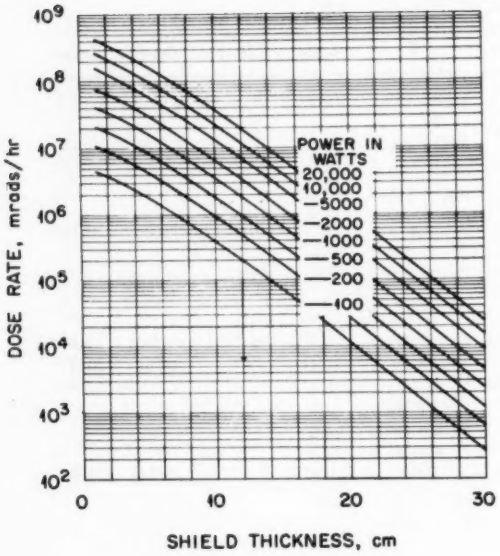

(a)

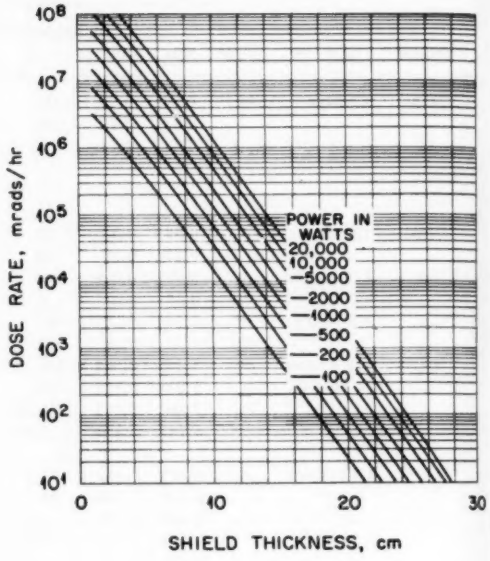

(b)

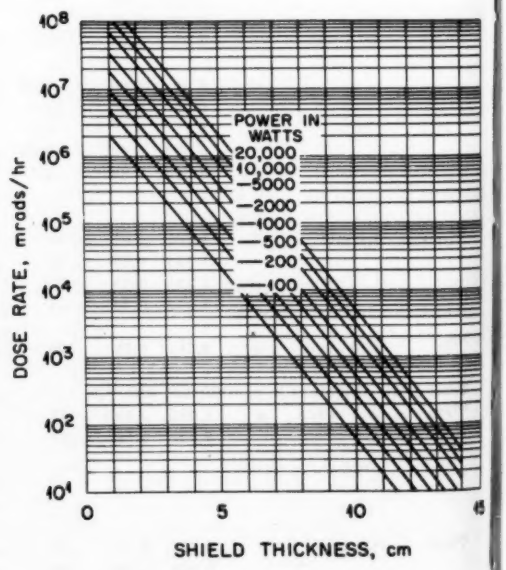

(c)

Fig. V-3 Gamma dose rates from shielded ^{60}Co power sources. Specific activity, 200 curies per gram of cobalt. *(a)* Iron shield. *(b)* Lead shield. *(c)* Uranium shield. Distance from source center to dose point, 100 cm.

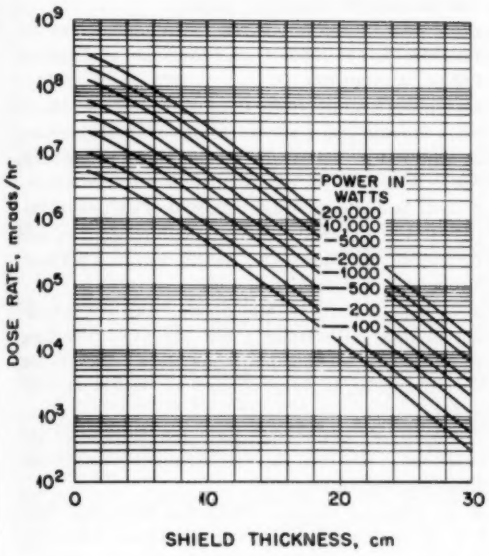

(a)

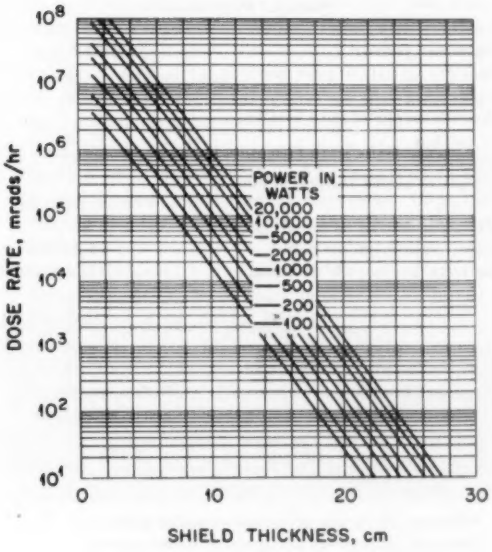

(b)

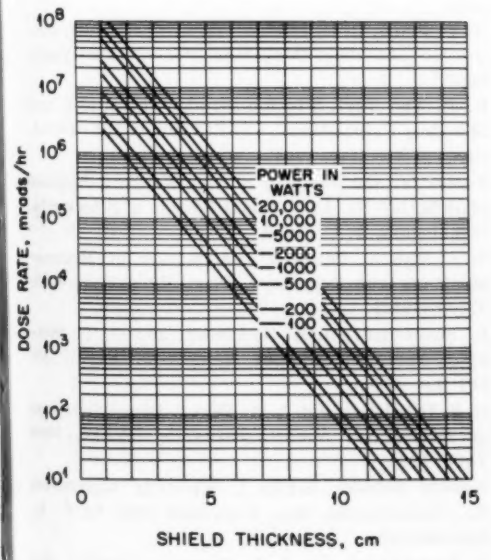

(c)

Fig. V-4 Gamma dose rates from shielded ^{60}Co power sources. Specific activity, 75 curies per gram of cobalt. *(a)* Iron shield. *(b)* Lead shield. *(c)* Uranium shield. Distance from source center to dose point, 100 cm.

Table V-3 PHYSICAL PROPERTIES OF ^{60}Co AS AN ISOTOPIC POWER SOURCE

General Properties	
Half-life, years	5.27
Specific activity of pure isotope, curies/g	1124
Specific power of pure isotope, watts/g	17.26
Compound	Metal
Weight of active isotope in metal, g/cm^3	0.59,* 1.58†
Effective density of metal, g/cm^3	8.9
Power, watts/cm^3 of metal	10.3,* 27.3†
Activity, curies/cm^3 of metal	667.5,* 1780†

Gamma-Radiation Properties	
Gamma emission rate for shielding calculations, photons/watt-sec	Photon energy, Mev
2.385×10^{12}	1.172
2.385×10^{12}	1.333‡

*Source: 75 curies per gram of cobalt metal.
†Source: 200 curies per gram of cobalt metal.
‡Predominant radiation from unshielded 5000-watt source.

a gamma component or in hard bremsstrahlung, an appreciable part of this energy is not easily recoverable because the penetrating radiation cannot be completely absorbed and converted to heat only in that section of the device in contact with the thermoelectric elements. The specific power of ^{60}Co is high, 17.4 watts/g, but concentrations that can be practically attained would limit the heat output to about 20% of that value. Even so, for metal, a power density of 27.3 watts/cm^3 (200-curie sources) appears achievable.

References

1. E. D. Arnold, Handbook of Shielding Requirements and Radiation Characteristics of Isotopic Power Sources for Terrestrial, Marine, and Space Applications, USAEC Report ORNL-3576, Oak Ridge National Laboratory, April 1964.
2. J. P. Nichols and E. D. Arnold, Shielding Isotopic Power Sources for Space Missions, *Nucleonics*, 22(2): 52-6 (1964).
3. C. A. Rohrmann, Radioisotopic Heat Sources, USAEC Report HW-76323, General Electric, February 1963.
4. H. H. Van Tuyl, E. P. Roberts, and E. J. Wheelwright, Shielding Requirements for Promethium Sources, USAEC Report HW-77375, General Electric, April 1963.
5. E. P. Blizard et al., Proceedings of Symposium on Protection Against Radiation Hazards in Space, USAEC Report TID-7652, 1962.
6. *Code of Federal Regulations*, Title 10, Part 20, revised Jan. 1, 1963, U. S. Government Printing Office, Washington, D. C.
7. Maximum Permissible Body Burdens and Maximum Permissible Concentrations of Radionuclides in Air and in Water for Occupational Exposure, *Natl. Bur. Std. (U. S.), Handbook 69*, Superintendent of Documents, Washington, D. C. (June 1959).
8. Oak Ridge National Laboratory, Procedures and Practices for Radiation, Health Physics Manual, Procedure A-5.3, August 1961.
9. E. D. Arnold and B. F. Maskewitz, SDC — A Shielding Design Calculation Code for Fuel Handling Facilities (a working but incomplete program for the IBM-7090, to be published as Report ORNL-3041).
10. J. Moteff, Miscellaneous Data for Shielding Calculations, USAEC Report APEX-176, General Electric, December 1954.
11. E. P. Blizard, Nuclear Radiation Shielding, Sec. 7-3 of *Nuclear Engineering Handbook*, edited by H. Etherington, McGraw-Hill, New York, 1958.
12. E. P. Blizard and L. S. Abbott, Shielding, in *Reactor Handbook*, Vol. 3, Part B, Interscience, New York, 1962.
13. H. Goldstein, *Fundamental Aspects of Reactor Shielding*, Addison-Wesley, Cambridge, Mass., 1959.
14. B. T. Price, C. C. Horton, and K. T. Spinney, *Radiation Shielding*, Pergamon Press, New York, 1957.
15. H. H. Van Tuyl, Fission Product Radiation and Shielding Calculations, USAEC Report HW-69533, General Electric, 1961.
16. *Tables for the Analysis of Beta Spectra*, Applied Math Series No. 13, National Bureau of Standards, Washington, D. C., 1952.
17. S. J. Wyard, Intensity Distribution of Bremsstrahlung from Beta Rays, *Proc. Phys. Soc.*, A65: 377-9 (1952).
18. D. Strominger, J. M. Hollander, and G. T. Seaborg, Table of Isotopes, *Rev. Mod. Phys.*, 30: 585-904 (1958).
19. B. S. Dzhelepov and L. K. Peker, *Decay Schemes of Radioactive Nuclei*, Pergamon Press, New York, 1961.
20. *Isotope Datadex*, Series I, Scientific Equipment Co., Indianapolis, Ind., Copyright 1960 by J. L. Sommerville.
21. G. Friedlander and J. W. Kennedy, *Nuclear and Radiochemistry*, Wiley, New York, 1955.
22. E. K. Hyde, A Review of Nuclear Fission. I. Fission Phenomena at Low Energy, USAEC Report UCRL-9036, 1960.
23. S. K. Penny et al., Cumulative Bibliography of Literature Examined by the Radiation Shielding

Information Center, USAEC Report ORNL-RSIC-1, Oak Ridge National Laboratory, 1963.
24. S. Katcoff, Fission-Product Yields from U, Th, and Pu, in *Handbook of Nuclear Technology*, pp. 236-43, reprinted by *Nucleonics*, McGraw-Hill, New York, 1960.
25. S. Katcoff, Fission-Product Yields from Neutron-Induced Fission, *Nucleonics*, 18(11): 201-8 (1960).
26. Royal Research Corporation, ^{137}Cs Fueled Generator, USAEC Report TID-12579 (RRC-CS-0100), p. 65, April 1961.
27. R. A. Robinson, Isotopes Division, Oak Ridge National Laboratory, personal communication, Sept. 16, 1963.
28. E. Von Halle, Operations Analysis Division, Oak Ridge Gaseous Diffusion Plant, personal communication, Jan. 20, 1964.
29. C. A. Rohrmann, Special Radioisotopes for Power: Availability and Applications of Thorium-230 (Ionium) from Uranium Ore Mills, Table 1, USAEC Report HW-71319(Rev.), General Electric, October 1961.
30. Oak Ridge National Laboratory, Status and Progress Report, USAEC Report ORNL-3351, p. 26, August 1962.
31. C. A. Rohrmann, Ionium–Uranium-232 and Thorium-228 Properties, Applications and Availability, USAEC Report HW-66600, Chart II, General Electric, August 1960.
32. W. H Sullivan, Trilinear Chart of Nuclides, Oak Ridge National Laboratory, January 1957.
33. D. R. Vondy, J. A. Lane, and A. T. Gresky, Production of ^{237}Np and ^{238}Pu in Thermal Power Reactors, paper presented at American Chemical Society Winter Meeting, Denver, Colo., Jan. 19, 1964.
34. Atomic Industrial Forum, *The Forum Memo to Members*, p. 14, November 1962.
35. *Nucleonics Week*, 3(10): (Mar. 8, 1962).
36. *Nucleonics Week*, 2(4): (Feb. 16, 1961).
37. W. D. Burch, E. D. Arnold, and A. Chetham-Strode, Production of the Transuranium Elements, *Trans. Am. Nucl. Soc.*, 5(1): 14-5 (June 1962).
38. W. D. Burch, E. D. Arnold, and A. Chetham-Strode, Production of the Transuranium Elements, *Nucl. Sci. Eng.*, 17: 438-42 (November 1963).

Section

VI

Isotopes and Radiation Technology

Medicine

Iodine-132*

The radioactive isotope ^{132}I, which has a half-life of only 2.3 hr, is of particular interest in the field of medicine, being used chiefly as a substitute for 8-day ^{131}I in diagnosis. Its principal advantages are the 100-fold decrease in radiation exposure of a patient when it is used and the possibility of repeated studies at short time intervals, even in pregnant women and in children. When double labeling of test compounds is needed, it may be used in conjunction with ^{131}I. This isotope has become well known only comparatively recently, chiefly after its successful use in medicine where ^{131}I had already become established. There is little information in the literature on its applications in other fields of science and industry, although its use for regulating the movement of products in pipelines in the petroleum industry has been mentioned.

The pertinent properties of ^{132}I and ^{131}I are:

	^{132}I	^{131}I
Half-life	2.3 hr	8.14 days
Average beta energy, Mev/dis	0.49	0.19
Average gamma energy, Mev/dis	0.79	0.40
Beta dose rate, rads/(hr)(μc)(g)	1.0	0.40
Total beta dose, rads/μc	3.15	110
Gamma dose rate at 1 cm, rads/(hr)(μc)	11.0	2.1
Gamma quanta produced per disintegration	2.52	1.06

*This section is a summary of a recent Russian compilation,[1] used because of its ready availability, of work from several countries, including the United States. A more detailed discussion of the current status of work on ^{132}I, with documentation, will be presented in an Isotopes Information Center brochure now in preparation, ORNL-IIC-4.

When ^{132}I is used instead of ^{131}I in studies of thyroid function, the gland itself receives 40- to 100-fold less radiation than when the same amount of ^{131}I is administered. In 6 hr the normal gland will usually absorb 50% of the radioactive iodine introduced into the body, during which time 85% of the ^{132}I—but only 2% of the ^{131}I—would have decayed. In addition, a smaller amount of ^{132}I may be used for gamma count measurements since the ^{132}I emits a larger number of gamma quanta per disintegration and their energy is higher. Other data indicate that irradiation of the sex glands is decreased 3- or 4-fold if ^{132}I is used instead of ^{131}I. Iodine-132 may also be used in evaluation of liver function, which is done with human serum albumin tagged with ^{132}I, and in determination of the location of brain tumors and metastases of cancer in the liver.

Physical Properties of ^{132}I

Iodine-132 is a beta-gamma emitter. Its gamma and maximum beta radiations are:

Gamma, Mev		Beta, Mev
2.200 (2%)	0.768 (75%)	0.730 (15%)
1.960 (5%)	0.673 (100%)	0.970 (20%)
1.400 (11%)	0.624 (6%)	1.160 (23%)
1.160 (8%)	0.530 (25%)	1.530 (24%)
0.960 (20%)		2.120 (18%)

The final product of ^{132}I decay is a stable isotope of xenon, ^{132}Xe (Fig. VI-1). One microcurie of ^{132}I weighs 0.97×10^{-10} g.

Production of ^{132}I

Iodine-132, a daughter of ^{132}Te, is continuously formed in beta decay of the latter (Fig. VI-2):

$$^{132}Te \xrightarrow{\beta^-} {}^{132}I \xrightarrow{\beta^-} {}^{132}Xe$$

Therefore the problem of obtaining ^{132}I is easily solved if there is a practicable method of producing ^{132}Te.

PROPERTIES OF ^{132}Te

Tellurium-132, like ^{132}I, is a beta-gamma emitter. Its half-life is 78 hr. Tellurium-132 emits electrons with maximum energies of 0.160 Mev (40%) and 0.280 Mev (60%) and gamma quanta whose energies are 0.220 Mev (40%) and 0.130 Mev (60%). One microcurie of ^{132}Te weighs 3.28×10^{-9} g (calculations based on a 77.7-hr half-life).

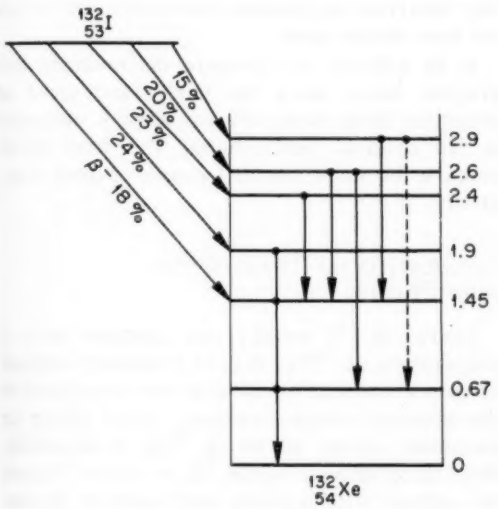

Fig. VI-1 Decay scheme of ^{132}I.

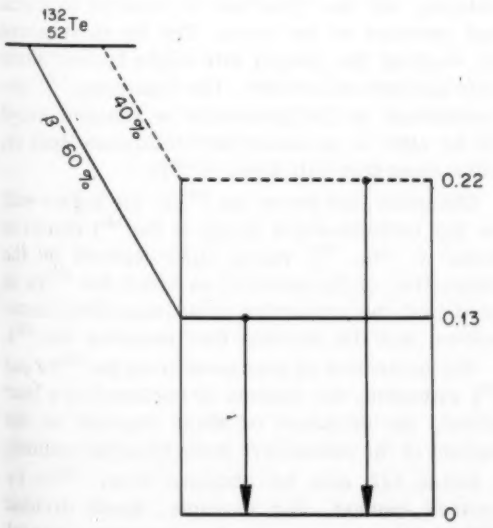

Fig. VI-2 Decay of ^{132}Te to ^{132}I.

PRODUCTION OF ^{132}Te

The best method of producing ^{132}Te is by neutron fission of plutonium, uranium, or thorium. Among the fission products of uranium irradiated in a nuclear reactor is 4.4 to 4.7% ^{132}Te, production of which increases with increasing energy of the neutrons. Calculations show that 32.5 μc of ^{132}Te will be formed in a 10-day irradiation of 1 g of natural uranium by thermal neutrons, at a flux of 10^{13} neutrons/(cm^2)(sec). At higher fluxes the production of ^{132}Te will be proportionally greater. Actually, ^{132}Sn forms in the reactor and decays to ^{132}Te:

$$^{132}Sn \xrightarrow[2.2\ min]{\beta^-} {}^{132}Sb \xrightarrow[2.0\ min]{\beta^-} {}^{132}Te$$

Tellurium-132 may also be obtained from stable (inactive) ^{130}Te, which makes 34.5% of natural tellurium, by cyclotron irradiation with accelerated alpha particles (^4He). Tellurium-132 is formed from ^{130}Te by the nuclear reaction $^{130}Te(\alpha,2p)^{132}Te$. However, pure ^{132}Te, i.e., without carrier, cannot be separated from alpha-irradiated targets by ordinary chemical methods, and the ^{132}Te yield is low.

SEPARATION OF ^{132}Te FROM OTHER URANIUM FISSION PRODUCTS

Since relatively pure ^{132}Te must be used to produce ^{132}I, the desired isotope must be separated from a mixture of 270 different radioactive isotopes formed in the fission of uranium. The separation should be completed by the tenth day after the end of the irradiation. With a relatively short irradiation time, significant amounts of long-lived radioisotopes do not appear in the reactor product, and in this 10 days some of the short-lived radioactive elements decay. The principal impurities that must be handled in the separation of ^{132}Te from irradiated uranium are:

^{238}U (4.5×10^9 years, macro amounts)	^{103}Ru (41 days, 2.9%)
^{99}Mo (67 hr, 6.2%)	^{95}Zr (63 days, 6.4%)
^{99m}Tc (6 hr, 6.2%)	^{95}Nb (35 days, 6.4%)

There are also some radioactive isotopes of tellurium, ^{131m}Te, ^{131}Te, and others, which cannot be separated by ordinary chemical methods.

In another method based on a series of hydrolytic precipitations, an irradiated compound of uranium—U_3O_8, UO_3, or $UO_2(NO_3)_2$—is dissolved in nitric acid and a carrier, e.g., TeO_2, is added to the solution. The solution is neutralized with alkali, and tellurium is precipitated by means of formic acid as TeO_2. The precipitate is filtered off, washed with dilute acid and water, dissolved in alkali, filtered, acidified, and precipitated from solution as metallic tellurium by a reducing agent, for example, $NaHSO_3$, $SnCl_2$, or $N_2H_4 \cdot 2HCl$. After a series of precipitations as the dioxide and element, tellurium is obtained finally as an alkaline solution of tellurite, Na_2TeO_3, which is used for producing ^{132}I. This method gives ^{132}Te in 70 to 80% yield, with 3 to 4% beta-active and 0.5% gamma-active impurities in the final product.

A chromatographic method of separating ^{132}Te from other products in the fission mixture is relatively simple. A solution of irradiated uranium in nitric acid is passed through a chromatographic column (glass tube) filled with a special type of acid-form Al_2O_3. The ^{132}Te and ^{99}Mo, without carrier, are held on the aluminum oxide as tellurite and molybdate, and the remaining fission products pass through the column. Pure ^{132}Te is obtained by washing the column with concentrated ammonia to remove the ^{99}Mo, of which only 0.01% remains on the column. Only 1% of the ^{132}Te is lost in this washing. Then a 7 to 14% alkali or ammonia solution is added to desorb the tellurium from the column, and the column effluent is alkalinized to *p*H 10 for use in producing ^{132}I.

The ^{132}Te may also be separated from the solution of irradiated uranium by precipitation with CuS. Some other radioactive impurities coprecipitate with the tellurium. The copper sulfide is dissolved in acid with the addition of an oxidizing agent, and trivalent iron is added and then precipitated as hydroxide with ammonia. The iron hydroxide carries the radioactive tellurium, antimony, and tin. The solution obtained by dissolving the $Fe(OH)_3$ in acid is used for making ^{132}I.

In another method a metallic uranium wire that has been neutron irradiated is dissolved in hydrochloric acid and 20 to 70 mg of tellurium carrier is added. The radioactive H_2Te formed is swept out with a current of nitrogen and is absorbed in a 5% solution of iron chloride in 3*N* hydrochloric acid, forming tellurite. Tin chloride is added to the solution, after which elementary ^{132}Te is precipitated, washed with 5*N* hydrochloric acid and water, and then used for making ^{132}I. The radioactive purity of ^{132}Te obtained by this method is high, and the overall yield is 90%.

There is also a chemical method for separating tellurium on platinum electrodes, but it has not been widely used.

It is difficult to compare the methods described above since the purity and yield of tellurium from them are not always indicated in the original publications. The first three seem to be more useful because of their simplicity.

SEPARATION OF ^{132}I FROM ^{132}Te (THE ^{132}I COW)

Users of ^{132}I usually are supplied with a preparation of ^{132}Te. This is frequently a glass column containing a material with adsorbent or ion-exchange properties (e.g., filter paper or aluminum oxide) on which ^{132}Te is adsorbed. When the consumer needs ^{132}I, he elutes it from the column with a dilute salt solution. In one ^{132}I generator the glass column is filled with cation-exchange material on which divalent tin has been adsorbed from $SnCl_2$ solution. A solution of ^{132}Te, as tellurite, is passed through the column, and the tellurium is reduced to metal and remains on the resin. The tin is removed by washing the column with dilute hydrochloric acid and then with water. The maximum ^{132}I accumulation in the generator is reached about 12 hr after it is loaded with tellurium (that is, after about five half-lives of ^{132}I).

Obviously, the purer the ^{132}Te, the higher will be the radiochemical purity of the ^{132}I removed from it. The ^{132}I purity also depends on the properties of the material on which the ^{132}Te is adsorbed, the properties of the impurities themselves, and the solution that removes the ^{132}I.

For protection of personnel from the ^{132}Te and ^{132}I radiation, the column is enclosed in a lead shield, the thickness of which depends on the amount of the radioactive isotopes on the column.

Iodine-132 may be obtained from ^{132}Te by another method. For example, finely divided ^{132}Te (with carrier) may be placed in a vessel with draw-off tubes made of low-melting mate-

rial. Periodic heating distills the iodine into collectors containing an appropriate absorbent solution. This method is used chiefly in establishments where ^{132}I is produced, since other places, as a rule, do not have the proper equipment for such operations.

Reference

1. V. A. Sokolov, A Short-Lived Isotope of Iodine, ^{132}I, Gosatomizdat, Moscow, 1963 (translated to English by Martha Gerrard, Oak Ridge National Laboratory, Isotopes Information Center, ORNL-tr-93).

Section

VII

Isotopes and Radiation Technology

Miscellaneous Items of Interest

Isotope Technology and Economics

Seventeen papers on isotope technology and economics were presented at an information meeting of government and industrial representatives on June 11–12 at AEC's Germantown, Md., headquarters. Production manuals from Brookhaven and Oak Ridge National Laboratories, Mound Laboratory, and the Savannah River Plant were made available to those attending the sessions. The contents of the manuals are discussed in Sec. I of this review, and the program and talks are summarized in the following paragraphs.

AEC

Glenn T. Seaborg	Introductory Remarks
E. E. Fowler	AEC Radioisotope Production Program and Policies
L. S. Lenderman	AEC Costing and Pricing Practices

ORNL

J. H. Gillette	Radioisotope Production and Distribution
E. E. Beauchamp	Reactor Products and Services
F. N. Case	Short Half-Life Fission Products; Separations and Radioactive Gas Handling
J. E. Beaver	86-Inch Cyclotron and Products

MOUND

F. D. Lonadier	Marketing and Sales; Polonium-210 Production and Processing

SAVANNAH RIVER

H. F. Allen	Cobalt-60 Production

BNL

Powell Richards	Marketing and Sales — General Product Information
Jack Floyd	Irradiation Facilities
Manny Hillman	Cyclotron Production and Cockcroft-Walton Neutron Generator
Powell Richards	Processing Facilities
Manny Hillman	Milking Systems; Reactor-Induced Triton Reactions
Powell Richards	Fluorine-18 Process

Fowler, Acting Director of AEC's Division of Isotopes Development (DID), and George Kavanagh, Deputy Assistant General Manager for Research and Development at AEC, were chairmen of the sessions. Rufus Shivers, DID, was general chairman of the meeting.

Chairman Seaborg, in his introductory remarks, noted that the AEC has a continuing interest in fostering private participation in the production and distribution of radioisotopes. He indicated that with the development of private capability the Commission has consistently sought to reduce or eliminate its activities in the areas relevant to private interests:

> Reviewing the past few years one finds an impressive record in this regard. Activities formerly carried out by the Commission, which have during these years been turned over to private industry, include the production of labeled compounds, the provision of film badge services, the distribution of processed cyclotron isotopes, as well as the encapsulation services and activation analyses once offered by the AEC.
>
> Until recently the functions undertaken by private industry, such as the foregoing, have been auxiliary to the prime production of the isotopes themselves. With the advancing technology and broadening of markets, however, the interest of private industry in producing its own supplies of radioisotopes has been increasing rapidly. Indeed, in the last nine months the Commission has withdrawn from the

production and distribution of seven radioisotopes because of their availability, on reasonable terms, from independent sources of supply.

He predicted more vigorous participation of private concerns in isotope production, although solutions to many difficult questions of probable policy will have to be found in years ahead:

> The over-all national objective of fostering widespread peaceful application of atomic energy, the legitimate interest of radioisotope users in being assured of adequate availability of required radioisotopes at reasonable prices, and the proper interest and desire of private enterprise to participate in serving these markets all must be properly balanced and equitably recognized.

Fowler, in further discussing production production programs and policies, noted that this was the first information conference for industry in which the accumulated technology existing in the AEC's radioisotope production program had been presented. Reviewing the programs at the four laboratories, he said that progress in fission-product separations and purifications and the development of technology for large-scale use of these materials as heat and radiation sources have provided the basis for the present Commission plan for soliciting industrial interest and financing and operating the large-scale fission-product plant at Hanford. He reiterated Seaborg's comment that private industry, since the late 1950's, has become increasingly involved in radioisotope production. At least six private firms are engaged in the commercial production and sales of some 30 different radioisotopes. He said that the criterions of adequate availability of required radioisotopes at reasonable prices and the proper interest and desire of private enterprise to participate in serving these markets must be properly balanced. However, he pointed out that some aspects of the Atomic Energy Act and these goals are sometimes contradictory:

> Those who tend to place greatest importance on development of a private production capability give the most weight to this criterion. Others consider that encouragement of research and development and increased beneficial use of radioisotopes has the greatest importance. Lastly, there are those who are occupied with full cost recovery and believe this to be requisite.

Lenderman said that AEC's accounting system combined the principles of general commercial accrual accounting, industrial cost accounting, budgeting, and governmental fund accounting into a single system. This system provides (1) the unit cost of items produced, (2) a system of functional budgeting on the basis of accrued costs, (3) cost information on which to base prices for materials and services furnished to outsiders, and (4) other needed information to all levels of management.

Oak Ridge National Laboratory

The radioisotope distribution program was started at ORNL in August 1946 with a shipment of a few millicuries of ^{14}C to the Barnard Free Skin and Cancer Clinic, St. Louis, Mo. *Gillette* noted that the irradiated units in the early stages of the program were packaged for shipment and sent to customers without any processing. In summarizing present practices, he said:

> The ORNL services offered at present are as follows: special service irradiations; provision of the routine materials listed in the *ORNL Radio and Stable Isotopes Catalog* which are sold mainly as chlorides and nitrates in solution form; packaging and purification of ^{85}Kr, ^{3}H, ^{37}Ar, and ^{133}Xe; and special services consisting of the preparation of special compounds and sources as requested by customers.
>
> In terms of shipments, the growth of the radioisotope distribution program has been constant for all isotopes through 1957. Since that time, the number of shipments has been averaging slightly less than 13,000 per year. The income from sales has risen with the number of shipments and is now stablized at about $2 million per year except for unusual sales, such as occurred in 1961 and 1962. During these two years, several isotopic power sources were sold and several large orders for ^{137}Cs were completed.
>
> The total radioisotope program cost has increased from about $1.5 million in 1954 to $3.5 million in 1963. This change is primarily due to increases in the amount of ^{137}Cs and ^{90}Sr handled to provide material for fairly large-scale research use, power sources, and stockpiling .... The total value of inventoriable isotopes as a finished product was $1.77 million as of April 30, 1964.

He concluded that the costs which are charged to the production of isotopes are department labor, maintenance labor, materials and supplies, technical services, costs from other divisions, and utilities. Other costs, such as depreciation, are related to the out-of-pocket cost accumulated for each product isotope. Table VII-1 and Fig. VII-1 show selected radioisotope production and sales data over the years.

Table VII-1 RADIOISOTOPE PRODUCTION COSTS* AT ORNL, 1954–1963

Product	1954	1955	1956	1957	1958	1959	1960	1961	1962	1963
^{14}C	$ 86,827	$ 27,931	$ 23,150	$ 29,608	$ 51,348	$ 36,963	$ 80,608	$ 98,178	$ 97,352	$ 96,078
^{137}Cs			99,392	199,918	253,814	190,323	233,806	525,850	551,007	509,592
^{60}Co	81,386	344,088	368,983	415,277	1,190,432	(37,122)†	102,716	81,374	49,886	57,298
^{147}Pm			3,542	19,277	186,951	135,759	133,601	14,178	34,935	51,677
^{85}Kr			87,737	127,837	341,744	237,704	94,149	35,734	33,902	12,576
^{131}I	167,342	172,982	172,408	227,494	180,334	131,693	62,819	82,077	79,359	40,362
^{192}Ir			22,752	46,845	48,006	35,943	15,716	25,542	33,944	29,981
Reactor service irradiations			93,312	77,263	81,330	78,875	110,145	70,945	52,660	36,393
^{32}P	141,435	143,453	159,297	217,278	204,902	156,940	122,690	91,664	54,731	61,577
^{90}Sr			2,453	9,799	78,129	84,366	447,068	883,741	811,368	1,694,480
^{3}H	13,663	15,080	6,106	18,252	10,327	14,694	16,926	39,404	54,670	91,417
All others	782,709	517,688	334,058	515,314	779,259	746,235	812,029	839,278	946,769	847,007
Total	$1,273,362	$1,221,222	$1,373,190	$1,904,162	$3,406,576	$1,812,373	$2,232,273	$2,787,965	$2,800,583	$3,528,438

*Fund costs only; calendar years.
†Adjustment for prior year's overcharge.

Table VII-2 COBALT FABRICATION COSTS AT SAVANNAH RIVER PLANT

Cobalt shape	Cobalt size	Fabricator	Activity		Cost	
			Total, curies	Specific, curies/g	Per slug	Per curie
Wafers	1 cm × 1 mm	Du Pont	150,000	27	$ 72	$0.005
Pellets	1/16 in. × 1/16 in.	Du Pont	150,000	100	216	0.014
Slabs	0.640 in. × 0.060 in. × 12 in.	BNL	977,000	100	200	0.009
Bars	0.725 in. × 10.25 in.	Curtiss-Wright	1,348,000	6	163	0.05

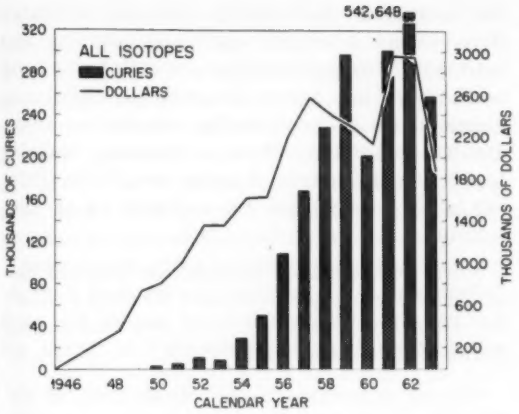

Fig. VII-1 Sales of isotopes at ORNL, 1946–1963.

Beauchamp noted that differences exist between published and available specific activities of radioisotopes. Lowest values are given in the *ORNL Catalog of Radio and Stable Isotopes*, and intermediate ones, in the *ORNL Radioisotopes Procedures Manual* (USAEC Report ORNL-3633). Available specific activities are higher and are scheduled on a special basis, for example:

	Specific activities, curies/g		
Isotope	Catalog	Manual	Product (after removal from reactor)
^{51}Cr	≅100	733	1200
^{59}Fe	10	20	40

Beauchamp also reviewed ORNL-3633, as well as target selection and preparation, irradiation, processing, analytical techniques, and shipping. He concluded, "One must do the work to learn the art."

Case noted that short-half-life fission products are prepared by short-term irradiation of enriched (>90%) ^{235}U. The fission products of interest are: ^{140}Ba-^{140}La, ^{141}Ce, ^{131}I, ^{95}Nb, ^{143}Pr, ^{103}Ru, ^{89}Sr, ^{133}Xe, and ^{95}Zr-^{95}Nb. He pointed out that chemical separation is required soon after discharge of the uranium target from the reactor because of the short half-lives of the products.

In a second paper *Case* noted that the general principles of gas handling (vacuum pumping, cold-trap pumping, leaktight systems, and protection against contamination) apply also to radiogas processing.

Beaver described the ORNL 86-in. cyclotron. [See J. J. Pinajian and T. A. Butler, ORNL 86-in.-Cyclotron Facility for Isotope Production, *Isotopes Radiation Technol.*, 1(2): 137-43 (Winter 1963–1964).] He said that the cyclotron was operated 52% of the scheduled time in 1963 and that 40 different radioisotopes were produced in some 280 separate service irradiations.

Mound Laboratory

Lonadier said that, beginning in 1960, the source-manufacture responsibility at Mound was turned over to private industry. The laboratory now makes only special sources that cannot be produced by industry but still supplies processed polonium. Sales have increased from about 2000 curies/year in fiscal year 1955 to a peak of about 9000 curies in fiscal year 1959; they decreased to about 5000 curies in fiscal year 1963. These sales include those to both AEC and private industry. The cost of ^{210}Po is $25/curie. Production of ^{210}Po is discussed in Sec. I of this review.

Savannah River Plant

In discussing the Savannah River plant capacity, *Allen* said that, if a reactor charge was designed to produce only cobalt, many tens of millions of curies per reactor could be produced in configurations with a maximum width of 3 in., in addition to about 8 million curies that could be produced (under current operating conditions) in 0.94-in. slugs. The overall cost of a ^{60}Co source includes costs for slug fabrication, irradiation, shipping, a reencapsulation after irradiation, and sales. Slug fabrication and irradiation costs are shown in Table VII-2. He noted that the base irradiation cost today is less than the lowest AEC price of $0.50/curie, and this cost includes the usual charges noted by *Gillette*.

Brookhaven National Laboratory

Richards mentioned that the Brookhaven Procedures Manual, USAEC Report BNL-864, a preliminary draft of which was distributed at the meeting, did not mention a few other isotopes that are available from Brookhaven, for example, ^{38}Ar, ^{67}Cu, ^{124}I, and ^{90}Y beads. He noted

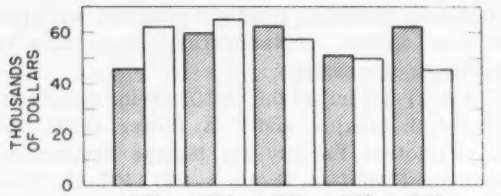

Fig. VII-2 Production expenses and dollar value of radioisotopes shipped from BNL, 1959–1963.

that the number of all shipments of isotopes over the years shows a gradual increase, but the number of users is erratic. There has been a drop in expenses due to an increase in efficiency and a reduction in personnel. Figure VII-2 shows the expenses and dollar values of radioisotopes shipped from 1959 to 1963. Figure VII-3 shows the trends in shipments of radioisotopes in the same years.

Richards also discussed radioisotope processing facilities, which are described in detail in BNL-864, and, in describing ^{18}F production and processing, made the following points:

1. Fluorine-18 is the only isotope of fluorine with a half-life long enough to be of value as a tracer.

2. Its half-life of 112 min creates problems in production and distribution at any distance from the production site.

3. In spite of these problems, there is interest in ^{18}F in certain medical applications.

He mentioned applications such as annihilation gamma scanning and bone scanning and said that ^{18}F is particularly valuable in medical uses where low doses are desired. Millicurie amounts can be made in the reactor by irradiation of lithium-oxygen compounds (usually Li_2CO_3) with thermal neutrons [$^{6}Li(n,t)^{4}He$; $^{16}O(t,n)^{18}F$]. Accelerator production is also feasible.

Floyd described the Brookhaven Graphite Research Reactor. (See *Graphite Research Reactor Facilities and Services Guide*, Brookhaven National Laboratory, June 1960).

Hillman summarized the capabilities of the BNL 62-in. cyclotron and the policies for use of this instrument. He noted that the cyclotron is equipped for acceleration of alphas, deuterons, protons, and ^{3}He ions with energies of 42, 21, 10.5, and 31 Mev, respectively. Both internal and external beams are available. Internal beams of about 50 μa and external beams of 30 to 50 μa are practical for use. The facility is designed primarily for research purposes for the staff at Brookhaven, and production time is limited.

He also described a Texas Nuclear Corp. neutron generator that is currently being set up for research. This instrument is capable of delivering 2.8- and 14.7-Mev neutrons, which are obtained by the $^{2}H(d,n)^{3}He$ and $^{3}H(d,n)^{4}He$ reactions, respectively. Deuterons are accelerated by a potential of 150 kv and strike a target containing ^{2}H or ^{3}H. With a fresh target the machine will be capable of delivering up to

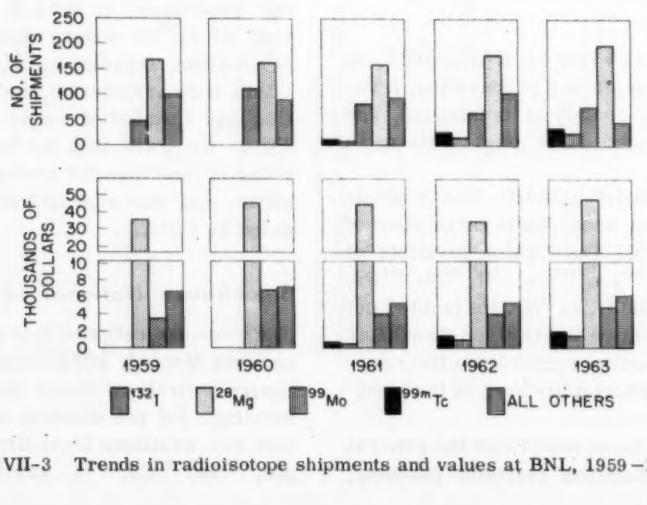

Fig. VII-3 Trends in radioisotope shipments and values at BNL, 1959–1963.

2×10^{11} neutrons/(cm^2)(sec) or about 2×10^{10} neutrons/(steradian)(sec) for 14.7-Mev neutrons and 10^8 neutrons/(steradian)(sec) for 2.8-Mev neutrons; it can also be used for production of thermal neutrons, 15-Mev protons, 20-Mev gammas, and X rays and will be equipped with a pneumatic device for fast irradiations. Policies for its use are the same as those for use of the cyclotron.

Generators or "milkers" are systems by which a desired radioisotope can be separated from its longer lived parent. *Hillman* showed the curve in Fig. VII-4, which illustrates the

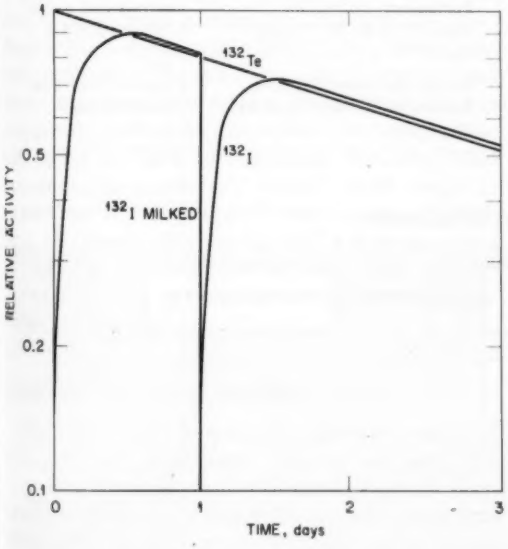

Fig. VII-4 Theoretical relative activities of ^{132}Te and ^{132}I. Iodine-132 is completely removed at time 0 and 1 day.

activity of a daughter in a generator before and after milking. [For review, see M. W. Greene, R. F. Doering, and Manny Hillman, Milking Systems: Status of the Art, *Isotopes Radiation Technol.*, 1(2): 152-3 (Winter 1963–1964).] *Hillman* said that milking systems are designed so that they will be easy and safe to handle and transport, simple and fast to use, and economical.

He described several generators listed in the Brookhaven manual. These are based on ion exchange, solvent extraction, and distillation and precipitation. He noted that other possible methods include use of a charged wire to collect a daughter from a gaseous parent, and electrolysis.

Table VII-3 POTENTIAL MILKING SYSTEMS

Daughter	Half-life	Parent	Half-life
^{44}Sc	4.0 hr	^{44}Ti	~100 years
^{131g}Te	25 min	^{131m}Te	1.2 days
^{129g}Te	67 min	^{129m}Te	33 days
^{127g}Te	9.3 hr	^{127m}Te	105 days
^{42}K	12.4 hr	^{42}Ar	35 years

Table VII-3 lists a number of possible generators for the future. The ^{42}K generator will be Brookhaven's first with a gaseous parent. The tellurium "ground-state" generators are of theoretical interest because the parent is also tellurium and the ^{44}Ti parent of ^{44}Sc has the longest half-life (around 100 years) of any parent for generators in which the Brookhaven group is interested.

In describing reactor-induced triton reactions, he noted that tritons can be produced in a reactor by the ^{6}Li$(n,t)^4$He reaction, the amount of ^{6}Li consumed depending on flux. Figure VII-5 shows that the number of neutron reactions per unit thickness will also vary with thickness for pure ^{6}Li. Lithium thicknesses of <100 μ gave the best results when it was important to achieve high specific activity in the product or to minimize the volume of material to be processed. In practice, however, this thickness must be corrected for dilution by the secondary target and other diluents.

Hillman also described some of the problems associated with using the triton reaction method.

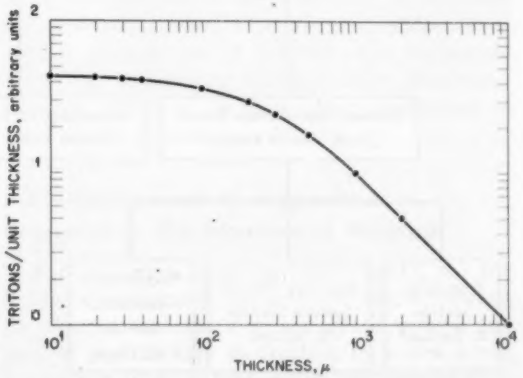

Fig. VII-5 Triton yield and thickness of ^{6}Li.

These include production of heat, low-energy availability for triton reactions in a reactor, and tenacity of ^{3}H for many materials at its removal during processing.

AEC Activities

New DID Organization Chart

Reorganization of AEC's Division of Isotopes Development recently was announced, and a new reorganization chart is presented below.

Joseph E. Machurek, formerly Chief of the Radiation Development Branch, has been appointed to a new position, Assistant to the Director for Planning and Evaluation.

A Radiation Applications Branch has been formed which combines the former Radiation Development Branch and the Isotopes Technology Development Branch. Justin L. Bloom has been appointed to head this new branch. His former position of Technical Assistant to the Director has been abolished.

Arnold Berman has been appointed Chief of a newly established Thermal Applications Branch. Along with development of thermal applications of radioisotopes, this new branch will accommodate all of the functions of the Production and Materials Branch, which has been abolished.

Other divisional units have been renamed and reconstituted as follows:

New title	Former title
Technology Utilization Branch, Oscar M. Bizzell, Chief	Analysis and Applications Branch
Budget and Administrative Branch, M. Edward Lockyer, Chief	Program Coordination Branch

DIVISION OF ISOTOPES DEVELOPMENT

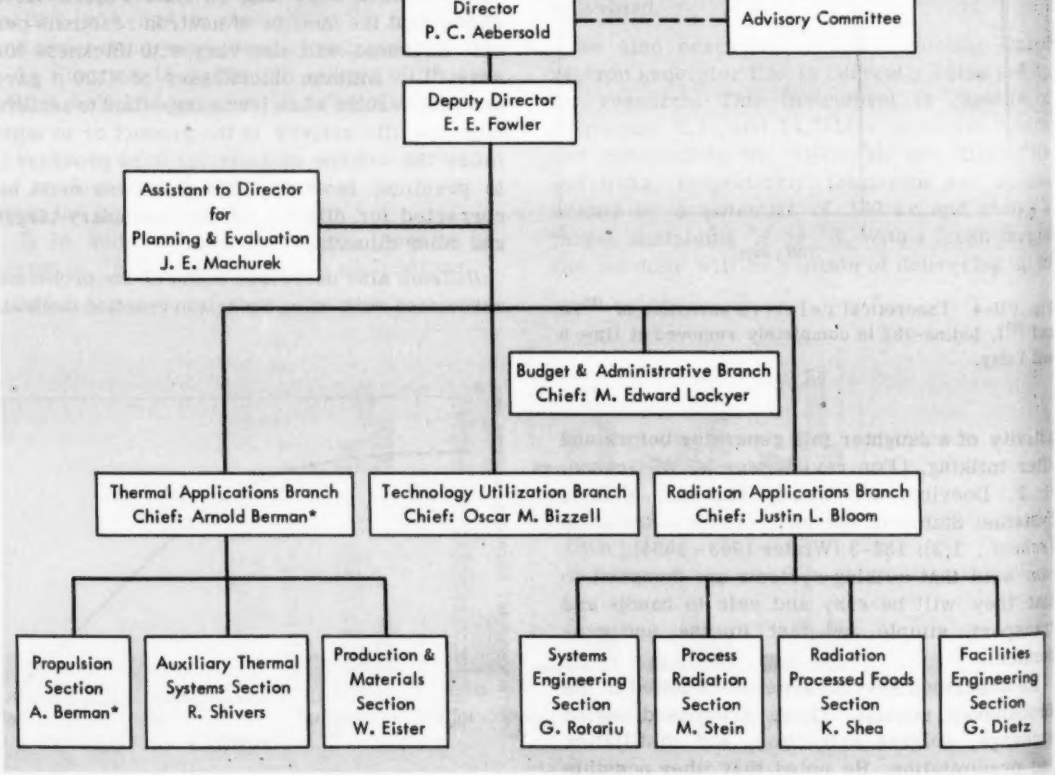

*Dual capacity.

AEC Ends Routine ^{85}Sr Production

AEC withdrew from the routine production and distribution of ^{85}Sr on October 15, and no new orders for the isotope have been accepted since August 15.

The new action adds ^{85}Sr to a list of seven other isotopes, produced mainly by Oak Ridge National Laboratory, recently withdrawn from routine AEC distribution. There are presently 10 domestic distributors of the isotope, and prices published by the producers are believed to be reasonable. Additional organizations were expected to begin producing the isotopes at about the time of AEC's withdrawal.

Five other isotopes—^{51}Cr, ^{55}Fe, ^{58}Co, ^{134}Cs, and ^{141}Ce—were similarly withdrawn [*Isotopes Radiation Technol.*, 1(3): 291 (Spring 1964)], and two others—^{125}I and ^{131}I—are produced only when higher quality fission-product material is required. AEC also continues the policy it established in 1961 of supplying ^{60}Co only when commercial producers cannot meet requirements under conditions of time, quality of product, or reasonable price. AEC's general policy is to discontinue providing materials or services that are reasonably available from commercial sources.

Proposal To Ease Medical Uses

AEC proposes to simplify regulations on medical uses of radioiodine, radiocobalt, and ^{51}Cr.

Under the new plan a physician files a registration form with the AEC and is authorized thereafter to procure the radiopharmaceuticals upon receipt of a registration number from AEC.

This would be done by establishing a general license, for which no application to the AEC is required, for the use of ^{131}I as sodium iodide for measurement of thyroid uptake and as iodinated human serum albumin for determination of blood and blood plasma volume; ^{58}Co or ^{60}Co for measurement of intestinal absorption of cyanocobalamin; and ^{51}Cr as sodium radiochromate for determinations of red blood cell volumes and survival time. A specific license from the AEC, or from a state with which the Commission has an agreement, now is required for these medical uses.

Two States Assume Authority

Florida and North Carolina recently became the seventh and eighth states to assume part of the AEC's regulatory authority over the use of radioactive materials.

Under the agreement the states will assume AEC's present regulatory responsibility for licensing, rule-making, and enforcement of the uses of radioisotopes, atomic energy source materials (uranium and thorium), and small quantities of fissionable material. There are about 260 AEC licenses in Florida and 185 in North Carolina. The states' boards of health are responsible for carrying out the radiation-control program.

The six other states that have previously executed similar agreements with AEC are Kentucky, Mississippi, California, New York, Texas, and Arkansas.

General License Established for Ownership of Radioisotopes Under New AEC Amendment

Under a new amendment to AEC regulations, a general license is established for ownership of radioisotopes in any quantity. This license requires no application to the Commission but does not authorize possession, use, import, or export of the material.

This means that a firm or individual, for example, no longer needs a specific AEC license to buy radioisotopes from a licensed manufacturer and have it shipped directly to a licensed user.

AEC believes it is desirable to issue a general license since ownership alone presents no radiation-safety problems. A similar general license already exists for the source materials uranium and thorium. The action is intended to simplify licensing requirements in cases where firms or individuals take title to, or transfer ownership of, radioactive material without ever having possession of it. The rule change to Part 30, "Licensing of Byproduct Material," became effective 30 days after publication in the *Federal Register* on July 21.

AEC–Department of Agriculture Cooperative Developmental Program

A cooperative program between AEC and the U. S. Department of Agriculture (USDA) on ways to control insects in stored grain without the use of insecticides is typified in a new grain irradiator (Fig. VII-6). Vitro Engineering Co., New York, recently was given a contract to de-

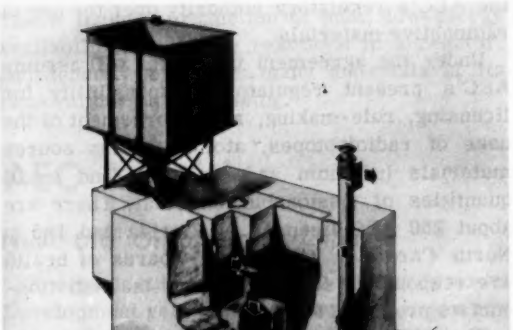

Fig. VII-6 Cobalt-60 bulk grain irradiator.

sign and supervise construction of this experimental facility at USDA's Stored-Product Insect Laboratory at Savannah, Ga. Operation of the irradiator is expected by July 1965. It will treat 2½ tons of grain an hour. Commercial models probably would operate at 250 tons an hour.

AEC Seeks Public Comments on Formal Procedures for Withdrawal from Routine Production and Distribution of Radioisotopes

The USAEC has published for public comment proposed formal procedures for Commission withdrawal from routine production and distribution of radioisotopes that are reasonably available from commercial producers. In doing so, the Commission reaffirmed its policy and intent to transfer its commercial radioisotope production and distribution activities to private industry as rapidly as possible, consistent with the overall national interest. The Commission would continue to produce some radioisotopes as necessary for governmental use or sale.

Under the procedures the Commission may withdraw either voluntarily or when industry files a formal petition. The contemplated procedural steps and withdrawal guidelines were published in the *Federal Register*, Sept. 16, 1964, and may be obtained from the Isotopes Sales Department, Isotopes Development Center, Oak Ridge National Laboratory, P. O. Box X, Oak Ridge, Tenn., 37831. Interested persons are asked to submit written comment to the Secretary of the Commission by Nov. 14, 1964.

Availability of Isotopes and Services

Mound Laboratory To Distribute Enriched Gaseous Isotopes

Mound Laboratory has recently taken over the handling and distribution of enriched gaseous isotopes for the AEC. Gases separated both at ORNL and at Mound are involved and include ^{3}He, as well as enriched isotopes of neon, argon, krypton, and xenon, which are, or will ultimately be, included in the program.

General

^{90}Sr Powers Navigational Aids in Lighthouse, Atlantic Ocean

Two power sources recently were placed in operation—the first U. S. Coast Guard nuclear-powered lighthouse and an Atlantic Ocean deep-water device.

An isotopic power generator developed for the AEC is operating an unmanned beacon in Baltimore Lighthouse located at Chesapeake Bay, Md., south of Baltimore. It began operation on May 20.

The 60-watt generator—designed to operate unattended for 10 years—supplants batteries that had to be replaced every year. In about a year it will be moved to a lighthouse in a remote location, not yet selected, where it will replace batteries or diesel engines.

The nuclear generator is 34½ in. in height by 22 in. in diameter. It weighs about 4600 lb, including shielding. The generator is fueled with ^{90}Sr. A special high-strength corrosion-resistant metal, Hastelloy C, encases the 14 fuel capsules. Inside the generator, heat from the decaying fuel is converted into electricity through 120 pairs of lead telluride thermocouples which surround the fuel.

The Atlantic Ocean source, a ^{90}Sr generator composed of parts fabricated at Oak Ridge atomic energy installations, is powering navigational aids 750 miles off the east coast of Jacksonville, Fla., at a depth of 15,000 ft. It began operation on July 13, 1964.

The generator is designed to provide about 7 watts of continuous electric power for at least 2 years. It is $14\frac{3}{4}$ in. in height and $9\frac{1}{2}$ in. in diameter.

The Nuclear Division of the Martin Company, Baltimore, Md., developed both generators.

Squibb Builds $2 Million Plant

A $2 million radiopharmaceutical plant recently was completed at E. R. Squibb & Sons site in New Brunswick, N. J.

The new manufacturing laboratory will more than double the company's capacity for making labeled compounds.

Squibb, a division of Olin Mathieson Chemical Corp., entered the radiopharmaceutical field in 1957 and now makes about 60 labeled compounds. Orders are currently filled on a prescription basis.

Production in Squibb's radiopharmaceutical manufacturing unit is on a laboratory scale. A large portion of the cost of the facility went into the elaborate provisions needed to protect personnel from radioactivity: shielding, remote-control units, special air conditioning, and facilities for disposal of radioactive wastes.

Each shipment that goes out must be prepared so that its level of radioactivity will be at the specified level on the day the physician plans to administer it to the patient. Future radioactivity levels must be calculated in advance and the current level checked carefully as the sample leaves the laboratory. More than 90% of the prescriptions are packaged and shipped by air the same day the orders are received.

Low-Energy X-Ray, Gamma Sources Production, Properties, Uses Topics of October Symposium

A symposium on low-energy X-ray and gamma sources and their applications was scheduled for October 20–21 at the Illinois Institute of Technology Research Institute (IITRI), Chicago. Cochairmen of this symposium were to be James W. Hitch, AEC, and Leonard Reiffel, IITRI.

The tentative program is shown on the following page.

Presiding on October 20 will be Leonard Reiffel, Director of Physics Research, IITRI, and G. J. Rotariu, DID. At the medical session on October 21, H. N. Wagoner, Assistant Professor of Medicine and Radiology at Johns Hopkins University, and E. Dale Trout, Director of the Radiation Laboratory at Oregon State College, will preside.

The program committee comprised G. J. Rotariu (DID), L. E. Preuss (Edsel B. Ford Institute), P. S. Baker (ORNL), Leonard Reiffel (IITRI), and H. D. Bruner (AEC). Local arrangements were made by William Finnegan, IITRI.

Paint Flecks Convict Burglar

Evidence from neutron-activation analysis recently helped to convict a private detective with no previous criminal record in the burglary of a San Francisco liquor store.

Paint flecks on a tire iron were found to match those from the jimmied door and the culprit's car. Vincent P. Guinn, General Dynamics Corp., and associates carried out the analysis. The incident is reported in the August 7 issue of *Time*.

Translations Available

As part of the effort to cover the foreign literature in the isotopes field, selected articles are translated by members of the ORNL Isotopes Development Center. These are available through usual USAEC information dissemination channels (see front cover). Some of the recent translations of interest in the field of production and applications of isotopes are:

1. AEC-tr-6138: H. H. Stamm and H. J. Schroeder, Paper Chromatographic Separation of Radionuclides with Iron(III) Hydroxide as Carrier, *J. Chromatog.*, 10: 392-5 (1963) (in German; translated by J. J. Pinajian).

2. AEC-tr-6163: K. Wagner, Some Studies in the Production of Carrier-free ^{7}Be by Bombardment of Lithium with Deuterons in the Cyclotron, *Kernenergie*, 6: 121-2 (1963) (in German; translated by J. J. Pinajian).

3. AEC-tr-6305: J. Mikulski and I. Stronski, Separation of Cr^{3+}, Mn^{2+}, and Fe^{3+} by Ion Ex-

October 20

Programmatic Objective	J. W. Hitch, Division of Isotopes Development, AEC
Important Considerations in the Production of X-Rays from Radioisotopes	Charles Terrell, IITRI
Recent Developments in the Production of Low-Energy-Emitting Radioisotopes	Neil Case or R. Pressly, Oak Ridge National Laboratory
Compilation of Beta-Excited X-Ray Spectra	Luther E. Preuss, Edsel B. Ford Institute
Containment Considerations When Using Low-Energy-Emitting Radioisotopes	Thomas Lahr, 3M Company
Bremsstrahlung from ^{90}Sr in Thin Absorbers	Thomas Bustard, Martin Company
Americium-241 as a Non-Destructive Testing Tool for the Aircraft and Space Industry	Gordon Locher, Western Radiation Laboratory
Analysis and Measurement of Materials with Low-Energy Radiation	Charles Badgett, Industrial Nucleonics Corporation
Portable Fluorescent X-Ray Developments	J. O. Karttunen, Argonne National Laboratory
Some Applications of Low-Energy Radiation from Radioisotopes	Harry Dooley, U. S. Radium Corporation
Industrial Analysis of ^{147}Pm X-Rays for Radiography and Imaging Readout	E. Coleman, Picker X-Ray
Round-Table Discussion	Leonard Reiffel, IITRI James Hitch Farno Green, Viso Corp. Luther Preuss Neil Case or R. Pressly

October 21

Use of ^{125}I for Intra-Oral X-Radiography	Rune S. A. Söremark, Harvard School of Dental Medicine
Radioisotopic Device for Measuring Bone Mineral	Lawrence Lanzl and Nels Strandjord, University of Chicago
Use of Monochromatic Low-Energy X-Rays for Body Composition Measurements	John Cameron and James Sorenson, University of Wisconsin
In-Vivo Measurement of Bone Mineral Content by Transmission Techniques	Leonard Goodman, ANL, and Bertrand Levin, Michael Reese Hospital, Chicago
An Autofluorography System for Use with Iodine-125	Michel Ter-Pogossian, Mallinckrodt Institute, Washington University
A Portable Device for Chest Radiography and Other Applications	Farno Green
Recent Research Developments at Polaroid Corporation and Their Application to Low-Energy Radiography	Herbert J. Frede, Polaroid X-Ray Research Laboratories, Waltham, Mass.
Proton-Excited X-Rays and Applications	Andrew Sterk, AMF Atomics, Alexandria, Va.
The Generation and Practical Use of Monoenergetic X-Rays from Alpha-Emitting Isotopes	Charles Ziegler, Parametrics, Waltham, Mass.

change, *Isotopen Tech.*, 2: 69-70 (1962) (in German; translated by J. J. Pinajian).

4. AEC-tr-6351: P. Schiller, Application of β-Backscattering to the Determination of Au, Ag, Sb, Zn, and Ca in Pharmaceutical Preparations, *Kernenergie*, 6: 514-6 (1963) (in German; translated by J. J. Pinajian).

5. ORNL-tr-24: H. Hugli, J. Peter, and P. Tempus, Installation for the Production of Radioisotopes, *Neue Tech.*, 5: 542-7 (1963) (in German; translated by J. J. Pinajian).

6. ORNL-tr-34: J. Mikulski, Investigations of the Extraction of Metal Ions Using Radioisotopes. Communication 3. Extraction of Mn(II), Fe(III), Co(II), Cu(II), and Zn(II) Ions with 8-Hydroxyquinoline-*N*-Oxide, *Kernenergie*, 6: 71-2 (1963) (in German; translated by Joe F. Allen).

7. ORNL-tr-93: V. A. Sokolov, ^{132}I, 23 pp., Gosatomizdat, Moscow (1963) (in Russian; translated by Martha Gerrard).

8. ORNL-tr-104: R. Münze, L. Baraniak, G. Reinhard, and W. Leuschke, Plant-scale Production of Carrier-free ^{32}P, *Kernenergie*, 6: 489-93 (1963) (in German; translated by J. J. Pinajian).

9. ORNL-tr-205: E. Hatzopoulos, A New Apparatus for Generation of ^{132}I, *J. Inorg. Nucl. Chem.*, 25: 462-3 (1963) (in French; translated by J. J. Pinajian and Martha Gerrard).

LEGAL NOTICE

This journal was prepared under the sponsorship of the U. S. Atomic Energy Commission. Neither the United States, nor the Commission, nor any person acting on behalf of the Commission:

A. Makes any warranty or representation, expressed or implied, with respect to the accuracy, completeness, or usefulness of the information contained in this journal, or that the use of any information, apparatus, method, or process disclosed in this journal may not infringe privately owned rights; or

B. Assumes any liabilities with respect to the use of, or for damages resulting from the use of any information, apparatus, method, or process disclosed in this journal.

As used in the above, "person acting on behalf of the Commission" includes any employee or contractor of the Commission, or employee of such contractor, to the extent that such employee or contractor of the Commission, or employee of such contractor prepares, disseminates, or provides access to, any information pursuant to his employment or contract with the Commission, or his employment with such contractor.

NUCLEAR SCIENCE ABSTRACTS

The U. S. Atomic Energy Commission, Division of Technical Information, publishes *Nuclear Science Abstracts (NSA)*, a semimonthly journal containing abstracts of the literature of nuclear science and engineering.

NSA covers (1) research reports of the U. S. Atomic Energy Commission and its contractors; (2) research reports of government agencies, universities, and industrial research organizations on a world-wide basis; and (3) translations, patents, books, and articles appearing in technical and scientific journals.

Complete indexes covering subject, author, source, and report number are included in each issue. These are cumulated quarterly, semiannually, and annually providing a detailed and convenient key to the literature.

Availability of *NSA*

SALE *NSA* is available on subscription from the Superintendent of Documents, U. S. Government Printing Office, Washington, D. C., 20402, at $30.00 per year for the semimonthly abstract issues and $22.00 per year for the four cumulated-index issues. Subscriptions are postpaid within the United States, Canada, Mexico, and all Central and South American countries, except Argentina, Brazil, British and French Guiana, Surinam, and British Honduras. Subscribers in these Central and South American countries, and in all other countries throughout the world, should remit $37.00 per year for subscriptions to semimonthly abstract issues and $25.00 per year for the four cumulated-index issues.

EXCHANGE *NSA* is also available on an exchange basis to universities, research institutions, industrial firms, and publishers of scientific information. Inquiries should be directed to the Division of Technical Information Extension, U. S. Atomic Energy Commission, P. O. Box 62, Oak Ridge, Tennessee, 37831.

TECHNICAL PROGRESS REVIEWS may be purchased from Superintendent of Documents, U. S. Government Printing Office, Washington, D. C., 20402. *Isotopes and Radiation Technology* at $2.00 per year for each subscription or $0.55 per issue; the other four journals at $2.50 per year and $0.70 per issue. The use of the coupon below will facilitate the handling of your order.

POSTAGE AND REMITTANCE: Postpaid within the United States, Canada, Mexico, and all Central and South American countries except as hereinafter noted. Add $0.50 per year, or $0.15 per single issue for the *Isotopes and Radiation Technology* journal and $0.75 per year or $0.20 per single issue for the other four journals for postage to all other countries, including Argentina, Brazil, British and French Guiana, Surinam, and British Honduras. Payment should be by check, money order, or document coupons, and MUST accompany order. Remittances from foreign countries should be made by international money order, or draft on an American bank, payable to the Superintendent of Documents, or by UNESCO book coupons.

order form

SUPERINTENDENT OF DOCUMENTS
U. S. GOVERNMENT PRINTING OFFICE
WASHINGTON , D. C., 20402

Enclosed:
document coupons ☐ check ☐ money order ☐

Charge to Superintendent of Documents No._____

Please send a one-year subscription to

☐ NUCLEAR SAFETY

☐ POWER REACTOR TECHNOLOGY

☐ REACTOR FUEL PROCESSING

☐ REACTOR MATERIALS

(Each subscription $2.50 per year; $0.70 per issue.)

☐ ISOTOPES AND RADIATION TECHNOLOGY

(Each subscription $2.00 a year; $0.55 per issue.)

SUPERINTENDENT OF DOCUMENTS
U. S. GOVERNMENT PRINTING OFFICE
WASHINGTON, D. C., 20402

(Print clearly)

Name _____

Street _____

City _____ Zone ____ State _____